Aus dem Institut für Anatomie und Zellbiologie
Abteilung Molekulare Neurowissenschaften
Geschäftsführender Direktor: Prof. Dr. E. Weihe
des Fachbereichs Medizin der Philipps-Universität Marburg

in Zusammenarbeit mit dem

Department of Microbiology & Immunology
Direktor: T. L. Manser, PhD
M. J. Schnell, PhD & B. Dietzschold, DVM
der Thomas Jefferson Universität Philadelphia

RABIES VIRUS REPLICATION OUTSIDE THE CENTRAL NERVOUS SYSTEM

Implications for Disease Transmission

Inaugural-Dissertation
zur Erlangung des Doktorgrades der gesamten Humanbiologie
dem Fachbereich Medizin der Philipps-Universität Marburg
vorgelegt von

Mirjam Preuß aus Wertheim

Marburg, 2008

Angenommen vom Fachbereich Medizin der Philipps-Universität Marburg
am: 02. Juli 2008

Gedruckt mit Genehmigung des Fachbereichs.

Dekan: Prof. Dr. M. Rothmund
Referenten: Prof. Dr. E. Weihe; M. J. Schnell, PhD
1. Koreferent: Prof. Dr. S. Becker

TABLE OF CONTENTS

1. Abstract [English]

Rabies is a fatal disease in mammals which is transmitted by the neurotropic Rabies virus (RV). Most often, classical RV infections originate from muscle tissue after a bite through an infected canine and ascend to the central nervous system (CNS) *via* peripheral nerves. In contrast, transfer of non-classical RV by bat bites or scratches, the most common cause for human rabies in North America and also an emerging disease in Europe, most likely introduces RV in rather small amounts superficially into a new host. In both cases, classical and non-classical RV can have access to lymph and/or blood. The impact and effects of the hematogenously and lymphatically distributed share of the viral inoculum is unclear.

Taking this into account combined with recent RV infections through unrecognized RV infected organ transplantations the questions arose whether RV is able to infect peripheral organs primarily *via* a vascular route or only by centrifugal spread *via* neuronal pathways from the CNS and if this postulated route is strain dependent. Subsequently it was thought to be elucidated, whether RV is able to replicate in organs and if its target cells for direct invasion of organs are different from those it reaches after centrifugal spread from the CNS. With regard to the transmission of RV by tissue transplants it was also investigated whether RV originating from organs is more likely to ascend into the CNS by neuronal pathways or on alternative routes.

In order to answer these questions, mice were infected either with a dog-derived classical RV (DOG4) or a bat-derived non-classical RV (rSB) as representatives for the two RV strains with the largest impact in naturally occurring human rabies, and monitored for weight loss and disease symptoms. To maximize the hematogenous dissemination of the inoculum, mice were infected intravenously (i.v.) and compared to mice inoculated intramuscularly (i.m.). A TaqMan® probe based quantitative reverse-transcription polymerase chain reaction (qRT-PCR) assay was developed to quantify strain-specifically negative-stranded as well as positive-stranded viral RNA in various tissues. For confirmation of replicating RV, virus was isolated from tissues and the nature of virus-positive cells in the periphery determined by immunohistochemistry. A kinetic study was undertaken to trace the pathways of RV into and within the CNS after i.v. and i.m. inoculation.

I.m. inoculation with either DOG4 or rSB led to hind limb paralysis and death within twelve days. Viral RNA was detected in the CNS and all analyzed organs (lungs, heart, liver,

kidneys) from morbid animals. rSB killed mice in a dose-dependent way also when injected i.v., however without causing typical symptoms of rabies. Surprisingly, i.v. inoculation of DOG4 rendered the infection completely harmless. The mice recovered from a short period of mild weight loss and survived for longer than eight months, showing no signs of viral replication in organs, but low virus load in blood cells and CNS. This and persistent high virus neutralizing antibody (VNA) titers suggest an ongoing immune-controlled latent RV infection after DOG4 i.v. inoculation.

After rSB i.m. inoculation, the spread of RV to the periphery was only detected after viral progression throughout the CNS. Importantly, viral RNA was detected at early time points in organs after i.v. inoculation and infectious RV was isolated from the heart before it was isolated from the brain. After i.m. as well as after i.v. inoculation with rSB only neuronal cells were found to be positive for viral antigen. This data reveal for the first time the possibility of a primary infection of peripheral ganglionic cells in organs by rSB *via* a non-neuronal route.

Immunohistochemical kinetic studies of CNS tissue after rSB i.m. inoculation confirmed the motor pathway from the muscle to the brain as the main route for viral invasion whereby the sensory system was affected only secondarily through its connections to the motor system. In contrast, the forebrains of i.v. inoculated mice were infected independently from the presence of viral antigen in spinal cord and brain stem. Our immunohistochemical findings suggest for the first time a direct invasion of the CNS by rSB from the vascular system, most preferentially through hypothalamic neurosecretory axons in the neurohypophysis and the median eminence, whereas retrograde neuronal transport of RV from peripheral organs to the CNS proved to be unlikely.

2. Abstract [German]

Tollwut ist eine für Säugetiere tödliche Erkrankung, die durch das neurotrope Tollwutvirus (RV) übertragen wird. Meist gehen klassische RV-Infektionen nach dem Biss eines infizierten Hundes vom betroffenen Muskelgewebe aus und wandern durch periphere Nerven ins Zentralnervensystem (ZNS) ein. Im Gegensatz zur Infektion durch einen Hundebiss ist die Menge an RV, die durch Fledermausbisse oder -kratzer übertragen wird, relativ klein und oberflächlich. Solche nicht-klassischen RV-Infektionen sind die häufigste Ursache für Tollwut beim Menschen in Nordamerika und werden auch in Europa zunehmend registriert. In beiden Fällen kann klassisches und nicht-klassisches RV Zugang zu Lymphe und/oder Blut haben. Die Bedeutung und Auswirkungen des hämatogenen und lymphatischen Anteils des Inokulums ist unklar.

Diese Überlegungen warfen im Zusammenhang mit Transplantationen RV-infizierter Organe in der jüngeren Vergangenheit die Frage auf, ob RV periphere Organe direkt aus Gefäßen heraus oder nur über neuronale Wege vom ZNS aus infizieren kann und ob dieser postulierte Infektionsweg abhängig vom Virusstamm ist. Nachfolgend sollte geklärt werden, ob RV in Organen replizieren kann und ob seine Zielzellen dort für eine direkte Invasion sich von denen unterscheidet, die es nach zentrifugaler Ausbreitung aus dem ZNS erreicht. Mit Blick auf die Übertragung von RV durch Gewebstransplantate wurde außerdem untersucht, ob RV aus Organen über Nerven ins ZNS einwandert, oder ob die Ausbreitung über alternative Wege wahrscheinlicher ist.

Zur Beantwortung dieser Fragestellungen wurden Mäuse entweder mit einem klassischen Hunde-RV (DOG4) oder einem nicht-klassischen Fledermaus-RV (rSB) als Vertreter der zwei RV-Stämme mit der größten Bedeutung für natürlich vorkommende Tollwutinfektionen im Menschen infiziert, und Gewichtsverlust und Entwicklung von Symptomen beobachtet. Um den hämatogenen Anteil des Inokulums zu maximieren, wurden die Mäuse intravenös (i.v.) infiziert und mit intramuskulär (i.m.) infizierten Mäusen verglichen. Eine TaqMan®-Sonden basierte quantitative Reverse-Transkription Polymerasekettenreaktion (qRT-PCR) wurde etabliert, um Virusstamm-spezifisch negativ- als auch positiv-strängige virale RNA in verschiedenen Geweben quantifizieren zu können. Zur Bestätigung viraler Replikation wurde Virus von Geweben isoliert und die Art virus-positiver Zellen in der Peripherie durch Immunhistochemie bestimmt. Eine kinetische Studie wurde durchgeführt, um die Wege von RV ins und innerhalb des ZNS zu verfolgen.

I.m. Inokulation mit DOG4 oder rSB führte zur Lähmung der Hinterläufe und Eintreten des Todes innerhalb von zwölf Tagen. Negativ- und positiv-strängige RV RNA wurde im ZNS und allen analysierten Organen (Lunge, Herz, Leber, Nieren) aus schwer kranken Tieren

detektiert. rSB tötete Mäuse auch dann, wenn es i.v. injiziert wurde, allerdings ohne Tollwut typische Symptome zu verursachen. Überraschenderweise machte die i.v. Inokulation die Infektion mit DOG4 harmlos. Die Mäuse erholten sich von einer kurzen Phase geringen Gewichtsverlusts und überlebten danach länger als acht Monate, ohne Anzeichen von viraler Replikation in Organen zu zeigen. Allerdings war sowohl in Blutzellen als auch im ZNS virale RNA nachweisbar. Dies und anhaltend hohe Virus neutralisierende Antikörpertiter weisen auf eine immunologisch kontrollierte latente Infektion nach i.v. Inokulation mit DOG4 hin.

Nach rSB i.m. Inokulation wurde eine Etablierung der Infektion in der Peripherie nur nach vorangehender Ausbreitung im ZNS beobachtet. Bemerkenswert ist, dass nach i.v. Infektion virale RNA schon zu frühen Zeitpunkten in Organen gefunden wurde und infektiöse rSB Partikel vom Herzen isoliert wurden, bevor eine Isolation aus dem Hirn möglich war. Sowohl nach i.m. als auch nach i.v. Inokulation mit rSB konnte virales Antigen nur in neuronalen Zellen nachgewiesen werden. Diese Daten zeigen zum ersten Mal die Möglichkeit einer primären Infektion peripherer Ganglionzellen in Organen durch rSB *via* eines nicht-neuronalen Weges auf.

Immunhistochemische kinetische Studien an ZNS-Gewebe nach rSB i.m. Inokulation bestätigten die motorischen Bahnen vom Muskel ins Hirn als Hauptweg für die virale Invasion, wobei das sensorische System erst nachfolgend durch seine Verbindungen zum motorischen System infiziert wurde. Im Gegensatz dazu wurden die Vorderhirne i.v. infizierter Mäuse unabhängig von der Anwesenheit viralen Antigens in Rückenmark und Hirnstamm infiziert. Unsere immunhistochemischen Befunde weisen zum ersten Mal auf eine direkte Invasion des ZNS durch rSB vom Gefäßsystem aus, vorzugsweise über hypothalamische neurosekretorische Axone in der Neurohypophyse und der medianen Eminenz, hin, wohingegen sich der retrograde neuronale Transport von RV aus peripheren Organen ins ZNS als unwahrscheinlich erwies.

3. Introduction

3.1. The Rabies Disease in its Historical Context: Epidemiology and Pathogenesis

3.1.1. History

Rabies is an almost always invariably fatal infectious disease of the CNS, which affects exclusively mammals including humans. The name ‘rabies’ is adapted from the Sanskrit word *rabbahs*, ‘to do violence’, and from the Latin verb *rabere*, ‘to rage’. Both refer to the changes in the behavior of infected animals and humans to madness and violent aggression, which are typical symptoms for one of the three clinical profiles of the disease [163]. Because of its spectacular manifestations and its association with carnivores, human awareness of the rabies disease can be traced back until ancient descriptions from the Mesopotamian region of the twenty-third century BC [46]. Rabies was often linked to dark deities like the God of Death in the Vedic Age (1500 – 500 BC) of India, whose companion was a deathly dog, or the Egyptian god Sirius who was depicted himself as a furious, death-bringing dog. In the fourth century BC the disease is mentioned by the Greek philosopher Aristotle in his “History of Animals”, as well as in plays written by Euripides and Xenophon. First records of the term ‘hydrophobia’, another characteristic feature of rabies describing the fear of water observed in human patients, were made by Cornelius Celcius in the first century AD.

3.1.2. Development of Vaccines

Despite the long history of more than three thousand years, the knowledge about rabies is still rather incomplete. In 1584, the Italian Girolamo Fracastoro stated in his text “The Incurable Wound” the observation that infected humans have to be regarded as inevitably moribund once clinical symptoms manifest, which unfortunately remains true until now, more than four hundred years later. In 1885, Louis Pasteur generated the first vaccine against the disease, although he did not know about the actual nature of its causative agent, for which he defined the word ‘virus’ (Latin for ‘poison’). Building upon the work of the German scientist Georg Gottfried Finke, who transferred rabies from a rabid dog by sprinkling infectious saliva into wounds in 1804, and Pierre Victor Galtier, who described in 1879 the adaptation and the

serial transfer of the disease in rabbits, Pasteur studied the virus in rabbits. Originally he inoculated them with RV from an infected cow brain, followed by serially passing of aqueous suspensions of dried spinal cords from infected animals to healthy ones. After several rounds, the rabbits did not develop severe symptoms anymore and were protected effectively against a challenge with infectious material. Thus, Pasteur produced the first attenuated virus to be used as post-exposure vaccine in humans.

The development of safer vaccines and the production of larger quantities depended on two basic discoveries: (1) the recognition of viruses as biological entities, which was driven by the studies of Dmiti Iwanowski and Martinus Beijerinick in the following fifteen years; (2) the attribution of a virus as responsible cause for the rabies disease, which was made by Paul Remlinger in 1903. In 1964, the groundwork for a vaccine against RV was developed by cultivation of RV in a human diploid cell strain and therefore removing the risk of transferring neuronal tissue present in the vaccine which originated from brain [386]. Today, advanced derivatives of this tissue culture vaccine, for example Vero cell rabies vaccine, purified chicken embryo cell vaccine and purified duck embryo cell vaccine, are available and consist of inactivated virus that cannot cause disease but induces high titers of virus neutralizing antibodies (VNA). Nerve tissue originated vaccines, which are less safe and effective but cheaper, are also still in use, particularly in developing countries. According to the guidelines of the World Health Organization (WHO; http://www.who.int/rabies/resources/en/), vaccines are administered only as post-exposure treatment together with rabies immunoglobulin, or as pre-exposure prophylaxis for people at risk such as veterinarians or laboratory personnel, who come in contact with RV.

3.1.3. Epidemiology

Rabies is the most important viral zoonosis [265], although humans are usually a dead-end host. The virus is endemic in a plethora of hosts throughout the world except Antarctica and some island countries, for example Greenland, New Zealand, Iceland and Japan. In most of the developed countries however, at least the contamination of domestic animals with RV is under control due to the application of consequent vaccination strategies [146].

Globally, canines present the major reservoir and vector of RV and pose a serious health hazard especially in Asia, Latin America and Africa. Here, community and stray dogs are common, and often nobody feels responsible for their vaccination. Regionally, different RV

strains are endemic in distinct species, although the virus has been isolated from almost all mammalian species. Foxes, for example, are the main reservoir for RV in Europe. In North America, RV is present in raccoons, skunks and coyotes, and in Asia and Africa, mongooses are the most inflicted species beside canines. In addition to these ground dwelling animals, lyssaviruses are carried also in hematophagous vampire bats in Central and South America as well as in insectivorous bats in North America, Europe and Australia [79]. The true extent of infection rates with RV in these non-terrestrial wildlife populations is unknown and cannot be controlled by vaccination programs yet [5].

3.1.4. Impact on Human Health

Although the disease is preventable, it is estimated by the WHO that still more than fifty thousand people succumb to it worldwide annually, especially in Africa and Asia (http://www.who.int/mediacentre/factsheets/fs099/en/). Forty percent of the victims are children (http://www.who.int/rabies/human/en/). Exact numbers are not available, since infections often occur in rural regions and rabies surveillance in the most inflicted countries is incomplete or even non-existing.

Transmission usually occurs by contact with virus-laden saliva of a rabid animal, mostly through a bite. Interestingly, RV transmission normally occurs within a species, but can occasionally spread to other ones including humans. Also, in very rare cases the disease was probably contracted by an aerosol or through contact of a mucous membrane with infectious material [83, 393, 394]. Transmission from human to human has not been described. However, there are eight documented cases of RV infections caused by corneal transplantations [66, 138, 175, 191], and in 2004, in two unrelated cases, seven people in the USA (Texas) and Germany contracted RV and succumbed to the disease after having received solid organs or vascular conduits from undiagnosed RV infected organ donors [15, 160, 347].

According to the WHO, ten million people receive post exposure treatment annually after having had contact with an animal suspected to be rabid, which poses a great financial burden on the health care system. There is also an increase of cases of rabies, in which an exposure to a rabies infected animal cannot be recalled. These so-called cryptogenic infections challenge the diagnosing medical personnel and can be attributed retrospectively most often to bat-derived RV strains [133]. The risk of contracting RV by contact with a rabid animal ranges from five to eighty percent, depending on the size of the inoculum, the severity

of the lesion, nerve density in the affected area, proximity of the entry site to the CNS as well as the RV strain and host factors [118].

3.1.5. Clinical Picture of the Rabies Infection

If post-exposure prophylaxis (PEP) cannot be administered immediately, a delay up to five days may be justifiable [161]. First symptoms of rabies usually manifest after an incubation period of one to two months. However, time spans between infection and outbreak of seven days up to six years have been documented [343], although the latter are extremely rare. The prodrome is rather unspecific, resembling a common cold, with fever, headache and general malaise, but this stage usually indicates the end of the ability to prevent a fatal outcome by PEP.

After infection, RV progresses centripetally within nerve fibers from the site of entry into the CNS, causing often numbness, itching and neuropathic pain in the affected skin region [163]. After a few days up to one week, patients enter an acute neurological phase, which can manifest in three forms. People suffering from encephalic (furious) rabies develop the classical aggressive behavior and hyperactivity, which is the most common reception people have of rabies. Other possible symptoms include cerebral dysfunctions such as attention deficiency, sleeplessness, hallucinations, aerophobia and the already mentioned hydrophobia, as well as autonomic dysfunctions like hypersalivation, hyperventilation, abnormal pupil reactions, and generalized goose skin. Symptoms may deteriorate by thirst, anxiety, light, noise and other triggers. After only a few days, the patient lapses into coma and eventually dies due to cardiorespiratory failure.

The second clinical form of the infection, paralytic (dumb) rabies, causes an ascending paralysis by involving peripheral nerves and is likely to be mixed up with Guillain-Barré syndrome (GBS), an autoimmune disorder of unknown cause that has the same effects [335]. But unlike GBS, RV infection leads inevitably to death, although the survival period is usually longer than in the furious manifestation of the disease [169]. The reason why a patient develops the furious or the dumb form of rabies is still unknown, but it is assumed that the RV strain, the location of the entry site, the incubation period and the virus localization in the CNS as well as the genetic background of the patient have an influence on it [164, 168, 270]. Often, patients, who contracted the virus from bats, present with atypical symptoms, for example neuropathic pain, myoclonus, hemiparesis or ataxia. These cases of non-classical

rabies, the third form of the disease, show in general very heterogeneous symptoms and are most often associated with RV transmitted by bats [163].

3.1.6. Invariably Fatal?

Up to today there are only six documented cases, in which people with rabies symptoms survived the infection. Five of them had been either previously vaccinated or received PEP treatment before the onset of symptoms [9, 157, 250, 301]. All but one suffered from massive sequelae [157, 163]. The survival and complete recovery of a fifteen-year-old girl after a bat bite in 2004 presents a unique case since neither pre- nor post-exposure prophylaxis in any form was administered before the development of symptoms [391]. An experimental protocol was applied, inducing coma and giving ketamine, a N-methyl-D-aspartate antagonist, to reduce brain excitotoxicity and autonomic reactivity. Since 2005, this protocol was repeated with other rabies patients, who contracted RV from bat or dog bites, but failed in all cases [67, 165], indicating that other reasons than the treatment were responsible for the survival.

3.1.7. Pathophysiology

The exact mechanism by which RV causes the fatal encephalomyelitis is still unexplained [121, 360]. The infection proceeds non-lytically and apoptosis seems to play only a role in experimental infections with attenuated RV strains [188, 274]. The pathogenesis is largely independent from the extent of virus load. It is likely that the depletion of cellular metabolic supplies by excessive viral replication leads to inhibition of the synthesis of neurotransmitters, which is responsible subsequently for altered neurotransmission and electrophysiological dysfunctions of the infected neurons [121, 360]. Immunologic reactions to the viral infection turn out rather mild, with only some perivascular accumulations of lymphocytes and polymorph-nuclear cells. Histologically, neurons - especially hippocampal pyramidal cells and the Purkinje cells of the cerebellum - often show eosinophilic inclusion bodies, which were described first by Adelchi Negri in 1903. He misinterpreted them, however, as a parasitic pathogen causing the rabies disease [214]. Today this so-called Negri bodies still serve as one of the criteria for the *post mortem* diagnosis of rabies and it is known now that they present aggregations of randomly oriented RV nucleocapsids [178].

3.2. The Rabies Virus: Structure, Genomic Organization and Cellular Cycle of Infection

3.2.1. Taxonomy

The RV has a non-segmented, negative-sense, single-stranded RNA genome, which is encapsidated in an enveloped helical nucleocapsid. According to these features it was classified by the International Committee on Taxonomy of Viruses within the order of the *Mononegavirales* to the family of the *Rhabdoviridae* [305], which comprises beside four others the two genera Vesiculovirus and Lyssavirus. The latter summarizes seven genotypes (GT): type I refers to the classical RV, whereas GT II (Lagos bat virus; LBV), III (Mokola virus; MOKV), IV (Duvenhage virus; DUV), V (European bat lyssavirus 1; EBLV 1), VI (European bat lyssavirus 2; EBLV 2) and VII (Australian bat lyssavirus; ABLV) are outlined as RV related viruses (RRV). Recently, new isolates from Central Asia, East Siberia and the Caucasian region are under discussion to represent four more GT: Aravan [16], Khujand [218], Irkut and West Caucasian bat lyssavirus [217].

Lyssaviruses and vesiculoviruses are similar in their structure and their protein functions. Initially, the majority of the knowledge about rhabdoviruses was gained by extensively studying the animal pathogenic vesicular stomatitis virus (VSV), which serves as the prototype for this family. In many areas these findings are transferable on RV, but there are also some striking differences, which define unique characteristics of the lyssaviruses leading to a slow, progressive disease in the case of rabies in contrast to the acute, self-limiting disease caused by VSV. In the following description of the structure and function of RV, it was tried to cite RV specific references wherever available.

3.2.2. Virion Structure

Analysis by electron microscopy shows that the rabies virions are on average about 180 nm long and 75 nm wide with a rod- or bullet-like shape. This feature is shared by all rhabdoviruses, hence the name (*rhabd-*: rod, rodlike).

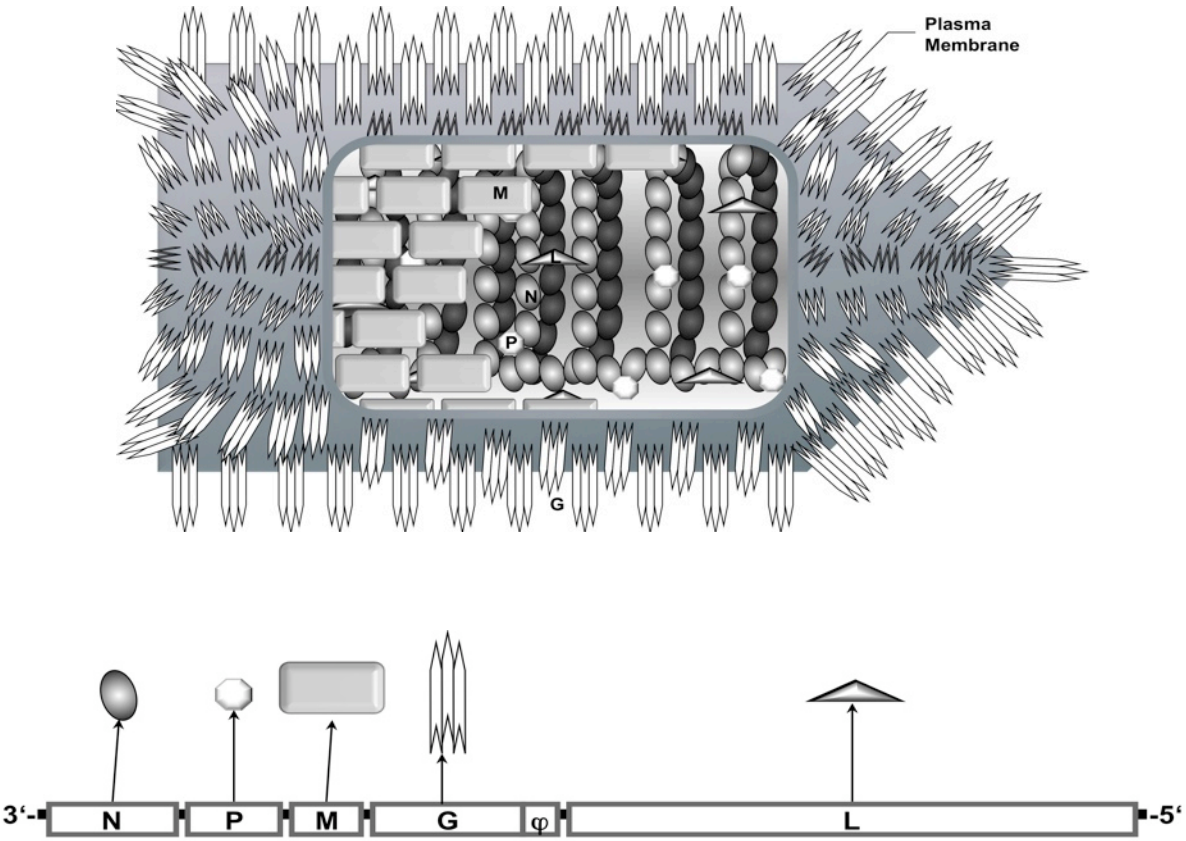

Fig. 1: Schematic presentation of a laterally opened rabies virion (top) and the RV genome (bottom).

The genomic RNA (gRNA) molecule contained in each virion is about twelve thousand nucleotides long. It encodes for five monocistronic messenger RNA (mRNA), which are translated into the following structural proteins: a nucleoprotein (N), a phosphorylated protein (P), a matrix protein (M), a glycosylated transmembrane protein (G) and a large RNA-dependent RNA polymerase (L) (Fig. 1). A stretch of about four hundred bases at the 3‘ end of the G gene is not translated. Based on the flanking sequences it has been speculated that this is a further functional gene, which is called pseudogene (φ). A function for this sequence has not been identified yet. Upstream of the coding region for the N protein is a leader sequence of about sixty nucleotides, which might be important for the regulation of replication and encapsidation of the viral genome [399, 400]. The 5‘ end of the genome consists of seventy bases, which are not translated (trailer sequence). The genomic RNA is tightly encapsidated by N proteins, of which each has contact with nine RNA nucleotides [7]. The N-RNA-polymers form a right-handed helical chain of about one thousand and five hundred N proteins with fifty-three protomers per helical turn by strong hydrophobic interactions [346]. Together with approximately eight hundred P and fifty L proteins, this structure makes up the ribonucleoprotein (RNP) core of the virion. Genetic information is

accessible only in this complex and naked RNA cannot be used as template for transcription or replication. Hence, it is suggested to prefer the term 'RNP genome' in this context instead of 'RNA genome' [33]. The about one thousand four hundred M proteins in each virion build the connection between the RNP core and its host-derived envelope, which is penetrated by up to six hundred G protein homotrimers [129, 383].

3.2.3. Cellular Cycle of Infection

3.2.3.1. Adsorption

In order to replicate, the virus needs to enter a susceptible cell (see Fig. 2: 1 Adsorption). It is proposed that the G proteins on its surface play a crucial role for the adsorption by interacting with specific receptor molecules in the host cell membrane, thus defining the tropism of RV [273]. Several molecules are under discussion as possible targets for the virus-cell recognition event, among them the low-affinity neurotrophin receptor p75NTR [221, 367], the neuronal cell adhesion molecule NCAM [355] and the nicotinic acetylcholine receptor nAChR [226, 231]. The first two suggested molecules are neuron specific which would provide an explanation for the neurotropism of RV, one of its hallmark features. nAChR is especially expressed on the postsynaptic membrane of motor end plates, hence the most common site affected by RV after violent contact with a rabid animal [378].

All three suggested molecules, however, cannot satisfactorily explain the infection *in vivo*. The receptor p75NTR, for example, fulfills an important role in the development of the nervous system by providing a key for nerve growth factors into neurons and serving as a transport vehicle from the axon terminal to the cell soma. However, it is rarely expressed in adults, usually only if axonal injury or other pathologic situations in the CNS occur. Thus, although it was convincingly shown that the trimeric RV G can interact with p75NTR [221, 367, 368], it does not seem conclusive that this receptor constitutes the main entry port into cells for RV *in vivo* [187].

NCAM belongs to the immunoglobulin superfamily and exists in three isoforms on the cellular surface, especially concentrated in presynaptic membranes in axon terminals and neuromuscular junctions, where it is involved in synaptogenesis and the synaptic vesicle cycling [321]. Its location and ubiquitous expression in the adult nervous system makes NCAM a promising candidate for the role as RV entry receptor. *In vivo* studies with NCAM knockout mice, however, revealed, that NCAM cannot be the sole responsible molecule, since

death by RV infection was only delayed but not prevented and the spread into and within the CNS was not reduced in all regions [355] when compared to RV infected control mice.

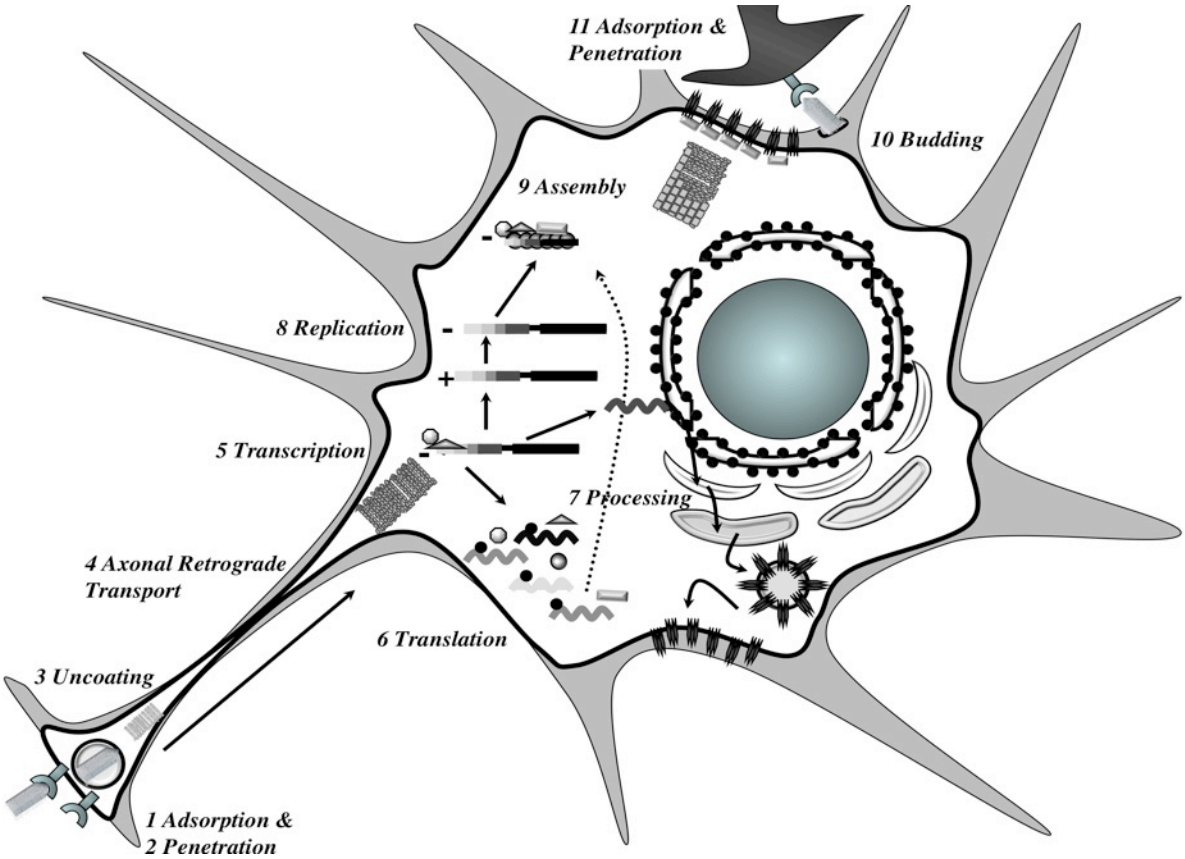

Fig. 2: Cellular cycle of RV infection.
Presentation not true or consequent to scale. See text for details.

The third molecule under discussion, nAChR, is a ligand gated ion channel built of different combinations of five out of seventeen possible subunits (α1-10, β1-4, γ, δ, ε) dependent on the site and time of expression. The amino acid (aa) sequence of RV G from aa 170 to 255 is homologous to the snake venom α-bungarotoxin, which can bind to α1 and α7-10. It was shown that the viral G protein, too, is able to interact with these nAChR subunits [126, 227] and behaves as an antagonist [150]. The cell recognition by RV is best studied on the nAChR α1 subunit, which is present only at the postsynaptic membrane of neuromuscular junctions [56, 63, 225, 226, 231, 361]. Thus, nAChR could provide the means to concentrate virus particles in the synaptic cleft between muscle fiber and motoneuron axon terminal and to facilitate the uptake into the nerve fiber. However, this cannot explain the neuroinvasive nature of RV by itself. In the CNS, the predominant alpha subunit is α4, which does not bind α-bungarotoxin. The same is true for α2-3 and α5-6, which are also present in the brain. However, it could be shown for at least one alpha subunit in the CNS, which does

not interact with the snake venom, to be susceptible for RV binding [224]. In general, the interaction of RV G with nAChR variants in the CNS has not been really consequently studied. Most nAChR molecules concentrate in the presynaptic membrane to mediate modulation of the excitability of neurons and the release of other neurotransmitters. Cholinergic innervation is sparse but broad, from the brain stem through the rostral diencephalon to the telencephalon. Both features make the nAChR a more conclusive candidate for allowing the virus to spread within the CNS rather than to directly enable its invasion at a peripheral site. The other α-bungarotoxin sensitive nAChR subunits α7-10 are mainly distributed at non-synaptic sites in the CNS, which makes them less likely to play a role during RV infection, since the virus is preferentially taken up at synapses [134], but they can be found also on non-neuronal cells like endothelial cells and lymphocytes throughout the body [58, 204, 382].

However, in *in vitro* studies, cells of a broad range of types and species origins are susceptible for infection, independent of the expression of p75NTR, NCAM or nAChR, which favors the assumption that RV is able to enter cells also by a ubiquitous receptor [312]. In this context it is hypothesized that carbohydrates, phospholipids and gangliosides might also serve as G protein interaction sites [85, 351, 397].

Taken together it remains still elusive, which molecule holds the key role for RV to get access to peripheral nerve fibers and if there are differences between the peripheral invasion of neurons and the transneuronal spread within the CNS. It is likely that not only several interaction partners for RV are decisive for the susceptibility of a certain cell type, but that also the intracellular environment presents an important determinant for the success of the infectious processes.

3.2.3.2. Penetration & Uncoating

After adhesion to the cell surface, studies suggest that the virus is ingested rather by adsorptive endocytosis with involvement of clathrin pits and clathrin coated vesicles [230, 232, 350] than by direct fusion of the viral envelope with the cellular plasma membrane (Fig. 2: 2 Penetration and 3 Uncoating). Superti *et al.* and Lewis *et al.* showed in the three cited articles that early after uptake, virus co-localizes with endosome markers and the release of RNP is mediated by the acidification of the endosomal compartment through proton pumps. Fusion of the viral envelope and the vesicle membrane is observed at an intravesicular pH

below 6.5 with maximal fusion activity at pH 6.15 [319]. The pH shift leads to the conformational transition of RV G into a fusion-active state [266], which is reversible [131]. This conformation is in a pH dependent equilibrium [128] with a fusion-inactive state at low pH values during its modification in the golgi network and its vesicular transport to the plasma membrane [130], and a fusion-inactive state at neutral pH on the cellular and viral surface. For VSV it could be shown that a stretch of fourteen amino acids of the membrane-proximal ectodomain of G is essentially required for the fusion process [194, 195].

3.2.3.3. Intraneuronal Transport

In order to get access to the neuronal protein synthesis machinery and to be able to replicate, RV has to be carried from the site of uptake to the cell soma (Fig. 2: 4 Axonal Retrograde Transport). Therefore, RV needs to utilize cytoskeleton mediated cellular transport through the neurite since its transport can be prevented by chemically inhibiting the microtubule network [60, 362]. It was observed in several studies with fixed RV strains *in vitro* as well as *in vivo* that the preferred direction is retrograde, which is achieved by the dynein mediated transport along axonal microtubules [205, 206, 353, 372]. Nevertheless, there are some studies indicating that an anterograde transport might occur, too, which could be a strain dependent feature or restricted to the spread within the CNS [88, 134, 366].

The actual mechanism of RV transport has been only vaguely elucidated yet. It was observed that not all endosomes containing virus are acidified, thus, the virus could be transported either within endosome-like organelles or as naked RNP cores, or both [62]. The P protein of RV features a binding site for the light chain of dynein (LC8), a motorprotein involved in the retrograde transport of vesicles along microtubules [190, 309]. In the past years, some researchers proposed the direct interaction between RV P and LC8 as the most likely transport mechanism for RV, since LC8 has two binding sites, with which it could bridge between the RNP core and the motorprotein. Recent findings however clearly exclude this possibility by revealing that this would contradict thermodynamic principles [388]. In addition, own work and that of others could show that virions lacking the LC8 binding site forfeit some of their pathogenic potential *in vitro* as well as *in vivo*, but that they are nevertheless still able to invade the CNS from peripheral sites [261, 352]. Indeed, the reason for this attenuation lies rather in the diminution of the *de novo* transcriptional activity of the virus [352]. The fact that LC8 is incorporated in rabies virions indirectly supports that it might facilitate primary transcription after transition into another host cell [190, 309].

In summary, although it could be shown that an intact microtubule and actin network is an essential prerequisite for RV transport [246], the mechanisms for RV neuroinvasion from the periphery into the brain and within the CNS have not been understood yet.

3.2.3.4. Viral Protein Synthesis

Like all viruses, RV depends on the protein synthesis machinery of its host cell to produce progeny virions. The RV RNA genome however is not directly accessible for transcription by the cellular machinery since it consists of a single negative-stranded RNA. Therefore, all members of the order *Mononegavirales* bring their own RNA-dependent RNA polymerases (L, for large protein), which transcribe the genomic minus RNA strand into subgenomic, non-overlapping mRNA molecules [30] (Fig. 2: 5 Transcription).

In the past, extensive studies analyzed the transcription and translation processes of VSV. Here, three molecules of P proteins interact as non-catalytic co-factors [33, 104] with one L molecule [148] to form the active transcriptase complex [96], which is associated with the RNP core [153]. Beside elongation, for which the presence of P proteins is essential [96], the L protein also polyadenylates the mRNA on their 3' end [32, 103] and catalyzes their 5' capping [34, 147, 159].

The five monocistronic genes are separated from each other by short sequences. These genome segments consist of a stop signal, seven uracils serving as template for mRNA polyadenylation, an untranscribed intergenic region (IGR) and a conserved start signal for the subsequent gene. The IGR contain variable sequences and differ in length, increasing in nucleotides (nt) in the 5' direction (N/P: 2 nt; P/M: 5 nt; M/G: 5 nt; G/L: 24 – 29 nt) [86, 87, 359]. This arrangement leads to a differential attenuation of transcription of the downstream lying genes [116]. For VSV it was shown that, after transcription is initiated by the genomic promotor in the 3' leader sequence, the less product is synthesized during the sequential downstream directed synthesis of the individual mRNA [315], the farther 5' a particular gene is located [183, 376], based on the additive probability for the L protein to be dissociated from the protein-RNA complex and to fail at reinitiation at one of the gene separating genome sequences [183]. Thus, the gene order and the resulting 3'-5'-gradient of transcripts mirror the ratio of required amounts of the five viral proteins to form functional progeny [26, 119].

The achievement of an optimal - and not necessarily maximal - protein synthesis is also important in order to preserve cellular functions, which are needed for virus amplification and

transcytotic transport of infectious particles. Also, it is favorable for the virus to avoid provoking a host immune response, for example by displaying too many RV G trimers on the cell surface, which lead to apoptosis and present the major immunogenic RV constituent [109, 274].

Beside the gene expression gradient, the M protein takes over an important role in transcription regulation by acting as a strong endogenous inhibitor [182]. For VSV it is suggested that the downregulating properties of its M protein [65, 82] are based on an ionic strength dependent interaction with the RNP core [392] by inducing a conformational change in RNP from an extended, accessible structure to a highly compact form. Thus, the elongation of the nascent RNA chain is prevented [98]. The M protein not only inhibits viral mRNA synthesis, but also host gene expression. Glodowski and colleagues [137] confirmed the observation made earlier by Lyles and others [249] that VSV M protein can migrate into the nucleus, and identified two nuclear localization signals in its amino acid sequence, of which one was involved in the inhibition of the nucleocytoplasmic transport of the host cell. For RV, an inhibitory effect on host cell translation was recently shown, involving a protein-protein interaction between RV M and the transcription factor eIF3 [210].

After translation of the processed mRNA into proteins realized by free ribosomes in the cytoplasm, RV N, P, M and L are ready to be assembled into new virions. In contrast, the RV G amino acid chain is produced by ribosomes bound at the endoplasmic reticulum and subsequently glycosylated in the Golgi network before being inserted into the cellular plasma membrane (Fig. 2: 6 Translation and 7 Processing).

3.2.3.5. Replication

The L polymerase has to switch from the mode, in which it recognizes internal gene start and stop sites, to a mode, in which it ignores those signals in order to produce full-length RNA genomes for the virus progeny (Fig. 2: 8 Replication). Several potential regulatory mechanisms for this functional transition of the L protein are under discussion. For example, studies on VSV suggested that the ratio of plus-strand leader RNA, which is the first product during the serially transcription of the genome [27, 81] and neither polyadenylated nor 5' capped but phosphorylated at the 5' end [80], as well as available N protein [19] play major roles for the change of mode. After synthesis in the cytosol, RV and VSV N proteins are chaperoned by P proteins [255] in order to be kept in a soluble, reactive form [95, 256]. The N

protein binds preferentially to the positive sense leader sequence [212]. While the RNA binding motif of VSV and RV N proteins has affinity to all kinds of RNA, the specificity for the viral leader RNA is realized by the P protein [254, 294, 399]. For RV as well as for VSV, the encapsidation signal is probably an adenin-rich stretch within the first thirty nucleotides of the leader RNA [49, 50, 399].

Unlike in VSV, not only the nominal phosphoprotein P but also RV N is phosphorylated [345]. It has been shown that free or P-complexed RV N protein is unphosphorylated and binds with high affinity to the newly synthesized positive sense leader RNA [400]. Only then it is phosphorylated, which leads to a weaker protein-RNA interaction [203]. This conformational change may make it easier for the L polymerase to access the RNA template and favor transcription as well as replication [396, 400]. The actual trigger for the functional switch of the L protein from a transcriptase to a replicase is currently not known. A prerequisite however is that enough N proteins are available to enable the encapsidation of newly synthesized full-length positive-strand RNA [19, 294]. It was shown for VSV that the production of complementary RNA is mechanistically linked to the polymerization of preformed N-P and P-L complexes [1]. Gupta and coworkers [148] argue that this also includes the reorganization of the polymerase complex from a L-$(P)_3$ structure to a N-P-L unit.

Further factors may influence the switch from transcription to replication. For VSV it was shown that the P protein has different phosphorylation states during transcription and replication which regulate the differential functions of the L polymerase [179, 293]. Also, the presence or absence of certain host proteins that bind to the viral protein-RNA complex could play a role [52, 93, 97, 216]. Most recently, the impact of RV M for the regulation of transcription and replication was discovered. Finke and colleagues found out that the M protein is not only the major factor for the suppression of gene expression, but concurrently also stimulates replication [117]. They were able to attribute this function, which is also very important for the host cell survival as described above, to an arginine residue at position 58 [115].

When the replicating polymerase arrives at the 5’ end of the negative-stranded genome, it does not interrupt at the 5’ gene border of the L gene as it does during transcription, but it also replicates the 5’ terminal, which is in part complementary to the 3’ end. Thus, like the

leader RNA of the negative sense genome, the cRNA genome possesses a strong promotor at its 3' end that finally initiates the synthesis of encapsidated negative-stranded progeny genomes.

3.2.3.6. Assembly & Budding

Already during the transcription of viral proteins, the assembly of new virions starts with the formation of N-P- and L-P-complexes, and proceeds later with enwrapping the nascent cRNA and RNA genomes by these complexes (Fig. 2: 9 Assembly). The assembling process was mostly studied on VSV. Here, the M protein plays the most crucial role for the next steps. Most of the available M proteins reside in the cytoplasm [76] in order to completely cover the RNP cores [263] which leads to the shut down of viral transcription by condensation of the nucleocapsids into the compact form found in native virions [98, 284, 289]. In addition, Barge and coauthors suggested that the rod-like shaped M molecules also build an inner scaffold around which the helical RNP coils [38, 39].

In case of VSV, the interaction between RNP and M protein cannot be initiated by the cytoplasmic M pool. In fact, the M molecules have to undergo specific structural changes to become able to bind to RNP and to enable the association of further M proteins [192, 247]. The RNP-M complexes then migrate to the plasma membrane, with which a smaller share of available M proteins – probably in a different chemical or conformational state – is already tightly and specifically associated [76, 77]. This happens preferentially at sites where viral G proteins are concentrated, to which the M proteins reversibly bind [248]. The association with the inner leaf of the membrane is realized by two sites in the highly charged basic N-terminus of the VSV M amino acid chain, of which one interacts through electrostatic forces and the other one stably integrates into the membrane by a hydrophobic loop [77, 127, 401]. For VSV as well as for RV, the membrane associated M proteins are essential for the stable interaction of the RNP cores with the membrane and spike proteins during the process of viral egress [259, 263]. The M molecules possess an intrinsic budding activity independent from all other viral proteins, causing the evagination of the plasma membrane and releasing exocytotic vesicles [201, 235] (Fig. 2: 10 Budding). Nevertheless, efficient viral budding is also promoted by RV G [262]. Particularly in the case of VSV, the membrane-proximal stem of the G ectodomain, that is thought to induce the curvature of the membrane at the initial stage of budding [193, 318], is necessary for this process.

The final steps in the release of infectious particles are probably an interplay between viral and host cell proteins. Craven and colleagues identified a conserved prolin-prolin-prolin-tyrosin (PPPY) motif in the N terminal of the VSV M protein [89], which serves as a so called late domain for effective cell-virus – pinch-off, by interacting with tryptophan-tryptophan (WW) domains of cellular proteins [156, 193]. As one of the possible players in this context the membrane-localized ubiquitin ligase Nedd4 was identified. Indeed, it was confirmed that the M protein is ubiquitinated and that free ubiquitin is important for efficient budding [155]. How this mechanism works exactly and if other host proteins are also required for an optimized viral egress has still to be further elucidated.

After budding from the neuronal cell membrane, it is assumed that the nascent virions diffuse across the synaptic cleft and adsorb at the presynaptic membrane of the adjacent neuron (Fig. 2: 11 Adsorption and Penetration). Thus, the cycle is closed and starts over in a new host cell.

3.3. Rabies Virus Replication at Peripheral Sites

On the level of the infected host, RV follows a certain path through the body during its life cycle within the host (Fig. 3). The virus invades the neural network from the site of entry and amplifies in the perikaryon of the first neuron before traversing a synapse to an adjacent neuron and ascending further into the CNS. It is thought that its spread into the limbic system, especially the amygdala, causes a change of attitude, resulting in an aggressive, fearless behavior. Correlating with the time point of its appearance in these CNS structures is the occurrence of infectious particles in the saliva of the infected animal. Both features are prerequisites for the propagation of the virus into a new host. Beside the well-documented replication in neurons, the possible ability of RV to infect and to produce progeny in other cells along its way through the organism is always a topic under discussion, which this chapter aims to summarize.

3.3.1. Muscle Tissue

Although it is widely accepted that its neurotropism is one of the hallmark features of RV, different groups provided evidences for a first round of viral amplification directly at the entry site, namely in muscle tissue. Murphy and Harrison and their coworkers observed rabies

virions budding from plasma membranes and intracellular membranes of striated muscle fibers by electron microscoping muscle tissue of i.m. infected hamsters [154, 279]. In the same direction points a study from Charlton and Casey, who noticed RV in muscle tissue of street RV infected striped skunks (Mephitis mephitis) previous to its detection in the CNS [68]. Later, Charlton hypothesized that myocytes at the entry site might present a mean for the virus to persist in an organism during the occasionally long incubation periods, since he was able to detect viral RNA in muscle tissue by reverse transcription polymerase chain reaction (RT-PCR) even two months after infection [72].

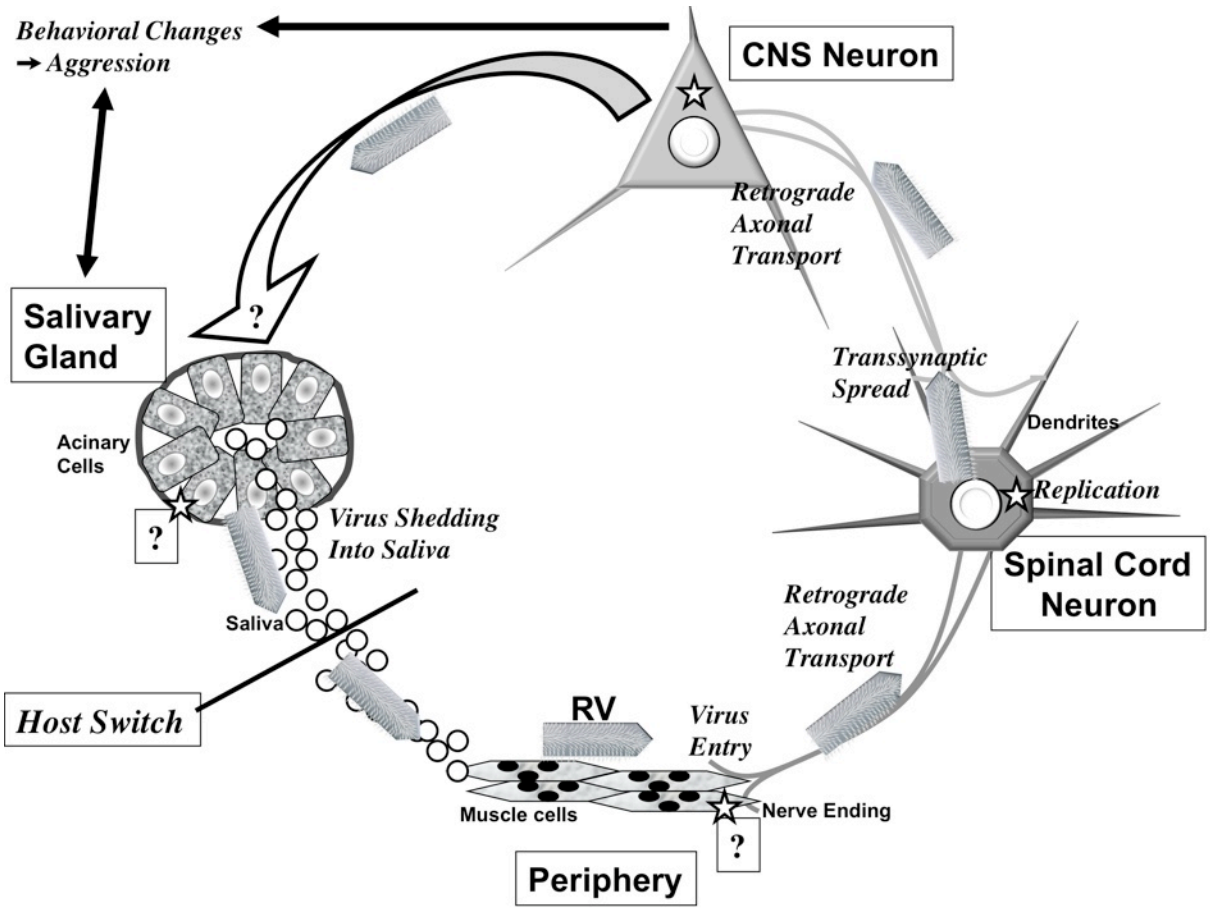

Fig. 3: The infection cycle of RV in an organism.
RV invades the body from the periphery. An initial round of replication in muscle cells at the inoculation site is under discussion. Virions penetrate the nervous system at axonal terminals and are retrogradely transported to the perikarya in the spinal cord. After replication, the nascent virions spread across synapses into adjacent neurons and reach the brain, where the infection is widely and rapidly dispersed. How the virions exactly get to the salivary gland and if another cycle of replication occurs there in acinary cells is still unclear. Virus shedding into the saliva correlates timely with the exhibition of aggressive behavior, leading to a host switch by transmission of RV within the saliva by a bite.

The susceptibility of myocytes to RV correlates with its ability to bind to α-bungarotoxin sensitive nAChR α1 subunits, which are found only in the plasma membranes of muscle fibers [63, 226]. Lentz and others investigated this topic *in vitro* with co-cultures of

spinal cord neurons and chick myotubes, which are embryonic muscle fibers that carry nAChR with a special subunit composition. In this developmental stage, the receptors are still equally distributed over the cell surface and not only concentrated where the nerve fibers come in contact with them. They inoculated these co-cultures with the mouse adapted laboratory RV strain challenge virus standard (CVS) and observed that the virus is adsorbed preferentially at neuromuscular junctions, timely followed by the presence of virions in synaptic vesicles in nerve terminals. In addition, RV was also taken up by the myotubes via receptor mediated endocytosis all over the cell surface [231].

On the other hand, Tsiang and colleagues reported more than ten years earlier that, although CVS invades myotubes (which originated from rat in this case), viral replication is abortive and non-infectious particles are released [363]. Street RV, in contrast, was not only able to infect myotubes but the inoculum was also successfully amplified in these cells [361]. This shows that the results in such studies are highly dependent on the RV strain that is used in the specific experimental set-up. Most researchers choose to use different strains of CVS for their experiments, which in general lead to negative findings regarding the replication in muscle fibers. Coulon and coworkers, for example, stated that the CVS strain enters motor as well as sensory fibers of mice directly without prior amplification in muscle [88] and Johnson found that the lethal outcome of the infection cannot be prevented by removing the injection site contemporarily to the inoculation [198]. Nevertheless it was shown that, although CVS does not amplify before entering the neuronal network, the virus is able to spread back from the CNS to the muscle later during the disease progress and replicates in myocytes only then [292, 334, 378].

In summary, though tried to elucidate for a long time, it is still not clear, if viral multiplication in muscle fibers at the entry site is only a possibility or an obligate stage in the infection cycle of RV, since it was not studied in consequent experimental settings. Neither embryonic myotubes nor laboratory adapted or attenuated RV strains can be regarded as appropriate means to clarify the importance for RV to replicate at the entry site.

3.3.2. Salivary Glands

Similar to the findings for RV replication in myocytes, the question of a final round of viral multiplication in the salivary glands before being released from the current host's body is also a topic under discussion and thought to depend on the virus strain, the host species, and

the time point within the disease progress. The topic has been mostly studied in street RV infected striped skunks, where the submandibular gland was found to be the most affected among the salivary glands [71, 176]. The same was found to be true also for rabid raccoons [395]. Balachandran and Charlton observed virions in skunks and foxes budding from mucous cells of the submandibular gland as well as from interstitial neurons and their processes [25]. This is in accord with the findings of Li *et al.* in human tissue, but only less than fifty percent of the salivary glands that they examined showed RV at all [236].

It seems that in RV infected humans the tongue plays a more prominent role as viral output tissue than the salivary glands. RV can be detected there in a much higher load, involving myocytes, serous glandular cells, nerve fibers as well as epithelial cells including taste buds from which virus shedding could be a possible alternative to the release from salivary glands [189, 236]. Another unsolved problem in this context is how the virus actually reaches the salivary glands, since they are only innervated by sympathetic and parasympathetic fibers. Virus migration from the CNS to the periphery along these pathways would contradict the dogma of an exclusively retrograde virus transport. A more logical way would be the re-infection of the visceromotor nerve fibers of the salivary glands by virus particles that were released from superficial taste bud cells of the tongue, which are sensorily innervated. However, there have been no further studies in the past to elucidate this issue.

3.3.3. Solid Organs

It has been noticed for several host species that RV can be detected in various organs in the periphery late during the disease progress. Balachandran and Charlton, for example, found street RV in naturally infected striped skunks and red foxes in chromaffin cells of the adrenal medulla [25]. Also, in experimentally infected mice RV spreads centrifugally from the CNS and can be demonstrated by polymerase chain reaction (PCR) from the tenth day on after inoculation with a dog-derived street RV in lungs, liver, spleen, kidney and urinary bladder [237].

Immunohistochemical analyses, in order to clarify the exact localization of RV within these tissues, have been realized mostly for human organs. Jogai and coworkers could show that RV resides mainly in nerve plexus that innervate the capsules and walls of solid organs such as the gastrointestinal tract and the heart, but they detected it also in pancreatic acinus cells as well as in cells of the adrenal medulla [197]. Similar findings were reported by

Jackson *et al.*, but in contrast to Jogai and colleagues they also verified virus in myocardial fibers. Also, instead of the exocrine part of the pancreas they rather saw the endocrine Langerhans islets to be affected [189].

That viral particles in these solid organs are indeed infectious has not been assessed by experimental set-ups yet, but became unfortunately clear in 2004 and 2005, when several people developed rabies symptoms after having received organs from two donors which were not recognized to have died of an encephalitis caused by RV [160, 268]. If the involvement of peripheral organs happens purely by chance or if the presence of virus at these sites has any impact on the disease progress has not been satisfactorily assessed in the past.

3.3.4. Other Non-Neuronal Cells

It was demonstrated by *in vitro* experiments that both attenuated and street RV strains infect primary cultures of murine macrophages as well as murine and human macrophage-like cell lines [310]. The infection of activated murine lymphocytes and of the human lymphoblastoid Jurkat T cell line was also shown [354]. Baratawidjaja was able to verify the infectivity of leukocytes originating from rabid rabbits by transferring them intracerebrally (i.c.) into mice [37].

In general, the accessibility of blood cells for RV infection seems to depend on the virus strain, the time point along the disease progress as well as on the level of differentiation and activation of the potential host cells. The acute biological significance of RV viremia, however, is questionable. Ray *et al.* as well as Thoulouze *et al.* suggest that the persistence and slow replication in blood cells could propose a possible explanation for the sometimes rather long incubation periods *in vivo*.

Beside the cell types listed above, there are other which are incidentally found to be susceptible for RV, among them microglia and astrocytes [311, 365] as well as hair follicles and cells of the epidermis [25, 189]. Nevertheless, neuronal cells have been proven so far to show always a greater predisposition to RV and a greater aptitude to sustain viral growth than any non-neuronal cell under investigation.

3.4. Bat-Derived Rabies Virus Strains

Bats are the most abundant and geographically most widely distributed non-human mammals worldwide [132] and they present excellently adapted hosts for viruses and other disease agents. Up to date, sixty-six viruses have been isolated from bats all over the world [64], among these all officially accepted lyssavirus genotypes (GT I to VII) except MOKV (GT III) [374]. Five of twelve examined European and eleven out of twelve North American bat species are lyssavirus reservoirs [84]. Based on the sequence of the N protein, bat RV in the Americas is assigned to GT I, the classical RV [341], while the bat associated strains in Europe (EBLV 1 and 2), Africa (DUV and LBV) and Australia (ABLV) are phylogenetically distant [54, 55, 120, 140].

With regard to the many variants of RV and RRV that bats are suitable hosts for, it surprises that there is only one genotype, namely GT I, that shares terrestrial as well as aerial epidemiologic cycles, and that this is only common in the Americas, but not on any other continent. In Europe, for example, three of the seven genotypes are endemic. Each, however, is restricted to its preferred natural host species: GT I in foxes and raccoon dogs, GT V and VI in the insectivorous bats *Eptesicus serotinus* respectively *Myotis dasycneme* and *Myotis daubentonii* [11, 342]. Although experimental host crossover is possible [377] and bat RV is distributed throughout the entire territory in contrast to the localized appearance of the terrestrial RV variants [53], natural spill over infections are very rare [278]. Also, adaptation to new hosts has not been observed.

Human infections with RRV strains resemble indistinguishably the clinical picture caused by GT I lyssaviruses. Therefore all encephalitic disorders caused by RV and RRV are summarized as rabies. Indeed, most indigenous human rabies cases in areas, where canine rabies is under control or not present at all, originate from bat-derived viruses [213, 286]. In Europe for example, EBLV 1 (GT V) and EBLV 2 (GT VI) have caused two lethal infections each since 1977 [245, 281, 332]. In Australia, ABLV is responsible for two human deaths since its discovery in fruit bats in 1998 [151, 325]. In North America, more than fifty percent of the human rabies cases since 1950 have been bat-related, mainly due to RV strains that are endemic in the solitary living insectivorous silver-haired bat, *Lasionycteris noctivagans*, and eastern pipistrelle, *Pipistrellus subflavus*, although rabid bats account only for approximately seventeen percent of all registered rabies cases in animals [79] and encounters with them are

usually rare. Fortunately it could be shown that current human diploid cell culture vaccines, that were developed against GT I, also neutralize other viruses from GT IV, V, VI and VII [57, 219, 220]. These genotypes are summarized as phylogroup I based on the similarities of their G protein sequences and the cross-reactivity of the VNA that are induced [23, 328, 387]. In addition, bat-related lyssavirus strains showed only relatively low virulence: when primary isolates of North American big brown bats, European bats and African DUV-1 were experimentally inoculated in mice, cats and dogs, most of the peripherally inoculated animals survived [112].

That bats might present special RV and RRV reservoirs becomes clear, when studies are evaluated that analyzed the proportional level of virus contamination in bat populations and the related lethality. Fifteen percent of examined bats in North America are RV positive [291], the rate of RV-caused deaths within bat populations, however, is not known. In a case of natural infection of a *Rousettus aegyptiacus* bat colony in a Danish zoological garden, even seventy-five percent of the animals tested positive for the presence of RNA of the a variant of EBLV 1, but the bats did not show any symptoms and only about seventeen percent of examined brains were positive in the standard fluorescent antibody test, confirming an active infection [381].

Amengual and colleagues observed two colonies of insectivorous *Myotis myotis* bats in Spain for over twelve years and reported also that on average about a third of the bats were seroconverted against EBLV 1, although all captured animals were apparently healthy and survived at least one year after seroconversion was registered. From seventeen dead bats, that they collected and examined, fluorescent antibody tests of all brains were negative, but RNA could be detected in two animals (brain in one bat; heart and tongue in the other animal). The group stated that bats recover from EBLV infection and develop a degree of immunological protection to future infections. Thus, low or non-productive infections in bats, which do not modify their mortality rate, seem to be normal, and lyssavirus contamination within a colony proceeds towards a stable equilibrium [10, 333].

In summary, this compendium indicates that bats as hosts as well as the RV and RRV strains that they harbor have special features that characterizes them in a unique way and distinguishes them from lyssaviruses endemic in other species.

4. Problem Statement

There is still a very high number of annual human deaths caused by RV which implies that more effort has to be invested to further elucidate epidemic cycles and to identify molecular events during infection and replication of lyssaviruses in order to find new ways for prevention and treatment of this ancient disease. The recent occurrence of rabies in tissue transplant recipients and the emerging infections with bat-related RV and RRV on six continents with an often cryptic virus transmission have re-introduced rabies onto the up-to-date list of topics in infectious biology research.

The most common mode of RV transmission is the bite of a rabid animal, mostly a canine, where infectious particles from the saliva of the animal are introduced deep into muscle tissue of the victim. In areas where terrestrial rabies is under control, transfers through bat bites and scratches are the rule. Due to the small teeth of some bat species such events are often unrecognized and only a low number of virions is introduced rather superficially into the body of the new host.

In both cases, the virus can have access to lymphatic and blood vessels and spread throughout the organism. While the effects of this hematogenous distribution might be masked after inoculation of a large amount of infectious particles into the muscle due to the high accessibility to peripheral nerve fibers, it might play a role after introduction of only few virions, and also after organ transplantation.

The current investigation was undertaken to find answers for the following questions:

1. Is RV able to spread to various peripheral organs *via* the vascular route? Is this postulated route strain dependent?

2. Can RV primarily replicate in organs? Are there differences in target cells for primary and secondary infection of organs?

3. Does RV originating from organs ascend into the CNS?

To maximize viral dissemination throughout the body on non-neuronal pathways, mice were inoculated into a tail vein and compared to i.m. inoculated mice. A dog-derived classical (DOG4) as well as a bat-derived non-classical (rSB) RV were used in the experiments, representing the two GT I RV strains with the largest impact in naturally occurring human rabies.

5. Materials & Methods

5.1. Animals and in vivo Experiments

5.1.1. Mice Strains

Six-to-eight-week old female Swiss Webster mice were purchased from NCI-Frederick Animal Production Area (Frederick, MD, USA) or Taconic Farms (Germantown, NY, USA). They were kept in the animal facility of the Thomas Jefferson University (Philadelphia, PA, USA) in groups of five mice per cage with food and fresh water *ad libitum* and controlled air pressure and humidity. From arrival in the facility until the beginning of an experiment, mice were allowed to acclimate for at least one week.

5.1.2. Infection and Observation of Mice

For i.m. inoculation virus-containing 1xDPBS (Dulbecco's Phosphate-Buffered Saline; Mediatech, Herndon, VA, USA) was injected into the right gastrocnemius muscle under isoflurane anesthesia.

For i.v. inoculation, mice were also anesthetized. In addition, they were restrained in a special plastic tube, which allowed dilating the blood vessels by warming up the tail with a mouse tail illuminator (Braintree Scientific, Braintree, MA, USA). After injection of the viral particles into one of the tail veins, the vein was treated with a cautery device (World Precision Instruments, Serasota, FL, USA) to minimize viral spread into the surrounding tissue.

Mice were monitored and scored daily for disease symptoms such as hind leg paralysis, seizures and the reduction of food and water intake. The progress of disease was categorized into six stages:

- 0: healthy
- 1: ruffled fur
- 2: negative trunk curl test (see below)
- 3: one-sided hind leg paralysis
- 4: two-sided hind leg paralysis

- 5: moribund.

The individual scores were averaged in groups for each day and the resulting curves analyzed using the Kruskal-Wallis one-way analysis of variance (ANOVA) on ranks with the Dunn's multiple comparison test to look for differences in dependence on inoculum size or infection route.

Also, the appearance of the mice and their performance in diverse tests were rated with points and the results summed up for each mouse to get a more differentiated pattern, especially since not all groups under investigation developed paralysis:

- Appearance of fur: somewhat disheveled fur was evaluated with one point, an obviously ungroomed and considerably disheveled appearance with two points.
- Piloerection: if most hairs were standing on end, one point was added to the profile of the mouse.
- Trunk curl test: the animal was held on its tail above a surface. Failure of stretching all four limbs was recorded as negative (one point).
- Reaching reflex: the mouse was held on its tail above a platform and approached towards it. Failure of reaching out towards it before the whiskers made contact with it was noted as negative. For reaching out upon contact of the vibrissae with the platform one point was assessed, two points for reaching out upon nose contact and three points were assigned if no reaction was observed.
- Grasp strength: the animal was seated onto the cage grid and pulled back slightly. An only moderate, but still effective grip was rated with one point, a semi-effective, slight grip with two points, and the total absence of active resistance against the applied force was counted as three points.
- Preyer reflex: a clicking noise was made about 30 cm above the head of the mouse. If the animal jumped in reaction to the sound, no points were recorded; if it showed only a backwards flick of the pinnae (Preyer reflex), it got one point, and two points if a response was totally missing.

- Tactile stimulus: the whiskers were touched cautiously with the handling forceps to assess if the mouse reacted with a head turn in direction of the stimulus or not (one point).

This parameter catalogue led to individual point profiles from 0 to 14. The data were averaged and analyzed in the same way as the data obtained with the clinical score from 0 to 5. For both methods, mice which died naturally due to the infection were rated with the maximum score value (5 respectively 14 points). Mice were sacrificed by neck dislocation as soon as a weight loss greater than fifteen percent than the weight on day zero (beginning of the experiment) was noticed, or at the end of the observation period.

Differences in body weight between day zero and selected time points were normalized and analyzed using two-way ANOVA with Bonferroni's multiple comparison test.

Survivorship in the mouse groups was compared using Kaplan-Meier's (log-rank) survival analysis.

All statistic analyses were done with GraphPad Prism 4.0 software (GraphPad Software, San Diego, CA, USA).

5.1.3. Tissue Harvest

Solid tissue for RNA isolation was immersed into an appropriate amount (1 ml per 100 mg tissue) of RNAlater RNA Stabilization reagent (Qiagen, Valencia, CA, USA) immediately after harvest from the mouse body according to the manufacturer's recommendations and stored at 4°C for maximal four weeks until further processing.

Tissue determined for immunohistochemical analysis was immersion-fixed in 4% buffered formalin or Bouin Hollande fixative for twenty-four to seventy-two hours (depending on the type and size of tissue) and washed with 70% isopropanol afterwards.

- 4% buffered formalin: 100 ml 37-40% formaldehyde solution - 6.5 g Na_2HPO_4 - 4.0 g NaH_2PO_4 - ad 1 l ddH2O - filtered and stored at 4°C
- Bouin Hollande stock solution: 25 g copper-II acetate - 60 g picric acid - ad 1 l ddH_2O - filtered and stored at 4°C for at most four weeks
- Bouin Hollande fixative: 100 ml Bouin Hollande stock solution - 10 ml 37-40% formaldehyde solution - 1 ml acetic acid

Tissue from which infectious particles were intended to be isolated was put promptly onto ice and processed within hours.

Tissue from mice which were infected with a recombinant green fluorescent protein-(GFP-) expressing RV was bathed in 1xDPBS after harvest and thinly sliced with a scalpel. The section was placed on a microscope slide, moistened with 1xDPBS and squeezed under a cover slip. The preparations were analyzed immediately with a fluorescence microscope.

Murine blood was drawn by heart puncture with a twenty-gauge syringe under isoflurane anesthesia before sacrificing the animal by neck dislocation. To prevent coagulation, syringe and collection tube were flushed with 8% ethylenediamine tetraacetic acid (EDTA). Blood intended for RNA isolation was kept on ice and processed further within few hours. Blood for serological tests were kept on ice until centrifugation for ten minutes at 16,000 x g. The serum was transferred into a fresh tube and kept at 4°C until analysis.

5.2. Cells and their Cultivation

All cells were kept in 37°C/5% CO_2 incubators in a humidified atmosphere. They were all adherent cell lines and grown in T75 cell culture flasks (BD Biosciences, San José, CA, USA). Every three to five days, cells were washed with 1xDPBS and detached by addition of trypsin-supplemented versene (Mediatech). After inactivation of the enzyme/chelator mixture by addition of fetal bovine serum (FBS; Mediatech) containing cell culture media, cells were split in a ratio of one to ten and seeded into a new cell culture flask.

- trypsin/versene solution: 10 ml trypsin (2.5% in Hank's Balanced Salt Solution) - 100 ml versene (0.48 mM EDTA)

Neuroblastoma (NA) cells from A/J mouse origin were grown in Roswell Park Memorial Institute medium (RPMI) 1640 (with L-glutamine) medium (Mediatech) supplemented with Penicillin-Streptomycin (Mediatech) and 5% heat-inactivated FBS (RPMI-5).

- RPMI-5: 500 ml RPMI 1640 with L-glutamine - 25 ml heat-inactivated FBS - 50,000 U penicillin G - 50 mg streptomycin sulfate

BSR cells, a derivative of the baby hamster kidney cell line BHK-21 [326], were grown in glucose, L-glutamine and sodium pyruvate containing Dulbecco's Modification of Eagle's

medium (DMEM; Mediatech) supplemented with 10% heat-inactivated FBS and penicillin-streptomycin (DMEM-10).

For the recovery of infectious particles from plasmids encoding the full-length sequence of recombinant RV, BSR cells were used which were stably expressing the bacteriophage T7 RNA polymerase (BSR-T7 cells). These cells were cultivated the same way as BSR cells, but with the addition of 1 mg/ml G418 sulfate (Mediatech) every third passage as selection antibiotic [59].

- DMEM-10: 500 ml DMEM with glucose - L-glutamine and sodium pyruvate - 50 ml heat-inactivated FBS - 50,000 U penicillin G - 50 mg streptomycin sulfate

5.3. Molecular Biological Methods

5.3.1. Restriction Digest of DNA

All restriction endonucleases used in this study for the site-specific digest of vectors and PCR products were purchased from New England Biolabs (NEB, Ipswich, MA, USA). Reactions were set up according to the manufacturer's recommendations regarding buffer (provided with the enzymes), supplementation of bovine serum albumin, amount of enzyme units per µg DNA, incubation temperature and duration.

5.3.2. Agarose Gel Electrophoresis

Gels made of 1% agarose in 1x tris-acetate-EDTA (TAE) buffer, dissolved by microwaving and poured into horizontal casting forms, were used to separate DNA fragments in dependence of their length. A comb in the gel chamber provided wells in the cooled, polymerized agarose to fill in aliquots of DNA for analysis. Before loading, the DNA was mixed with loading solution (fivefold concentrated) in the correct ratio. Electrophoresis was carried out at 10 V/cm in 1xTAE buffer supplemented with the fluorescing DNA intercalator ethidium bromide (100 ng/ml) in order to visualize and document the DNA bands in the gel afterwards by ultraviolet (UV) light and digital photography. As length standards, a 100 bp ladder and a 1 kb ladder, purchased from NEB, were used.

- 1x TAE: 40 mM Tris/HCl, pH 8.0 - 40 mM sodium acetate - 1 mM EDTA
- loading solution (5x): 30% glycerol - 0.25% bromphenol blue - 0.25% xylene cyanol

5.3.3. Determination of Concentration and Purity of Nucleic Acids by Photometry

DNA and RNA in aqueous solution were quantified by photometrical analysis at 260 nm. Knowing that 50 µg double-stranded DNA or 40 µg RNA in 1 ml solution lead to an extinction of 1.0 at this wavelength, their concentration can be calculated. To assess for the grade of proteinaceous contamination, the extinction at a wavelength of 280 nm was measured, too. The purity of the nucleic acid solutions was regarded as acceptable, if the ratio between the absorption at 260 nm and at 280 nm was above 1.5 (DNA) or 1.7 (RNA) respectively.

5.3.4. Gel Purification of DNA Fragments

To isolate DNA fragments from an agarose gel after electrophoresis, the desired band was excised with a scalpel using only weak UV light for visualization to decrease the risk for mutation generation. The DNA was separated from the agarose by a spin column kit (PerfectPrep Gel Cleanup, Eppendorf, Hamburg, Germany) according to the manufacturer's manual. First, the DNA-containing agarose slice, weighing maximal 400 mg, is dissolved in a chaotropic solution (3 µl per milligram gel) at a temperature of 50°C, and then mixed with isopropanol (1 µl per milligram gel) before placing the solution into a spin column. Up to 10 µg DNA binds to the glass fiber membrane in the column and can be washed then with the ethanol containing wash buffer to purify it from salts, organics, ethidium bromide and other contaminating molecules. DNA was eluted with 50 µl molecular biology grade water and stored at –20°C.

5.3.5. Alternative Purification of DNA Fragments from Enzymatic Reactions

Up to 20 µg of DNA from restriction analysis, dephosphorylation or polymerase chain reactions were purified with the IsoPure PCR purification kit (Denville, Metuchen, NJ, USA) following the protocol provided by Denville. The enzymatic reaction to be purified is mixed with three volumes of the kit's binding solution and incubated for two minutes at room temperature in the spin column to ensure complete binding of the DNA to the silica-based membrane. The bound DNA is washed then twice with an ethanol-containing wash solution before elution with 50 µl molecular biology grade water. If DNA molecules bigger than ten

thousand base pairs, such as plasmid vectors, were purified, the column was incubated five minutes at 50°C instead of two minutes at room temperature before the final centrifugation step. DNA was stored at –20°C.

5.3.6. Dephosphorylation of Linearized DNA by Calf Intestine Phosphatase

To avoid re-ligation, linearized vectors were treated with calf intestine phosphatase (NEB), which removes 5' end phosphate groups. Reactions were set up and incubated according to the manufacturer's recommendations.

5.3.7. DNA Ligation

In order to connect restriction endonuclease digested DNA molecules or to insert a DNA fragment into a linearized vector, the reaction partners were incubated with T4 bacteriophage ligase (NEB), which catalyzes adenosin-tri-phosphate dependent a covalent phosphodiester bond between the 5' phosphate end of one fragment and the 3' hydroxyl group of another fragment – provided the compatibility of the restriction endonuclease generated ends of the DNA fragments. The molar ratio between the reaction partners is especially important, if a small insert has to be ligated into a relatively big vector. Since a three- to sevenfold excess of the smaller fragment is recommended, several 20 µl-reactions were usually set up in parallel with different ratios according to the manufacturer's protocol. The reactions were incubated overnight at 16°C.

Ligation reactions could be used as template for polymerase chain reactions (PCR) or for transformation into *E. coli* bacteria without prior purification.

5.3.8. Non-quantitative Polymerase Chain Reaction

In a PCR a heat-stable DNA polymerase I supplements a single-stranded DNA molecule to double-stranded DNA and amplification of the template molecule is carried out by repeating a sequence of specific temperatures - provided that a short double-stranded section is present. This is achieved by two oligonucleotides, so-called primers, which are complementary to either one of the DNA strands, and bind to it at a specific annealing temperature (T_a). Two different DNA polymerases were used in this study, mainly for cloning strategies: the $Vent_R$ DNA polymerase (NEB) with a temperature optimum of 72°C, and the Platinum Taq DNA Polymerase High Fidelity (Invitrogen, Carlsbad, CA, USA), which works

best at 68°C. Both polymerases have an integral 3'-5' proofreading exonuclease activity and elongate primed DNA in the presence of a sufficient amount of desoxynucleoside triphosphates (dGTP, dTTP, dCTP, dATP) at a rate of thousand bases per minute. To be able to ligate DNA fragments independent from endogenous restriction sites, 5' overhang oligonucleotides were used to prime the PCR amplification, which introduced suitable restriction sites upstream of the amplified DNA molecule. For the PCR reaction set-up and the cycling conditions, the instructions provided with the polymerases were taken as guidelines. In general, one amplification cycle consists of the following steps:

1) denaturation of double-stranded DNA: 30 sec at 94°C

2) annealing of the primer molecules: 30 sec at primer pair specific temperature (see below)

3) strand elongation: 60 sec per thousand bases at 68°C (Taq) / 72°C ($Vent_R$)

Usually, thirty cycles were completed and the annealing temperature for the used primer pair was calculated as follows:

$$T_a = [(T_{m\ primer\ 1} + T_{m\ primer\ 2}) / 2] - 5°C$$

with primer specific melting temperature Tm

$$T_m = 4°C \bullet (n\bullet G + n\bullet C) + 2°C \bullet (n\bullet A + n\bullet T)$$

n•G, n•C, n•A, n•T:

number of each of the four nucleotide types in the primer sequence

If a PCR reaction with 5' overhang primers was carried out, the annealing temperature for the first five amplification cycles was calculated by ignoring the non-binding part of the primer molecules, followed by twenty-five cycles with an annealing temperature considering the complete oligonucleotide sequence.

5.3.9. Transformation of Chemically Competent Bacteria with Recombinant DNA

Chemically competent *E. coli* (DH5α and JM109) were purchased from Promega (Madison, WI, USA) and transformed with plasmids by a heat shock: either 11 µl of a 20 µl-

ligation reaction or 4 ng of plasmid DNA were mixed with 80 µl (DH5α) or 50 µl (JM109) ice-cold bacteria and kept on ice for twenty-five minutes, before being transferred to a 42°C warm water bath for fifty seconds. After another two minutes on ice, 200 µl SOC media (Invitrogen) were added and the bacteria were incubated at 37°C for forty-five minutes. The sequence of all vectors used in this study include a gene for ampicillin resistance, which allowed the selection of positive clones by spreading the transformed *E. coli* onto ampicillin-containing lysogeny broth (LB) agar plates, which were kept upside-down overnight at 37°C. Clones that were transformed with plasmid DNA were further cultivated in a liquid LB media overnight in a shaker at 37°C for a large-scale DNA preparation. Clones from a transformation with a ligation reaction were analyzed by a small-scale DNA preparation and restriction digest analysis first, and only positive clones were used for a successive large-scale DNA preparation.

- LB broth: 25 g Miller's LB broth powder (Fisher Scientific, Pittsburgh, PA, USA) - dissolved in 1 l distilled water - autoclaved for fifteen minutes at 120°C - 100 mg ampicillin trihydrate were added before use
- LB agar plates: 40 g Miller's LB broth powder (Fisher Scientific) - dissolved in 1 l distilled water - autoclaved for fifteen minutes at 120°C - 100 mg ampicillin trihydrate were added when hand warm - poured into petri dishes (ø 10cm)

5.3.10. Small- and Large-Scale Plasmid Preparation from Bacteria

For the isolation of plasmid DNA from *E. coli* liquid cultures, either the Plasmid Mini or Maxi kit from Qiagen was used, depending on the amount of DNA that was needed. The kits are based on a process that was described in 1979 [43]. Bacteria from liquid cultures are pelletized, and the cells lysed under basic conditions and sodium dodecyl sulfate, which also leads to the denaturation of DNA. In addition, RNase in the lysis buffer degrades bacterial RNA. Neutralization of the lysate enables the rehybridization of plasmid DNA molecules, since their circular conformation prevented the spatial separation of the two strands during the denaturation phase. In contrast, genomic DNA stays denaturated and can be removed by centrifugation together with most of the proteins in the lysate which are precipitated by sodium acetate included in the neutralization buffer. The supernatant that holds the plasmid DNA is then further purified over an anion exchanger column.

To analyze clones that were transformed with a ligation reaction, 3 ml ampicillin-containing LB media were inoculated with a single colony and incubated in a shaker at 37°C.

The next day, 1 ml of the bacteria suspension was then further processed with the Plasmid Mini kit according to the manufacturer's protocol. The DNA (10 – 20 µg) was eluted with 50 µl molecular biology grade water and the DNA was further analyzed by restriction digest with suitable endonucleases.

For a large-scale plasmid DNA preparation, 250 ml ampicillin-containing LB media were inoculated with a single colony from a selection plate or with 1 ml of an previously analyzed low-scale bacterial culture and kept overnight in a shaker at 37°C. Plasmid DNA was then isolated by the Plasmid Maxi kit following Qiagen's manual. The eluted DNA was precipitated with 70% isopropanol and the resulting pellet washed afterwards with 70% ethanol to remove salts. The DNA was dried and resuspended in 200 µl molecular biology grade water. Concentration and purity was measured by photometry and restriction digest analysis with suitable enzymes. Finally, the solution was adjusted to 1 mg/ml and the DNA was kept at –20°C.

5.3.11. Construction of a Recombinant Rabies Virus

The coding sequence for the G protein in the recombinant silver-haired bat RV (SHBRV) 18 strain cDNA clone cSB-0 (provided by Prof. B. Dietzschold, Philadelphia, PA, USA) was replaced by the DOG4 RV G sequence using a PCR strategy with Platinum Taq DNA Polymerase High Fidelity (Invitrogen) (Fig. 4). The DOG4 G gene was amplified with the primers RP387 and RP477M (introducing a BsiWI site at the 3' end) using a plasmid with the sequence for the DOG4 G gene as template. In addition, two fragments from the plasmid cSB-0 were amplified: one upstream of RV G, from the unique restriction site BstEII in RV M (position 3310) to the end of the IGR between RV M and RV G, using the primers RP472 and RP473b (introducing a XmaI site at the 3' end); and one downstream of RV G, from the beginning of the IGR between RV G and RV L to the unique restriction site PacI (position 6092), using the primers RP474b (introducing a BsiWI site at the 5' end) and RP475.

The three gel-purified amplicons were digested with XmaI (A1), XmaI and BsiWI (A2) or BsiWI (A3) and ligated in a single reaction. The ligation product was re-amplified using the primers RP472 and RP475. Following digest with HpaI and PacI, the column-purified amplicon was then cloned into the HpaI and PacI digested cSB-0 backbone resulting in the clone cSB-DOG4. Correctness of the construct was confirmed by sequencing (done by the

Nucleic Acid Facility of the Kimmel Cancer Center at the Thomas Jefferson University). All primers used for cloning are listed in table 1.

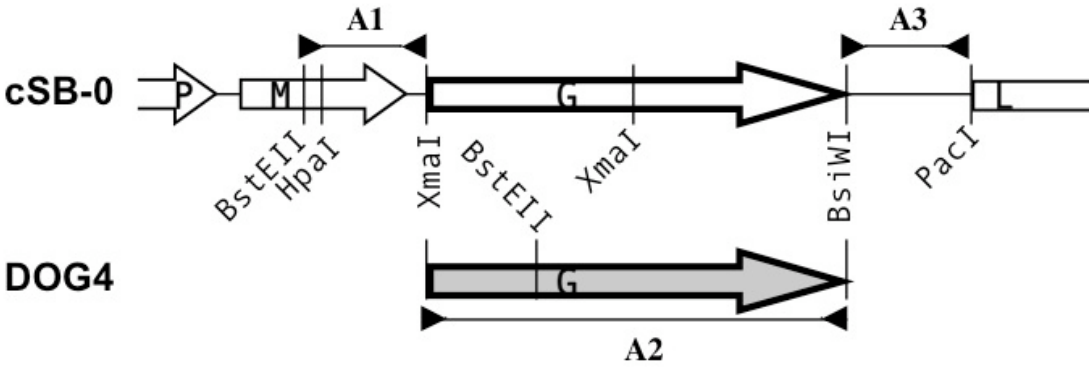

Fig. 4: Construction of cSB-DOG4.
See text for details.

5.3.12. RNA Isolation from Cells and Murine Tissue

Solid tissues that were harvested from mice were removed from the RNAlater reagent, weighed and disrupted by a handheld homogenizer with disposable probes (Omni International, Marietta, GA, USA) in 1 ml β-mercaptoethanol supplemented RLT buffer (Qiagen) per 100 mg tissue. The RLT buffer contains highly denaturing guanidine isothiocyanate, which leads to the immediate inactivation of RNases. 1 ml of the lysate was further homogenized by passing it five to ten times through a twenty-gauge syringe and clarified afterwards by centrifugation for three minutes at 16,000 x g. Total RNA was subsequently isolated from the 300 µl supernatant (representing 30 mg original tissue) according to the manufacturer's instructions using the RNeasy Mini kit (Qiagen) for brain, spinal cord, lung, liver and kidney. The addition of ethanol to the homogenate provides optimal conditions for the binding of total RNA to the silica gel-based membrane of the RNeasy mini spin columns. Contaminants are washed away afterwards by the two buffers RW1 and RPE in three spinning steps and the RNA is subsequently eluted by RNase-free water. For the RNA isolation from heart, muscle and tail, the RNeasy Fibrous Tissue Mini kit (Qiagen) was used, which differs from the described system only by an additional proteinase K digest before clarifying the lysate by centrifugation.

RNA isolation from murine blood collected by heart puncture was done immediately after harvest using the QIAamp RNA Blood Mini kit (Qiagen) according to the manufacturer's protocol. In short, erythrocytes are selectively lysed by incubation of the

whole blood with the kit's EL buffer on ice. The leukocytes that are recovered by subsequent centrifugation are lysed with β-mercaptoethanol supplemented RLT buffer as described above for the other tissues. The lysate was homogenized by centrifugation through a QIAshredder spin column. The remaining protocol is identical to that for the RNeasy kits.

RNA from cultured cells was isolated by lysing 1xDPBS-washed cells directly in the cell culture flask with β-mercaptoethanol supplemented RLT buffer. For a T75 flask, 3 ml lysis buffer were used. As described for animal tissue, the lysate was passed several times through a twenty-gauge needle to homogenize the sample, and centrifuged afterwards to clear it. RNA was extracted from the supernatant with the RNeasy Mini kit as described above, using one RNeasy-column for each 600 µl-cell lysate aliquot.

A fifteen minute on-column DNase I digest (Qiagen) was included for all samples between the wash spins. RNA was eluted with 35 µl RNase-free water and concentration and purity were measured by photometry at 260 nm and 280 nm. RNA was kept at –20°C for short term storage or transferred to –80°C if intended to use only much later.

5.3.13. Quantitative Real-time Two-Step RT-PCR Assay

In order to be able to quantify RV N gRNA and mRNA in murine tissue samples, a quantitative real-time two-step RT-PCR assay was established based on the TaqMan® method. In addition to the pair of primers used in conventional PCR to initiate complementary strand elongation, a third oligonucleotide is included in the reaction, which binds at the same temperature one of the DNA strands within the amplicon close to the forward primer binding site. The so-called TaqMan® probe is labeled with a fluorochrome at the 5' end and a quencher molecule on the 3' end, which prevents fluorescence by spatial proximity. A prerequisite for the assay is the 5'-3'-exonuclease activity of the Taq DNA polymerase I. During a combined annealing and elongation step in the cycling program at 60°C, the polymerase degrades the TaqMan® probe while generating a new complementary strand. Thus, the fluorochrome is separated from the quencher and is now able to emit light at its specific wavelength, which can be measured. With every new DNA amplicon molecule that is generated, more and more fluorochromes are released and the overall fluorescence increases proportionally. The cycle number (Ct value) at which the fluorescence surmounts a certain

threshold is determined for each sample and is the basis for the calculation of the initial template number in the reaction vessel.

5.3.13.1. Primer and Probe Design for Quantitative Real-time PCR

All primers and probes intended for quantitative real-time PCR (qPCR) were designed by the web-based program Primer3 (http://www-genome.wi.mit.edu/cgi-bin/primer/pimer3_www.cgi) using the leader and RV N nucleotide sequences of rSB and DOG4 as input. From the suggested possibilities those sets of oligonucleotides (primer pair and probe) were selected which amplified a DNA stretch shorter than two hundred base pairs and whose melting temperatures allowed a combined annealing and elongation step in the cycling program at 60°C. For the sets intended to use for the amplification of RV N gRNA, binding of one of the primers in the RV leader sequence was a prerequisite. The TaqMan® probes were labeled at the 5' end with FAM (6-carboxyfluorescent) as reporter dye and the quencher TAMRA (6-carboxy-tetramethyl-rhodamine) at the 3' end. All oligonucleotides used in this study were purchased from Operon Biotechnologies (Huntsville, AL, USA) and are listed in table 1.

5.3.13.2. Reverse Transcription

Before amplification by PCR, RNA molecules have to be reverse-transcribed into single-stranded complementary DNA (cDNA). This reaction is achieved by the RNA-dependent DNA polymerase reverse transcriptase, which is encoded in all retrovirus genomes, and has to be primed like conventional PCR. In this study, gene specific primers were used, namely the reverse primers designed for qPCR. In this way it was assured, that later only specifically either negative-or positive-stranded viral RNA was amplified and quantified.

Two microgram total RNA of all tissue and blood samples were reverse-transcribed using the Omniscript RT kit (Qiagen) and a gene-specific primer either for rSB/DOG4 RV N gRNA (RP381; 500nM) or for rSB/DOG4 RV N mRNA (RP406 and RP408 respectively; 500nM). To prevent the degradation of template RNA, ten units of the RNaseOUT Recombinant Ribonuclease Inhibitor (Invitrogen) were included in the reactions. Reverse transcriptions (RT) were carried out at 37°C for one hour and the enzyme was subsequently inactivated by five minutes at 95°C. The cDNA was stored at –20°C.

5.3.13.3. Quantitative Real-time PCR

The qPCR reactions were set up in LightCycler® capillaries (Roche Diagnostics, Indianapolis, IN, USA). Each 20 µl-reaction contained 1x QuantiTect Probe PCR Master Mix (Qiagen), 500 nM forward primer, 500 nM reverse primer, 100 nM TaqMan® probe and 200 ng of template cDNA. Reactions were performed as triplicates in a LightCycler® 1.5 instrument (Roche Diagnostics) along with a positive control triplicate and a no-template-control under the following cycling conditions: *hot start* 15 min at 95°C; *amplification* 45 cycles [15 sec at 95°C, 60 sec at 60°C]; *cooling* 30 sec at 40°C. The fluorescence of the hydrolyzed probes was measured in a single step at the end of each amplification cycle and Ct values were obtained by the second derivative method through the LightCycler® software 3.5.3 (Roche Diagnostics).

5.3.13.4. Generation of Standard Curves for Absolute Quantification of Viral RNA

To be able to transform the Ct values obtained for each sample by the LightCycler® instrument into actual numbers representing the absolute amount of initial cDNA template molecules in the reaction vessel, a standard curve from samples with known copy numbers had to be generated. For that, total RNA was isolated from rSB or DOG4 infected cells and reverse-transcribed using the Omniscript RT kit (Qiagen) and a bacteriophage T7 promotor introducing primer (RP413; 500 nM). Following PCR amplification by VentR Polymerase (NEB) with RP413 (500 nM) and a bacteriophage T3 promotor introducing primer (RP411; 500 nM), the resulting amplicon was column-purified and *in vitro*-transcribed using the MAXIscript T7/T3 kit (Ambion, Austin, TX, USA) according to the manual provided by Ambion. Transcription with T3 polymerase led to a RNA fragment containing the RV N gRNA template sequence for the primers RP381 and RP382 (DOG4) and for RP381 and RP405 (rSB) respectively, transcription with T7 polymerase to a RNA fragment containing the RV N mRNA template sequence for RP406 and RP407 (rSB) and for RP408 and RP409 (DOG4) respectively. The T3 and T7 RNA were purified by a RNeasy Mini column (Qiagen) following the additional protocol for RNA purification from enzymatic reactions included in Qiagen's manual, and the number of RNA molecules was calculated based on their concentration and the sequence-specific molecular weight of a single fragment determined by a web-based calculator (http://www.changbioscience.com/genetics/mw.html). A certain amount of T3 RNA and T7 RNA molecules (10^{11} or 10^{10}) was then reverse-transcribed in duplicates using the Omniscript RT kit (Qiagen) and either the primer RP381 (500 nM; T3

RNA) or one of the primers RP406 and RP408 (500 nM; T7 RNA). Each cDNA was serially diluted twice in tenfold steps using RNA isolated from uninfected BSR cells (0.05 µg/µl) as diluent. Subsequently, the Ct values of all dilutions from 10^2 to 10^8 molecules per reaction were determined in duplicates by qPCR as described for the tissue cDNA samples. The averages of those two duplicates per dilution step, that were closest to the average of all four duplicate averages per dilution step, were chosen as input for the table sheet program Exel (Microsoft Corp.) to determine the regression line and its equation for the correlation between Ct value and logarithm of the initial template number. The equations in the format y = slope • x + y-intercept which were finally used to calculate the initial copy numbers for every sample cDNA are:

- rSB RV N gRNA: $y = -3.3773x + 42.282$; $R^2 = 0.9998$; $E = 0.98$
- rSB RV N mRNA: $y = -3.4421x + 40.973$; $R^2 = 0.9998$; $E = 0.95$
- DOG4 RV N gRNA: $y = -3.3224x + 41.049$; $R^2 = 0.9999$; $E = 1.00$
- DOG4 RV N mRNA: $y = -3.5227x + 45.977$; $R^2 = 0.9994$; $E = 0.92$

With y = Ct value and x = lg(initial number of templates N): $N = 10^{(\text{Ct value} - \text{y-intercept})/\text{slope}}$

The R^2 value represents the strength of the linear correlation between the Ct values and the decadic logarithm (lg) of the initial copy numbers, with 1.0 being the maximum and 0 the minimum.

The efficiency E is calculated from the slope of the standard regression line

$E = 10^{-1/\text{slope}} - 1$

It is an indicator for the quality of the PCR. An optimal efficiency of 1.0 for example means that in every amplification cycle the number of present template molecules is doubled. The efficiency is mainly dependent on the primers, but is also influenced by inhibitors present in the reaction.

Table 1: Oligonucleotides used for cloning, RT and qPCR

ID	5'-3' sequence and purpose	comment
RP381	ACACCCCTACAATGGATGC rSB and DOG4 RV N gRNA: RT; reverse primer in qPCR;	rSB: together with RP405 194 bp amplicon. DOG4: together with RP382 138 bp amplicon; RV N start codon
RP382	GGGTTATACAGGGCTTTTTCA DOG4 RV N gRNA: forward primer in qPCR	
RP387	TTT*CCCGGG*AAGATGGTTCCTCAGGCTC DOG4 RV G (A2) forward primer	introducing *XmaI site*; RV G start codon
RP388	CCC*TTAATTAA*TCACAGTCTGGTCTCACCC DOG4 RV G reverse primer	introducing *PacI site*; RV G stop codon
RP405	ATTCATGCCAGACAAAATTGA rSB RV N gRNA: forward primer in qPCR	
RP406	CCCAGTCATCGGGACATGC rSB RV N mRNA: RT; reverse primer in qPCR	together with RP407 180 bp amplicon
RP407	ACCCGGCAATCAAAGACTCG rSB RV N mRNA: forward primer in qPCR	
RP408	CGTCAGTGCGCTTTATCTCCAA DOG4 RV N mRNA: RT; reverse primer in qPCR	together with RP409 174 bp amplicon
RP409	CAGGCATGAACGCTTCCAAA DOG4 RV N mRNA: forward primer in qPCR	
RP411	AATTAACCCTCACTAAAGGGACAAAAGGGGCTGTCTC	introducing T3 promotor; together with RP413 606 bp amplicon
RP413	TAATACGACTCACTATAGGGAGCAAAAATGTAACACCCCTAC	introducing T7 promotor:
RP472	TTT*GGTTACC*CCCTCCGGAG cSB-0 A1 forward primer	BstEII site
RP473b	AAAA*CCCGGG*GCTAGCTTTTCCTGAGATCCTTTGAGG cSB-0 A1 reverse primer	introducing *XmaI site*
RP474b	TTTTTAATTAA*CGTACG*AGGTGAGTCATCCCCTCC cSB-0 A3 forward primer	introducing *NheI site*
RP475	CCC*TTAATTAA*CTCCTCCATTCCAC cSB-0 A3 reverse primer	*PacI site*
RP477	CCCTTAATTAA*CGTACG*TCACAGTCTGGTCTCACCC DOG4 RV G (A2) reverse primer	introducing *BsiWI site*; RV-G stop codon
RTP-3	TACAAGTACCCGGCAATCAAAGACTCG TaqMan® probe for rSB RV N gRNA	
RTP-4	TCGACCCTGATGATGTATGCTCTTATCTAGCA TaqMan® probe for rSB RV N mRNA	
RTP-5	CAATAATCAGGTGGTCTCTTTGAAGCCAGA TaqMan® probe for DOG4 RV N gRNA	
RTP-6	TGATCCCGATGATGTATGCTCCTACTTGGC TaqMan® probe for DOG4 RV N mRNA	

5.4. Viruses and Virological Methods

5.4.1. Wildtype Rabies Virus Strains

The canine RV strain DOG4 (DRV4) was originally isolated from the brain of a human rabies victim and made available by B. Dietzschold [101]. The virus was passaged in cell culture on NA cells.

5.4.2. Recombinant Rabies Viruses

The recombinant RV vector rSB (SB0) was previously generated from the SHBRV 18 strain full-length cDNA clone pSB0 (cSB-0) as described [110] and passaged on BSR cells. The virus was provided by B. Dietzschold.

Recombinant SPBN-N2c-GFP, which consists of the backbone of the vaccine strain SPBN containing the coding sequence for the G protein of the mouse-adapted, highly pathogenic RV strain CVS-N2c and the insertion of the coding region for GFP after the G gene, was provided by M. J. Schnell. This strain was passaged on NA cells.

5.4.3. Recovery of Recombinant Rabies Viruses

Genetic manipulation and generation of infectious particles is not trivial for negative sense non-segmented RNA viruses such as RV, since i) a cytosolic RNA-dependent RNA polymerase has to be provided, ii) not the „naked“ RNA but only gRNA that is encapsulated by nucleoprotein and associated with phosphoprotein can be recognized as template, iii) gRNA cannot serve as mRNA which makes it necessary to provide all viral proteins that are required for replication and transcription of viral RNA in trans. Schnell *et al*. [330] developed a helper virus free system which fulfills all these prerequisites (Fig. 5).

Cells are transfected with transcription plasmids that encode positive sense full-length antigenomic RV RNA (cDNA clones; Fig. 5 FL). Plasmids encoding the Street Alabama Dufferin (SAD) B19 RV strain N protein (pT7T-N), P protein (pT7T-P), RNA-dependent RNA polymerase L (pT7T-L) and G protein (pT7T-G) are given in trans (Fig. 5 N, P, G, L). All coding sequences are framed by a T7 polymerase priming site and transcriptional terminator sequence. This allows transcription by the bacteriophage T7 polymerase (Fig. 5 II.), which is introduced either by another plasmid, or cells are used that stably express the enzyme (Fig. 5 I.). The support plasmids give rise to RV N and RV P proteins that encapsulate the negative-stranded gRNA, which is generated from the full-length cDNA clone (Fig. 5 FL) by the T7 polymerase (Fig. 5 light gray triangle). The newly formed RNP complexes can subsequently serve as templates for RV L, which produces viral mRNA and gRNA with the sequence of the recombinant RV (Fig. 5 IV. and V.). Virions are assembled from both SAD B19 and cDNA clone specific proteins (Fig. 5 VI.), and released into the cell supernatant (Fig. 5 VI.), which is transferred onto fresh cells. Since only the full-length cDNA clone gave rise

to the encapsulated genomes, the next generation of virions, designated as passage 1, consists only of RNA and proteins with the sequences specific for the recombinant RV.

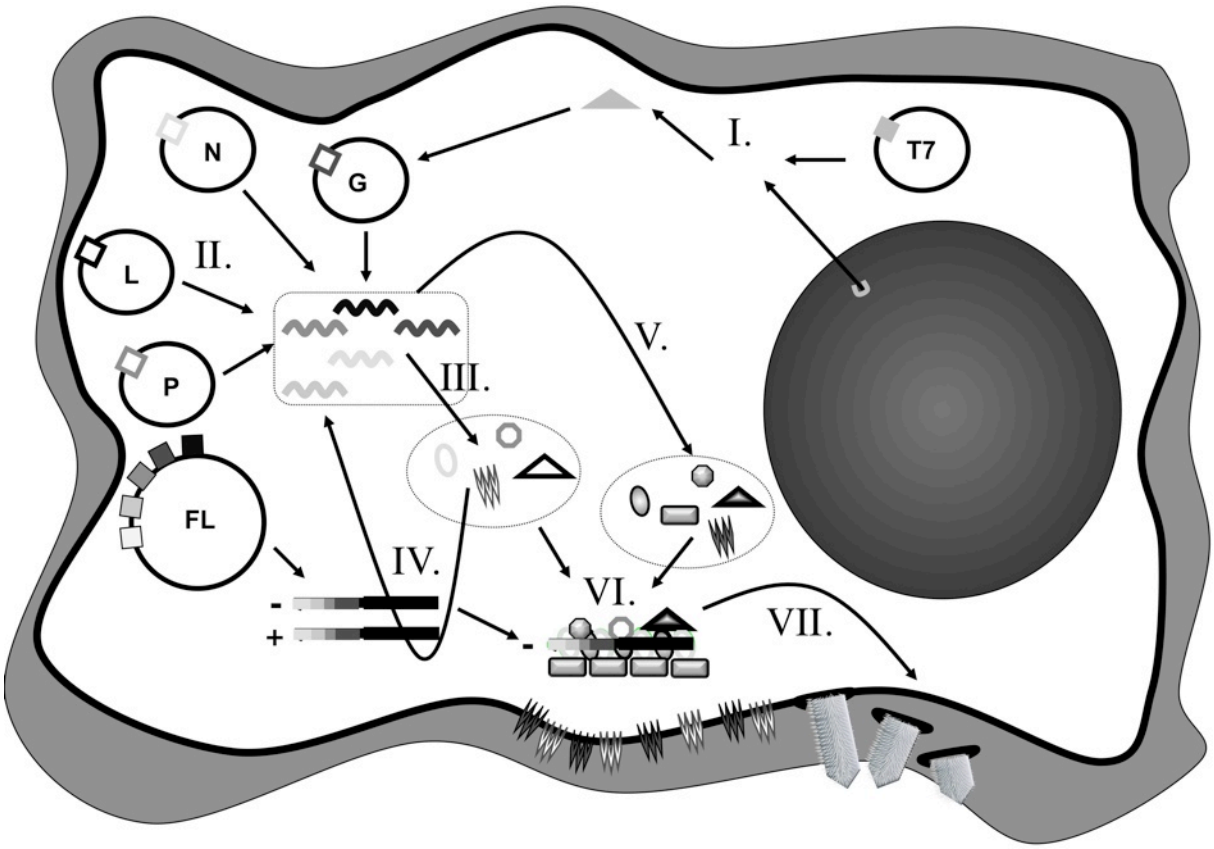

Fig. 5: Recovery of recombinant negative single-stranded non-segmented RNA viruses.
See text for details.

Infectious SB-DOG4 particles were tried to recover from the plasmid cSB-DOG4 as follows: BSR cells were seeded in six-well plates ($1.5x10^6$ cells per well) and transfected the next day with 830 ng of the full-length clone plasmid, 420 ng of pT7T-N, 210 ng of pT7T-P and pT7T-L, 170 ng of pT7T-G as well as 250 ng of a plasmid encoding the bacteriophage T7 RNA polymerase. For the transfection, FuGENE 6 transfection reagent (Roche Diagnostics) was used according to the manufacturer's recommendations. After three days at 37°C the supernatants were transferred onto NA cells, seeded the day before into twelve-well plates at a density of $6.25x10^5$ cells per well. After further three days at 37°C supernatants were saved and kept at 4°C, while the cells were washed once with 1xDPBS, fixed with 80% acetone at 4°C and checked for the presence of viral particles by immunostaining with a fluorescein-isothiocyanate- (FITC-) coupled anti-RV N protein-antibody (Centocor, Malvern, PA, USA). Cells and supernatants from passage 1 were checked by RNA isolation and sequencing of reverse-transcribed, PCR amplified genome stretches.

5.4.4. Production of Virus Stocks in vitro

In order to passage virus and to produce stocks for usage in experiments, one-day-old cells in T75 cell culture flasks, which were 80% confluent, were washed once with 1xDPBS. Virus from the previous passage was diluted in 2 to 5 ml serum-free cell culture media to achieve an inoculum that infected the cells at a multiplicity of infection (moi) of 0.1 ffu (focus forming units) per cell. The cells were incubated with the virus solution for ninety minutes at 34°C. After two wash steps with 1xDPBS, DMEM-10 or RPMI-10 – dependent on the cell line that was used – was added back and the cells were kept at 34°C for six days. On day three, the supernatant was saved and replaced by fresh media, and cleared in parallel with the second harvest on day six by centrifugation for two times ten minutes at 650 x g. Supernatants were titrated after being frozen at –80°C and only the harvest with the higher titer was saved and used for further experiments.

Virus stocks containing serum were only used for *in vitro* experiments. For the application *in vivo*, serum-free virus stocks were generated following the same procedure as described above but using serum-free OptiPRO cell culture medium (Invitrogen) supplemented with penicillin-streptomycin and L-glutamine (Mediatech) (OptiPro SFM) for viruses that were passaged on BSR cells such as rSB, and serum-free RPMI 1640 media (SF-RPMI) for viruses passaged on NA cells (DOG4, SPBN-N2c).

- OptiPro SFM: 1 l OptiPro, 100,000 U penicillin G, 100 mg streptomycin sulfate, 20 ml L-glutamine 200 mM
- SF-RPMI: 500 ml RPMI 1640, 50,000 U penicillin G, 50 mg streptomycin sulfate, 0.2% bovine serum albumin

5.4.5. Virus Titration

Viruses were titrated in triplicates on NA cells the following way: 10 µl virus solution were serially diluted tenfold in RPMI-10 in a ninety-six-well plate and about 1.9×10^5 NA cells were added to each well. After incubation for two days at 37°C, cells were washed with 1xDPBS, fixed with 80% acetone at 4°C and stained with the FITC-coupled anti-RV N antibody for at least two hours at 37°C. Fluorescing foci were counted and the average virus titers calculated from the triplicates in ffu/ml.

5.4.6. Concentration of Virus Stocks by Centrifugation

If titers of virus stocks were too low for the procedure of an experiment, the required total number of virions was spun down in an L8-M ultracentrifuge (Beckman Coulter, Fullerton, CA, USA) for one hour and ten minutes at twenty-two thousand rounds per minute (rotor SW28, acceleration 4, deceleration 4, temperature 4°C), and the pellet was resuspended in the correct amount of serum-free media to achieve the desired virus concentration, which was subsequently confirmed by titration.

5.4.7. Virus Isolation from Tissue

Tissues intended for virus isolation were weighed and sterile 1xDPBS was added to get a 20% organ suspension after disruption with a handheld homogenizer and disposable probes (Omni International). The homogenates were centrifuged for ten minutes at 1,000 x g. Subsequently, 100 µl cleared organ solution were added to a cell pellet of 7.5 x10^7 NA cells, together with 10 µg DEAE-Dextran and 100 µl SF-RPMI. After thirty minutes at 37°C, the mixture was spun down three minutes at 3,000 x g and the pellet resuspended in 1 ml RPMI-5. The cells were seeded in T25 flasks and the volume was raised to 10 ml RPMI-5. After two days at 37°C, cells were washed, fixed and stained as described for virus titration. Fluorescing foci were counted and the amount of ffu per mg tissue was calculated.

5.5. Immunological Methods

5.5.1. Determination of Virus Neutralizing Antibodies

Neutralizing activity of mouse serum was determined by using the rapid fluorescent focus inhibition test (RFFIT) as described [387]. NA cells (8 x10^4 per well) were seeded in a ninety-six-well plate and incubated at 37°C for two days. In a second ninety-six-well plate, sera were serially diluted in duplicates in threefold steps using SF-RPMI and starting with a dilution of one to fifty in a final volume of 100 µl per well. 10 µl virus at the tenfold of its individual working dilution (the dilution at which the virus infects ninety percent of cells within twenty-four hours) was added to every serum-containing well. The mixture was incubated one hour at 37°C and then transferred onto the NA cells seeded two days before after removing the old media. Twenty-four hours after infection, the cells were washed, fixed

and stained as described for the virus titration. The neutralization titer, which is defined as the inverse of the highest serum dilution that neutralizes 50% of the challenge virus, was determined for every serum and normalized to international units (IU) by using the WHO anti-RV antibody standard. Geometric mean VNA titers were calculated from individual titers in each group and statistically analyzed by the one-way ANOVA with Dunn's multiple comparison test, using the Prism 4.0 software (GraphPad Software).

5.5.2. Immunohistochemistry

Immunohistochemical staining of tissue sections was used to identify RV target cells in the periphery as well as to trace its way from the periphery respectively the vascular system to the CNS.

5.5.2.1. Silanization of Glass Slides

To guarantee a better adhesion of tissue sections, glass slides were silanized before their use. First, they were washed with dishwashing detergent in tap water for one hour and rinsed three times afterwards with hot tap water. It followed a bath in demineralized and analytic water. The clean glass slides were then washed with 70% isopropanol for forty-five minutes and dried afterwards at 60°C. After this treatment, the actual surface coating was carried out by dipping the slides in the following order: thirty seconds into 2% TESAP in acetone, twice thirty seconds into pure acetone, shortly into demineralized water, and shortly into analytic water. Finally, the slides were ready to use after drying at 42°C.

5.5.2.2. Tissue Sections

All tissues that were fixed for immunohistochemical analysis were dehydrated in an increasing isopropanol series and embedded in Paraplast Plus (Merck, Darmstadt, Germany). Afterwards, 7 µm-sections were produced by a microtome and unwrinkled in a 45°C water bath before being picked up with a silanized glass slide.

5.5.2.3. Antibodies

Table 2 lists the primary antibodies and their dilutions, which were used for the detection of proteinaceous antigens in paraffin-embedded tissue sections by enzymatic DAB/ nickel reaction or fluorochromes.

Table 2: Primary antibodies for immunohistochemical analysis of tissue sections

Antigen	Donor Species	Source	Dilution	
			DAB/nickel	fluorescence
CD3	rabbit	DAKO (Glostrup, Denmark)	1:2500	-
ChAT	goat	Chemicon (Temecula, CA, USA)	1:250	-
RNP	rabbit	B. Dietzschold	1:3000	1:300
TH	sheep	Chemicon (Temecula)	-	1:120
VAChT	goat	L. E. Eiden (Bethesda, MD, USA)	-	1:600

5.5.2.4. Information about the Detected Antigens

- The molecule CD3 is part of the T cell receptor complex and for that a marker for both types of T cells, namely αβ-T cells as well as the minor subpopulation of γδ-T cells.
- The choline acetyl transferase (ChAT) is an essential enzyme for the synthesis of the neurotransmitter acetylcholine. Thus, it is a marker antigen for cholinergic neurons such as motor nerve cells and parasympathetic neurons.
- The RNP served as a target structure for the detection of RV. Since it is mostly conserved, the used anti-RNP antibody labels the rSB as well as the DOG4 RV strain.
- The tyrosine hydroxylase (TH) is an essential enzyme for the synthesis of biogenic monoamines such as dopamine, epinephrine and norepinephrine and can be understood as a marker for sympathetic neurons.
- The transporter molecule for the neurotransmitter acetylcholine in synaptic vesicles (VAChT) flags, similar to ChAT, cholinergic neurons such as motor nerve cells, but also parts of the autonomic nervous system.

The primary antibodies were detected by either biotinylated or fluorochrome-coupled secondary antibodies, which are listed in table 3.

Table 3: Secondary antibodies for immunohistochemical analysis of tissue sections

Antibody	Donor Species	Source	Dilution
biotinylated anti-goat	donkey	Dianova (Hamburg, Germany)	1:200
biotinylated anti-rabbit	donkey	Dianova	1:200
Alexa 647-conjugated anti-goat	donkey	MoBiTec (Göttingen, Germany)	1:200
Alexa 647-conjugated anti-sheep	donkey	MoBiTec	1:200

5.5.2.5. Immunohistochemical DAB/Nickel Staining

Immunohistochemical analysis of CNS and heart tissue was done as follows: the tissue sections were deparaffinated in xylol and rehydrated in a decreasing isopropanol series. Endogeneous peroxidases were blocked by treatment with 0.1% H_2O_2 in methanol for thirty minutes. For optimal antigen retrieval, the tissue sections were treated with 10 mM sodium citrate buffer for fifteen minutes at 92 to 95°C. Successively, the tissue was incubated in phosphate buffered saline (PBS) containing 5% bovine serum albumin (BSA) to saturate free unspecific protein binding sites on the glass slides, and in the avidin-biotin blocking solutions of the Vectastain Elite ABC kit (Vector Laboratories, Burlingame, CA, USA) according to the manufacturer's protocol. Primary antibodies (table 2) were applied afterwards in 1% BSA/ PBS overnight at 16°C, followed by two hours at 37°C. Immunoreactions were detected with species-specific biotinylated secondary antibodies (table 3) by the Vectastain ABC method (Vector Laboratories), including 3,3-diaminobenzidine (DAB) (Sigma, Deisenhofen, Germany) reactions that were enhanced by ammonium nickel sulfate (Fluka, Buchs, Switzerland). The stained tissues were dehydrated again, sealed with DePeX media (SERVA Electrophoresis, Munich, Germany) and a cover slide, and finally analyzed with an Olympus AX70 microscope (Olympus Optical, Hamburg, Germany).

5.5.2.6. Immunohistochemical Double Fluorescence Staining

For confocal double immunofluorescence microscopy, tissue sections were treated as for DAB/nickel staining until the application of primary antisera, but skipping the H_2O_2 treatment. Pairs of primary antibodies raised in different donor species were added onto the tissue sections. After incubation overnight at 16°C followed by two hours at 37°C, the immunoreaction of one of the primary antibodies was marked with a biotinylated secondary antibody for forty-five minutes at 37°C. Afterwards, the sections were incubated with an Alexa 647-conjugated secondary antibody against the second of the primary antibodies, and Alexa 488-coupled streptavidin (MoBiTec) to label the biotinylated secondary antibody. After two hours at 37°C, the stained sections were covered by Fluorosafe (Calbiochem, La Jolla, CA, USA) and a cover slip, and analyzed with an Olympus Fluoview BX50WI confocal laser scanning microscope (Olympus Optical). Immunofluorescence staining was documented as digitized false-color images.

6. Results

6.1. Symptoms and Outcome of Infections in Mice after Intravenous Inoculation with a Recombinant Silver-Haired-Bat Rabies Virus Strain in Comparison to Intramuscular Inoculation

6.1.1. Concentration Dependent Survival after Intramuscular and Intravenous Inoculation

Transmission of RV into an organism by a bite or a scratch causes rupture of blood and lymphatic vessels and leads to the introduction of pathogenic particles into the vascular system. One of the aims of this study was to find out which effect the part of the viral inoculum that is distributed via the blood way has on the infection. Since previous studies were lacking an i.v. infection route it was first necessary to clarify if and how i.v. inoculation with RV would affect mice.

To assess if bat-derived RV elicits disease in mice after introduction into the vascular system, groups of ten young adult female Swiss Webster mice were inoculated into one of the tail veins with either 10^6 or 10^5 ffu of rSB. To minimize viral spread within the surrounding tissue, the vein was cauterized immediately after withdrawal of the injection needle. For comparison, the same number of mice was inoculated i.m. into the right gastrocnemius muscle, also with either 10^6 or 10^5 ffu of rSB.

It was well established in previous experiments that an i.m. infection with similar amounts of rSB causes a paralytic, lethal encephalitis. Indeed, in both groups, which were inoculated with RV *via* the ‘classical‘ route, mice got sick as indicated by weight loss (Fig. 6 A) around day five *post infectionem* (p.i.) and died within twelve (10^5 ffu) respectively ten days p.i. (10^6 ffu) (Fig. 6 B). Also, all twenty i.v. infected mice showed signs of sickness around day five p.i., but forty percent of the animals inoculated with the lower dose recovered over time and survived the twenty-eight day observation period. The last case of death in this group occurred at the seventeenth day. In contrast, all of the mice infected i.v. with 10^6 ffu succumbed to the disease until the sixteenth day. Although mice of all four groups entered the

final stage of disease between day eight and nine p.i., the progress after i.v. inoculation was less synchronized compared to i.m. infection.

Statistical analyses revealed that the infection route led to significant differences in the disease progress between the i.v. infected and i.m. infected groups inoculated with the same amount of virions in terms of body weight ($p \leq 0.001$), but that the size of the inoculum only significantly mattered if administered *via* the vascular route ($p \leq 0.001$ for i.v. versus $p > 0.05$ for i.m.).

From mice that had not died yet naturally, but were sacrificed for humane reasons because they already progressed to the final stage of the disease, blood was withdrawn from the heart and the serum was examined for VNA. The VNA titers in all accessible serum samples from mice in the final stage of the disease had already trespassed the threshold of 0.5 IU, which is considered as protective according to the information on the WHO website (Fig. 6 C). On average, the larger inoculum led to a higher titer within the groups infected by the same inoculation mode, and the i.v. infected animals developed a stronger antibody response than the corresponding i.m. infected group. However, differences were only statistically significant between the two groups infected with the lower dose ($p \leq 0.05$).

6.1.2. Differences in Symptoms after Intramuscular and Intravenous Inoculation

Beside the differences in body weight curves and outcome between i.m. and i.v. inoculation, the mice showed great varieties in accompanying symptoms. After i.m. infection, mice passed through the classical stages of experimental rabies disease. The onset of symptoms was marked by changes in the fur, from healthy-looking to a rather ruffled appearance (stage 1). Later on, the hind leg into which the virus was injected showed initial motor dysfunctions and was not stretched anymore in the trunk curl test, but mice sill used it for walking (stage 2). The complete paralysis of this leg (stage 3), which was observed in hundred percent of the mice at day seven p.i. (10^6 ffu) respectively day eight p.i. (10^5 ffu), was frequently followed by motor deficits in the other hind leg and sometimes also in the two front limbs (stage 4). In stage 3, mice were often still very mobile and agile, using only three legs for walking and ignoring the effects of the infection on their locomotor system. However, with the progress of the paralysis general disease symptoms increased, too, and the mice stopped going after food and water, even if made available on the cage ground where they

could reach it easily in spite of their restricted motility. In stage 5, the moribund mice lost severely weight due to reduction of food and water intake as well as polyuria.

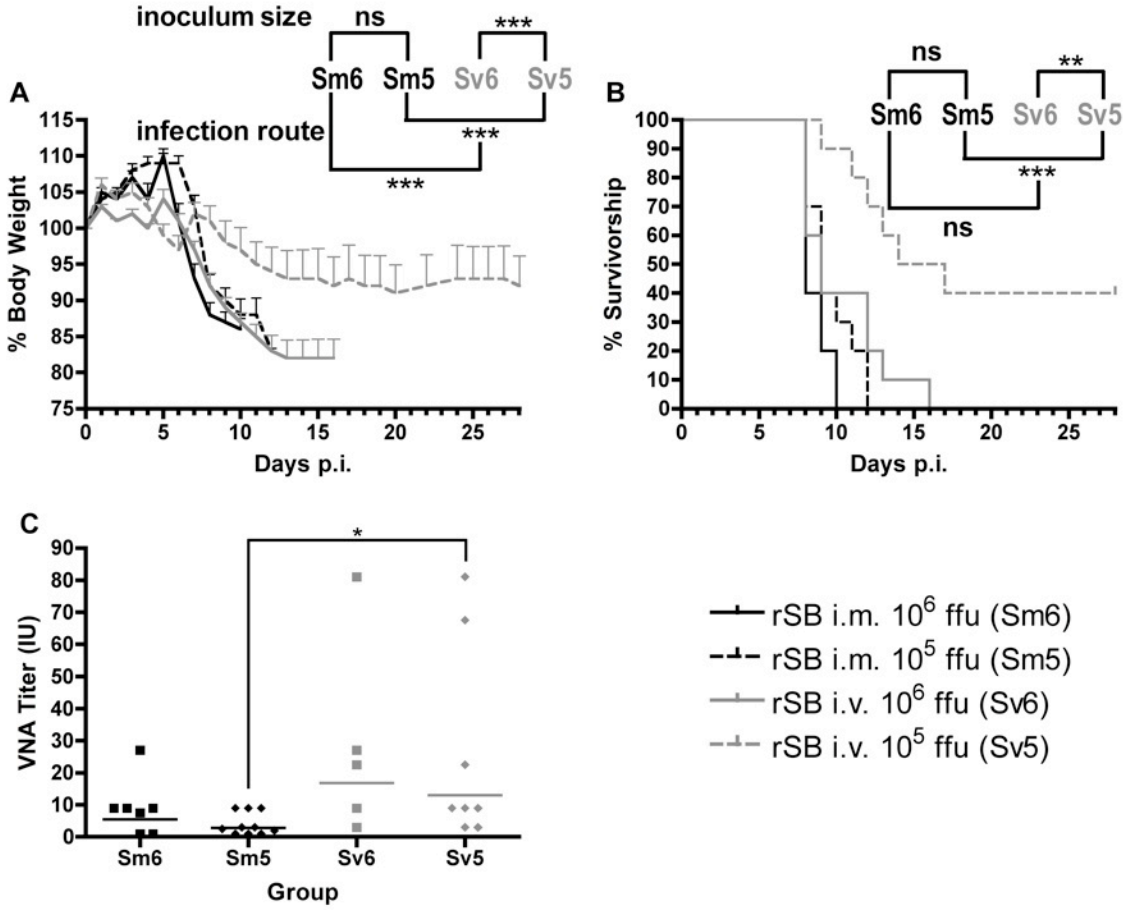

Fig. 6: Concentration dependent body weight (A), mortality (B) and VNA titers (C).
Ten Swiss Webster mice were infected i.m. or i.v. with 10^5 or 10^6 ffu of rSB. **A**: Body weight was recorded daily and normalized to the weight on day zero. Data are group average values (mean ± standard error). Asterisks indicate significant differences in the decrease of body weight in dependence of inoculum size or infection route. **B**: Percentages of surviving mice per day for each group. Asterisks indicate significant differences in the survival curves in dependence of inoculum size or infection route. **C**: If possible, blood was obtained immediately before death, and serum VNA titers (in IU) were determined. Data are presented as scatter plot with lines indicating the geometric mean for every group. (*, $p \leq 0.05$; **, $p \leq 0.01$; ***, $p \leq 0.001$; ns, not significant)

In contrast, i.v. inoculated mice never showed any signs of paralysis, but rather general sickness symptoms such as limited explorative behavior, increasing lethargy and reduction of food and water intake. These symptoms are not taken into account in the ranking from 0 to 5 (Fig. 7 A) that is usually applied to track the disease after i.m. inoculation, and mice had to be categorized constantly in stage 2 until they were moribund, although their conditions worsened continuously over time. This masks their real disease progress in the graphical

presentation and brings in artificial differences between the two inoculation routes as far as the severity of symptoms and not their quality is concerned.

In the attempt to get a more comparable representation of the disease progress, which would be valid for i.m. as well as for i.v. infected animals, another parameter catalogue was composed evaluating motor as well as sensory functions. Mice were subjected to several tests, which are described in 8.1. With their help it was possible to assess and to compare how alert an animal was by applying visual (reaching reflex), auditory (Preyer reflex) and tactile stimuli, as well as motor functions (trunk curl test, grasp strength) and the general body condition (piloerection, fur care).

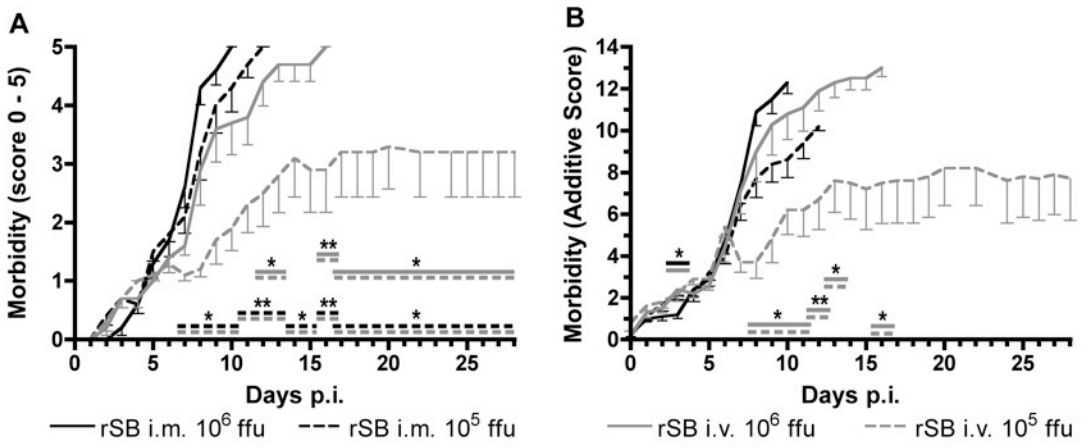

Fig. 7: Clinical score.
Ten Swiss Webster mice were infected i.m. or i.v. with 10^5 or 10^6 ffu of rSB. **A**: Clinical symptoms were rated from 0 to 5 (0, healthy; 1, ruffled fur; 2, negative trunk curl test; 3, one-sided hind leg paralysis; 4, two-sided hind leg paralysis; 5, moribund) **B**: Clinical symptoms were rated from 0 to 14 by summation of the results obtained by several tests. Data in both panels are group average values (- standard error). Asterisks indicate significant differences in the progress of symptoms in dependence of the inoculum size or infection route between one group and the corresponding other group (line format; *, $p < 0.05$; ** $p < 0.01$).

In both evaluation set-ups, the disease progress was similar fast in the two groups infected with the larger amount of virions and differences between i.m. and i.v. inoculation were more distinct for the mice that received only 10^5 ffu. While the classical score provides more artificial differences in the curves between the i.m. and the i.v. infected groups due to the rating in the progressed stages mainly based on motor functions (Fig. 7 A), the concentration dependency of the outcome of infection is better represented with the alternative parameters (Fig. 7 B). Especially, since in later stages of the disease i.v. inoculated mice also performed negative in the trunk curl test as well as in the reaching reflex, and they showed only a decent grasp strength like their i.m. inoculated counterparts. These failures,

however, were rather caused by exhaustion and general infirmness than by motor dysfunction, since they still were able to walk if motivated from exterior, for example by a stroke with a finger.

In summary, rSB causes disease in mice if administered i.v. and the major differences in comparison to intramuscular inoculation are the stronger dose-dependency and the lack of motor dysfunctions, while the disease itself progresses only slightly slower but not less aggressive.

6.2. Strain Dependency of the Outcome of Intravenous Inoculation

6.2.1. Outcome of Intravenous Inoculation with DOG4

Previous studies in cell culture already showed that bat RV strains differ greatly in some characteristics from canine strains. In order to analyze whether the ability to cause disease if administered i.v. is another feature that distinguishes classical and non-classical RV strains, or if the effects of the vascular component of i.m. inoculation is the same, six-to-eight-week old female Swiss Webster mice were inoculated i.v. with 10^6 ffu DOG4 and compared to i.m. inoculation as well as to mice infected i.v. or i.m. with the same amount of infectious rSB particles.

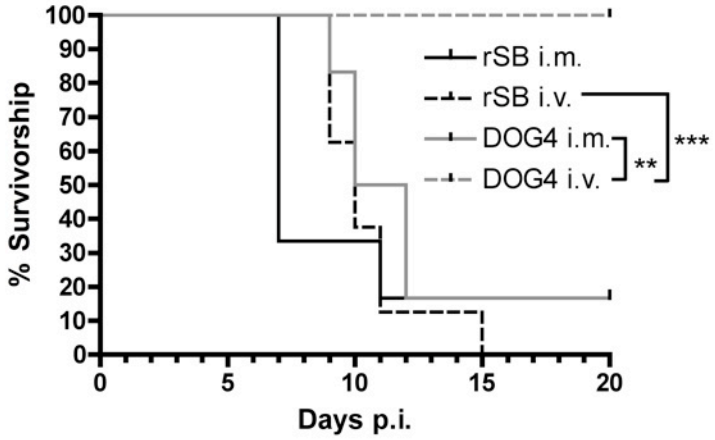

Fig. 8: Strain dependent mortality.
Swiss Webster mice were infected i.m. or i.v. with 10^6 ffu of DOG4 or rSB. The graph shows the survivorship per day for each group in percent. Asterisks indicate significant differences between curves (**, $p \leq 0.01$; ***, $p \leq 0.001$).

As expected and seen previously, ninety to hundred percent of mice infected i.m. with 10^6 ffu rSB or DOG4 died within twelve days (Fig. 8). However, while all mice succumbed to the disease after i.v. rSB infection, none of the mice got sick after i.v. inoculation with DOG4 until the end of the observation period of twenty days.

6.2.2. Strain and Infection Route Dependent Distribution of Viral Antigen in the CNS

Brain and spinal cord of one mouse from each of the four experimental groups were harvested when the mice had died (rSB i.m. day seven p.i., rSB i.v. day eleven p.i., DOG4 i.m. day twelve p.i.) or at the end of the observation period (DOG4 i.v. day twenty p.i.) and fixed in Bouin Hollande solution. Brains and spinal cords were sagittally sectioned and immunohistochemically stained against RNP.

The spinal cords of the rSB i.m. and i.v. infected animals showed a rather moderate amount of viral antigen, both with a prevalence for the ventral part (Fig. 9 B, D). In contrast, the DOG4 i.m. inoculated mouse had higher amounts of RV N in the ventral as well as in the dorsal part of the spinal cord, whereas nothing was detected for the i.v. infected mouse that was sacrificed twenty days after the inoculation. Similar observations were made in the brain of this animal, which was completely free of detectable RNP (Fig. 10 D). RV N antigen in the brain of the DOG4 i.m. infected mouse concentrated heavily on the dorsal tegmental and raphe nuclei of the midbrain (Fig. 10 C), but was also found in the deeper layers of the cortex (retrosplenial granular b cortex) dorsal of the splenium of the corpus callosum as well as in the septal nuclei, ventral of the genu of the corpus callosum. In addition, some hypothalamic areas and the reticular formation in the medulla oblongata were positive for RNP.

In contrast to the cerebellum of the DOG4 i.m. infected animal, which had only a moderate number of virus-laden Purkinje cells in the sixth cerebellar lobule, that of the rSB i.m. inoculated mouse was heavily affected and bore the main viral antigen, especially in the first to the fifth lobules. In addition, the medial layers of the retrosplenial granular b cortex were more involved, too. The tegmental and raphe nuclei in the midbrain and the reticular formation, however, showed only moderate immunoreactivity against RNP. Mostly spared after DOG4 i.m. inoculation, thalamic areas (paraventricular, central medial and reuniens thalamic nuclei) as well as the dorsomedial central gray substance of midbrain were positive for RNP after i.m. infection with rSB (Fig. 10 A).

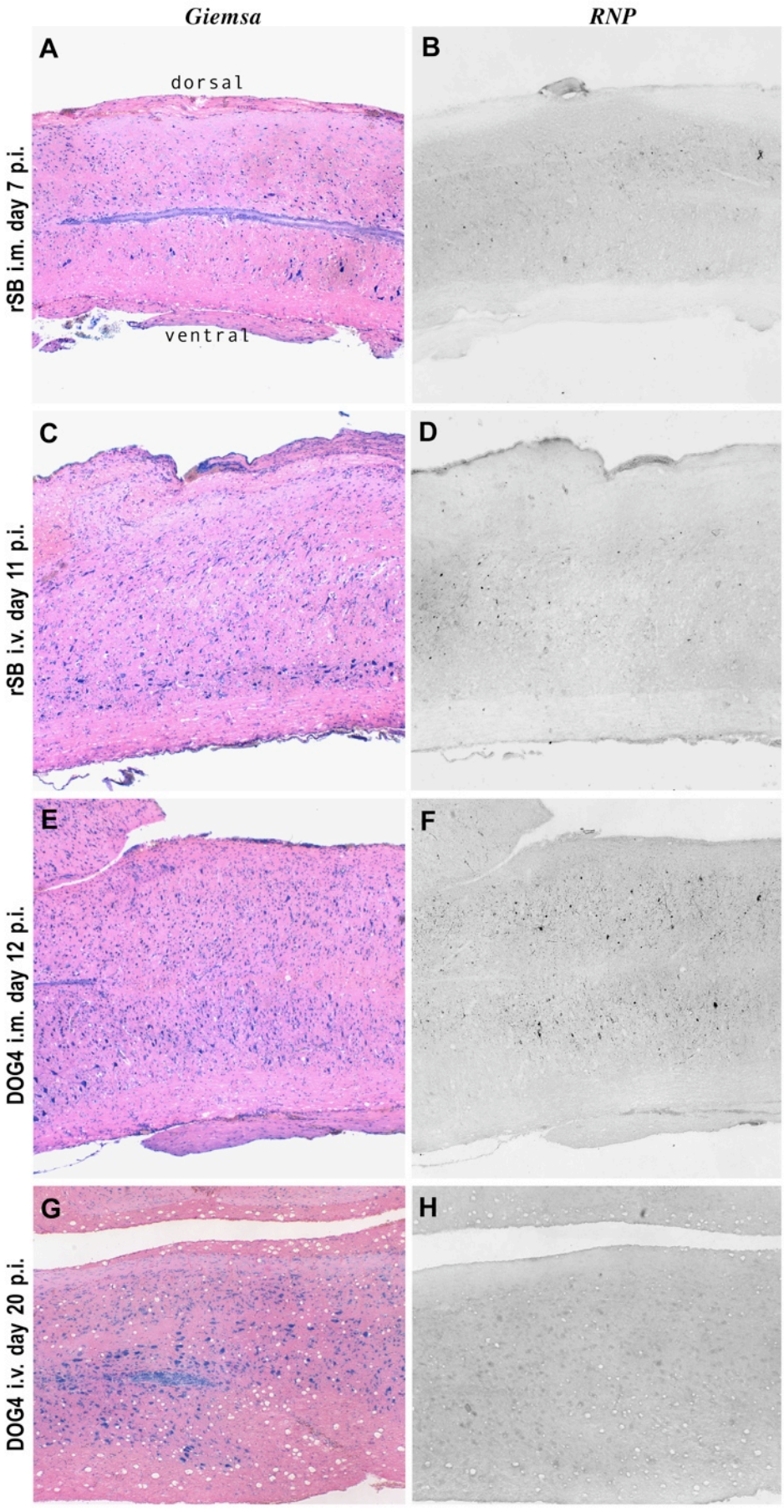

Fig. 9: Strain and infection route dependent distribution of viral antigen in the spinal cord.

Fig. 9 continued:
Spinal cords of rSB or DOG4 i.m. or i.v. infected Swiss Webster mice were harvested when the animals were moribund or at the end of the twenty-day observation period as indicated in the panels. Sagittal sections were stained with Giemsa (**A**, **C**, **E**, **G**) or immunohistochemically with a primary antibody against RNP, subsequently visualized by an enzymatic reaction (**B**, **D**, **F**, **H**).

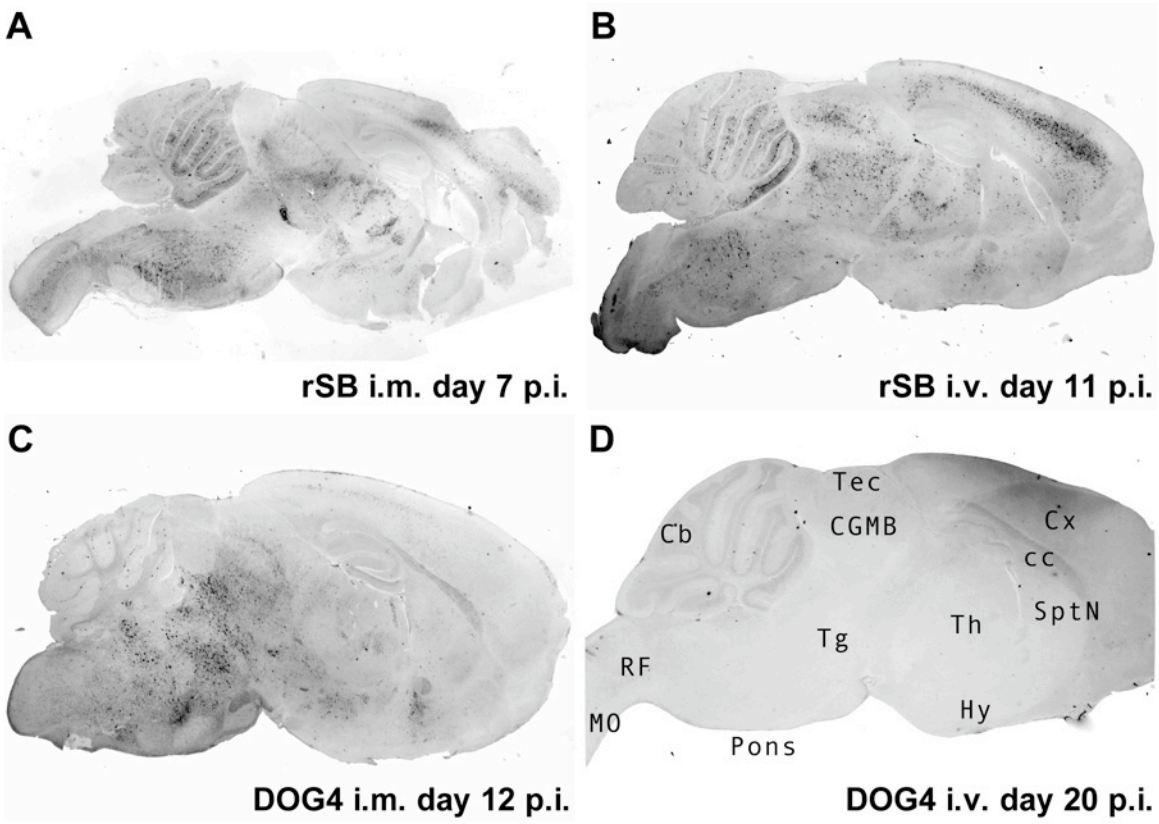

Fig. 10: Strain and infection route dependent distribution of viral antigen in the brain.
Brains of Swiss Webster mice were harvested when the animals were moribund or at the end of the twenty-day observation period as indicated in the panels **A** to **D**. Sagittal sections were stained immunohistochemically with a primary antibody against RNP, subsequently visualized by an enzymatic reaction. Abbreviations: Cb, cerebellum; cc, corpus callosum; Hy, hypothalamus; MO, medulla oblongata; CGMB, central gray substance of midbrain; RF, reticular formation; SptN, septal nuclei; Th, thalamus; Cx, cerebral cortex; Tg, midbrain tegmentum; Tec, tectum.

The i.v. inoculation with the bat-derived RV strain rSB led to a similar picture as the i.m. route; the main burden of antigen however, was not found to be in the cerebellum, but rather in the dorsomedial central gray substance of midbrain (Fig. 10 B). Aside from this area, the virus was not concentrated in special nuclei as it was seen after i.m. inoculation with DOG4 or rSB, but evenly moderately dispersed over the whole brain section.

In summary, the main virus load after DOG4 i.m. inoculation is seen in the midbrain tegmentum, whereas the cerebellum is the most afflicted CNS region in rSB i.m. infected

animals. Following the i.v. infection route, rSB concentrates mainly around the aqueduct, while DOG4 cannot be detected on the proteinergic level at all.

In order to clarify if the strain dependency of the lethality after RV i.v. inoculation as well as the differences in the distribution patterns of RNP immunoreactivity in the CNS after i.m. injection of rSB or DOG4 is influenced mainly by the RV glycoprotein, the attempt was undertaken to construct a chimeric virus based on the backbone of rSB, exchanging only its own glycoprotein against that of DOG4. Since the glycoprotein is thought to be the major determinant for the tropism of RV, it was expected that this RV, termed rSB-DOG4, would be able to reduce considerably the hundred percent lethality of rSB after i.v. inoculation and also to assimilate its distribution pattern in the CNS to that of DOG4.

The construction of the full-length clone of the chimera, cSB-DOG4, is outlined in 8.2. The correct sequence was verified by sequencing. Nevertheless it was not possible to produce infectious rSB-DOG4 particles from this clone with the recovery system that is described in 8.4, although it was successful in generating virus from other RV full-length clones that were proceeded as controls in parallel. Thus, a detailed analysis regarding the influence of RV glycoprotein on the strain dependent outcome of i.v. inoculation and viral distribution in the CNS after i.m. injected could not be met.

6.2.3. Long-term Infection with DOG4 after Intravenous Inoculation

From five of the six DOG4 i.v. infected mice, total RNA was isolated from brain, spinal cord, leukocytes, lungs, heart, kidney and liver tissue, reverse-transcribed and subjected to qPCR in order to analyze if virus would be detected somewhere in the organism or if it was cleared completely. Indeed, viral RNA could be detected in CNS tissue and in blood cells, whereas all peripheral organs were negative.

Since the possibility existed that the DOG4 i.v. inoculated animals had a prolonged incubation period longer than the twenty days that the experiment lasted, the experiment was repeated with the DOG4 strain. As previously observed, ninety percent of the i.m. inoculated animals died within twelve days p.i. (Fig. 11 B), all i.v. infected mice survived until the twenty-eighth day of infection, having completely recovered from a short period of slight weight loss from days six to ten after infection (Fig. 11 A).

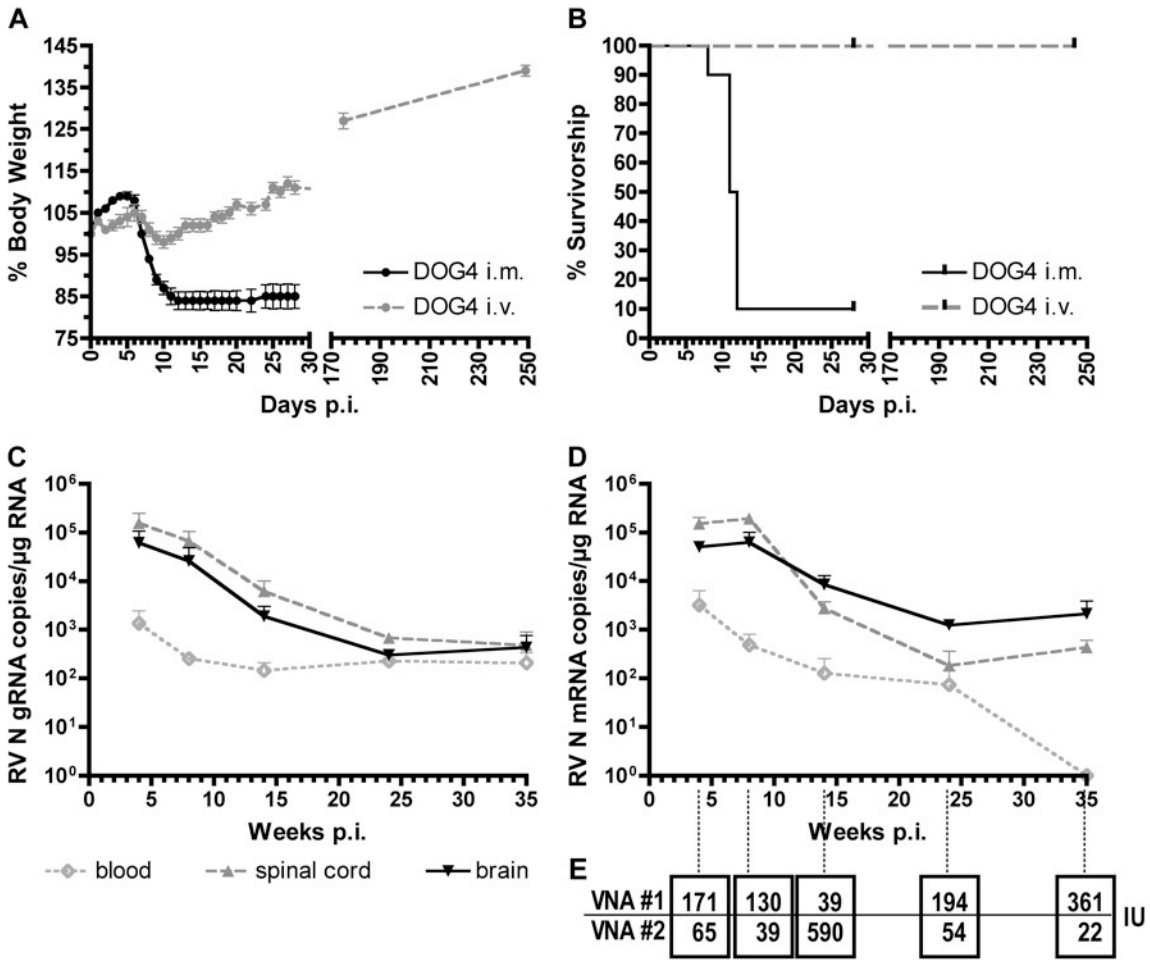

Fig. 11: Long-term observation after DOG4 i.v. inoculation.
Ten Swiss Webster mice were infected i.m. or i.v. with 10^6 ffu of DOG4. **A**: Body weight was recorded and normalized to the weight on day zero. Data are group average values (mean ± standard error). **B**: Percentages of surviving mice per day for each group. Mice which were infected i.v. were sacrificed pairwise after four, eight, twenty-four and thirty-five weeks p.i. and RV N gRNA (**C**) and mRNA (**D**) copy numbers per microgram total RNA isolated from leukocytes, spinal cord and brain were quantified by qPCR. Data are mean RNA copy numbers (+ standard error) calculated for each mouse pair. **E**: Serum VNA titers were determined for each individual mouse. Values are given in IU.

In order to analyze if DOG4 was still present in the organism, two mice each were sacrificed four, eight, fourteen, twenty-four and thirty-five weeks p.i. and spinal cord, brain and blood were harvested. RNA was isolated from CNS tissue and blood cells, reverse-transcribed and the cDNA analyzed by qPCR. Interestingly, viral negative-stranded as well as plus-stranded RNA (Fig. 11 C, D) was demonstrated in all three tissues for every time point, although the quantities were rather low, ranging from 10^2 to $5x10^5$ copies per microgram total RNA. Only RV N mRNA in blood cells from the last pair of mice was below the detection limit of the assay. During the surveillance period the amount of quantifiable virus genomes decreased about one to two lg levels in the brain and two to three lg levels in the spinal cord, while it stayed relatively stable in blood cells after eight weeks post infection. The first three

time points revealed constantly more copies of positive-stranded than negative-stranded RNA in all types of tissues under investigation, which could be evaluated as evidence for viral replication. At the last time points this observation was sustainable for brain tissue only, while the amount of putative RV N mRNA dropped below the level of RV N gRNA.

Since the PCR signals could also originate from fragmented RNA or non-productive RNP cores and not from intact, replicating RV, the attempt was undertaken to isolate infectious virions from the brains of the two mice that were sacrificed thirty-five weeks p.i., but failed.

In addition to the qPCR analysis, blood of all ten animals was also examined for the presence of VNA in the serum, which could be shown for all mice in very high titers (Fig. 11 E).

In summary, while rSB is able to cause an infection in mice when administered i.v., which does not differ significantly from i.m. inoculation concerning progress and outcome, DOG4 kills animals only following the classical infection route. Interestingly, DOG4 RNA can be detected in CNS and blood cells at least over a period of more than eight months after inoculation.

6.3. Presence of Rabies Virus at the Inoculation Site

Twelve young adult female Swiss Webster mice were infected with $5x10^6$ ffu rSB either into the right gastrocnemius muscle or into one of the tail veins. Two hours and two, five and seven days later, three mice of each group were sacrificed and the inoculation site was removed for RNA isolation and subsequent qPCR analysis.

The whole gastrocnemius muscle (338 mg ± 69 mg) was dissected from the i.m. infected mice, and from the i.v. inoculated mice an about 1.5 cm long stretch of the tail centered around the injection site was cut off (207 mg ± 24 mg) in order to control for differences in the virus load at the two inoculation sites. Calculated from the share of tissue homogenate that was used for RNA isolation (30 mg original tissue: about nine percent of the muscle versus about fifteen percent of the piece of tail), and the RNA yield per milligram tissue (0.41 µg RNA per milligram muscle versus 0.71 µg RNA per milligram tail), it is valid to compare the virus load data for both groups after normalization to one microgram of total

RNA (one microgram RNA represents 0.71% (i.m.) respectively 0.69% (i.v.) of the original tissue).

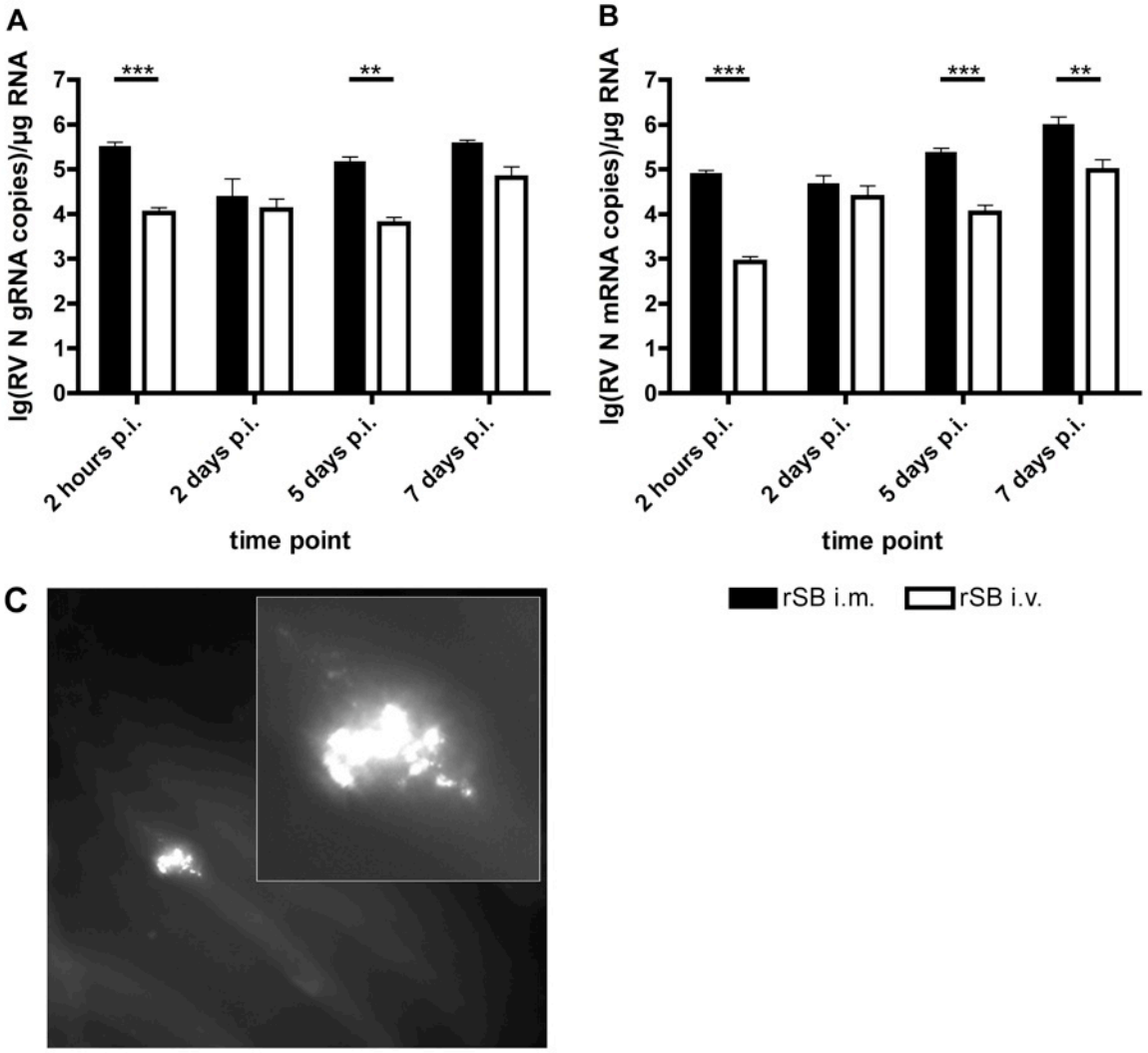

Fig. 12: Rabies virus at the inoculation site.
A and **B**: Twelve Swiss Webster mice were infected i.m. or i.v. with $5x10^6$ ffu of rSB. Three mice per group were sacrificed after two hours, two, five and seven days p.i. and RV N gRNA (**A**) and mRNA (**B**) copies were quantified by qPCR in tissue from the inoculation site (i.m., muscle; i.v., tail). Data are presented as lg of the mean RNA copy numbers (+ standard error) calculated for three mice per time point. Asterisks indicate significant differences in the virus load at the inoculation site in dependence of the infection route (**, $p < 0.01$; ***, $p < 0.001$). **C**: Mice were infected i.m. with $3.5x10^5$ ffu of SPBN-N2c-GFP and unfixed muscle tissue was examined for fluorescence. The picture shows a GFP positive muscle fiber in a group of negative fibers from a mouse sacrificed four days after infection. GFP is represented in white color. The insert is a digital magnification of the photo.

Figure 12 A shows that a considerable amount of virions is retained in the tail after injection, but it is still highly significantly less than in the muscle ($p \leq 0.001$). While the number of viral genomes per microgram of total RNA remains about the same in the tail at day two p.i., it drops about eighty-five percent in the muscle compared to the day of infection. In both tissues, the level of RV N mRNA copies is always higher than that of genomic copies

except for the two hour p.i. time point (Fig. 12 B). Both copy numbers increase over time until the seventh day. However, the gradient of virus multiplication differs significantly between the two inoculation sites ($p \leq 0.05$), suggesting that viral replication meets more favorable conditions in muscle tissue.

In order to elucidate where in the muscle tissue the viral amplification takes place, a RV was injected that expresses GFP in addition to its five genes. Ectopic or foreign accessory genes often cause unsurmountable problems for the recovery of a recombinant RV or, if viral particles still can be generated, lead to a significant drop in pathogenicity compared to the original strain. Since previous attempts failed to recover a GFP expressing rSB from a cSB-0 plasmid that carried the GFP gene downstream of the RV G gene, the virus SPBN-N2c-GFP was used for the approach [352]. The genome of this strain is identical to that of the vaccine strain SPBN, with the exception that the gene for RV G is replaced by that of the highly pathogenic, mouse-adapted strain CVS-N2c. In addition, the gene for GFP was introduced as an independent gene between RV G and RV L. This construct leads to the expression of free cytosolic GFP in RV infected cells whenever the transcription of viral genes start. The principle of the co-expression of rabies proteins and GFP in the same cells was proven by double immunofluorescence staining with antibodies against RNP and GFP [304]. Ten young adult female Swiss Webster mice were inoculated into the right gastrocnemius muscle with $3.5x10^5$ ffu of SPBN-N2c-GFP and one of these mice was sacrificed each day starting twenty-four hours after inoculation. In order to conserve the native fluorescence of GFP, the muscle tissue was not fixed after its dissection but moistened with 1xDPBS and cut into rough slices, which were flattened between a glass slide and a cover slip. The samples were scanned for fluorescence with a fluorescence microscope immediately after dissection. Due to the weak resolution caused by the crude preparation technique and the thickness of the tissue slices, the incidence of detecting expressed GFP was expected to be low. Nevertheless, single muscle fibers could be discriminated as shown in figure 12 C where five cells in longitudinal orientation can be recognized. One of them is marked by clear patches of green fluorescence (depicted as white color in the figure) resembling rather strongly the structure of a neuromuscular junction than a putative free distribution of GFP in the cytosol.

Altogether these findings reveal that replication at the inoculation site takes place after both i.m. and i.v. injection of rSB. It could be shown that more than ninety percent less virions are retained in the tissue surrounding the i.v. injection site compared to the i.m. inoculation

site and that the increase of viral particles over time is faster in the muscle than in the tail. Experiments with a GFP expressing RV suggest a strong spatial association between the site of replication in muscle tissue and neuromuscular junctions.

6.4. Primary and Secondary Infection of Peripheral Organs

It has been noticed for a long time that RV can be found in the skin and also in numerous peripheral organs during the late phase of the infection. Due to two independent cases of human rabies in 2004 and 2005 with lethal outcome, where RV was transferred from an undetected RV infected organ donor to several organ acceptors, these findings became of interest again. In the present study, the presence of RV in peripheral organs was sought to be brought into a timeframe in relation to the virus progress into and within the CNS. In addition, we wanted to clarify if the organs presented only a dead-end route of infection for RV, where viral particles are transported on neuronal pathways without further consequences, or if replication still could take place at such peripheral sites.

The site-by-site comparison of animals that were inoculated *via* the vascular route with i.m. inoculated mice would reveal if there were any differences in the patterns of peripheral organ infection over time and indicate if a primary infection of organs is possible and, if so, has an impact on the disease progression. The following data were obtained from tissues that were harvested from the same mice which were infected i.m. or i.v. with rSB for the analysis as described in section 9.3.

6.4.1. Time Dependent Progress of Viral CNS Infection after Intramuscular and Intravenous Inoculation of Mice with rSB

RNA from spinal cord and brain tissue that was harvested from three mice per time point and inoculation mode was analyzed for rSB RV N gRNA and mRNA (Fig. 13). After i.m. infection, gRNA was detectable in the spinal cord in fairly low amounts at day two p.i. (less than hundred RNA copies per microgram of total RNA), but the virus load amplified over more than six lg levels within the following three days (Fig. 13 A). Between 10^8 and 10^9 genomes per microgram of total RNA seem to be the maximum number of copies that can be produced in the spinal cord with the infection parameters that were applied, since almost no

further increase was observed from day five p.i. to day seven p.i., at which the animals were in the final stage of the disease.

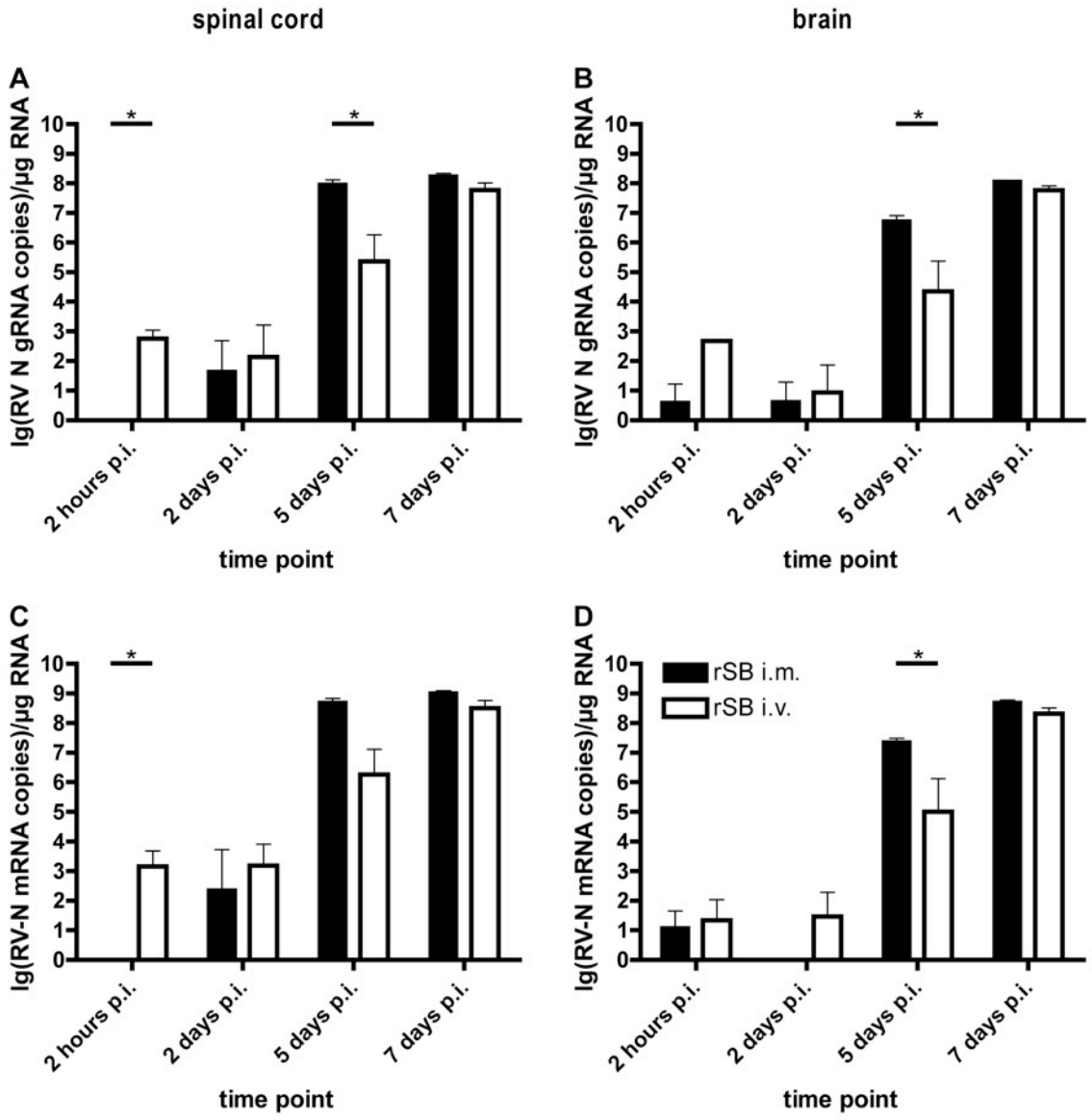

Fig. 13: Kinetics of virus load in the CNS.
Twelve Swiss Webster mice were infected i.m. or i.v. with $5x10^6$ ffu of rSB. Three mice per group were sacrificed after two hours and two, five and seven days. RV N gRNA (**A**, **B**) and mRNA (**C**, **D**) copies were quantified in total RNA from spinal cord (**A**, **C**) and brain (**B**, **D**) by qPCR. Data are presented as lg of the mean RNA copy numbers (+ standard error) calculated for three mice per time point and group. Asterisks indicate significant differences in the virus load of a tissue in dependence of the infection route at the indicated time point (*, $p \leq 0.05$).

Genomic rSB RNA was detectable in higher concentrations in the brain only at day five p.i., but in very low amounts also at day two p.i. and even already two hours after the inoculation. The latter supports the working hypothesis that indeed viral spill over into the vascular system and spread throughout the whole organism occurs, if inoculated i.m. (Fig. 13

B). The amount of virus in the brain slightly succeeded the viral burden in the spinal cord as expected. And here also, between 10^8 and 10^9 genomes per microgram of total RNA seem to present the upper limit for the virus load, as seen in the spinal cord.

Overall, the time pattern of the virus load is not significantly different between i.m. and i.v. infected mice. It can be observed however that after introduction into the bloodstream rSB is detectable in significantly (spinal cord, $p \leq 0.05$) or slightly (brain) higher amounts especially at the early time points, whereas the amplification slope from the day of infection to day seven p.i. is significantly steeper in the CNS of i.m. inoculated mice ($p \leq 0.05$) which becomes particularly noticeable at day five p.i. in both CNS segments. The findings for the temporal mRNA distribution paralleled the gRNA pattern as expected and was usually one to two lg levels higher in copy numbers per microgram of total RNA (Fig. 13 C, D). The fairly similar results obtained for the two inoculation modes regarding the extent of viral burden are also an indicator for the assumption that not the virus load in the CNS *per se* is responsible for the different clinical symptoms between the groups, but that rather the spatial localization within the CNS is likely to differ. Also, the slightly slower progress into the CNS after i.v. inoculation could be a sign for possibly different pathways from the periphery into the brain. These speculations will be further addressed later.

6.4.2. Presence of rSB at Peripheral Sites after Intramuscular and Intravenous Inoculation

Beside inoculation site and CNS tissue, heart, lungs, kidneys and liver were dissected from the same mice already described in 9.3. Analysis was concentrated on these four organs since they play major roles in transplantation medicine. In addition, they were found to have the highest incident to be positive for virus when different tissues from rSB and DOG4 i.m. infected mice in the final stage of disease were subjected to qPCR in pre-experiments.

Figure 14 depicts VNA titers and life data of the i.m. and i.v. infected mice and figure 15 compares the results of the qPCR for the organs mentioned above, subdivided according to the time point of harvest (two hours p.i., Fig. 15 A, E; two days p.i. Fig. 15 B, F; five days p.i., Fig. 15 C, G; seven days p.i., Fig. 15 D, H) and the type of RNA (rSB RV N gRNA, Fig. 15 A – D; rSB RV-N mRNA, Fig 15 E – H).

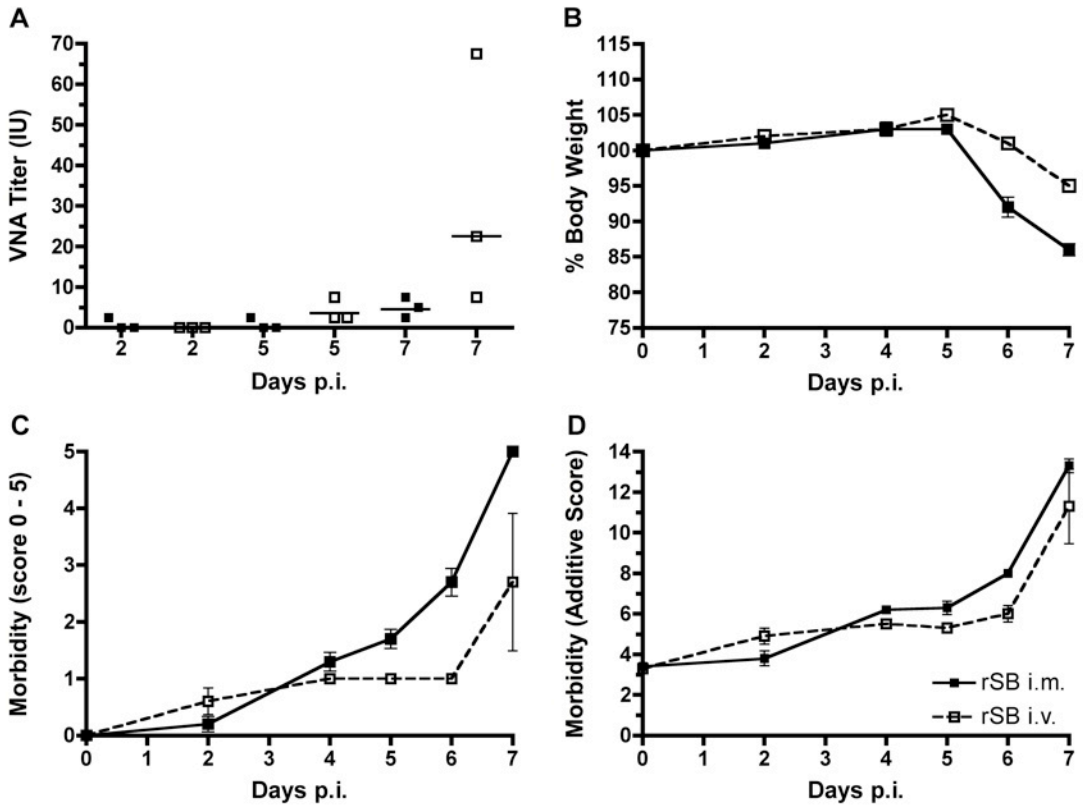

Fig. 14: VNA titers (A), body weight (B) and morbidity (C, D).
Twelve Swiss Weber mice were infected i.m. or i.v. with $5x10^6$ ffu of rSB. **A**: Blood was obtained from all mice by heart puncture immediately before sacrificing them, and serum VNA titers (in IU) were determined. Titers for all six mice sacrificed at day zero were negative. Data for the three other time points are presented as scatter plot with lines indicating the geometric mean for every group **B**: Body weight was recorded daily and normalized to the weight on day zero. Data are group average values (mean ± standard error). **C**: Clinical symptoms were rated from 0 to 5 (0, healthy; 1, ruffled fur; 2, negative trunk curl test; 3, one-sided hind leg paralysis; 4, two-sided hind leg paralysis; 5, moribund) **D**: Clinical symptoms were rated from 0 to 14 by summation of the results obtained by several tests. Data in both graphs of the lower panel are group average values (± standard error).

A two-way ANOVA test revealed that the inoculation route in general had a significant influence on the amount of virus found in peripheral organs only at two hours p.i. as well as after two days p.i. ($p \leq 0.001$). While at the earliest time point viral burden was distributed fairly equally between the different types of organs, significant differences emerged for all other three time points (RV N gRNA: two days p.i. $p \leq 0.001$, five and seven days p.i. $p \leq 0.01$; RV N mRNA: five and seven days p.i. $p \leq 0.001$). Two hours after i.m. inoculation, RV N gRNA and mRNA could be detected in very low amounts (less than four-hundred copies per microgram of total RNA) randomly in all types of peripheral organs under investigation but systematically only from five days p.i. on.

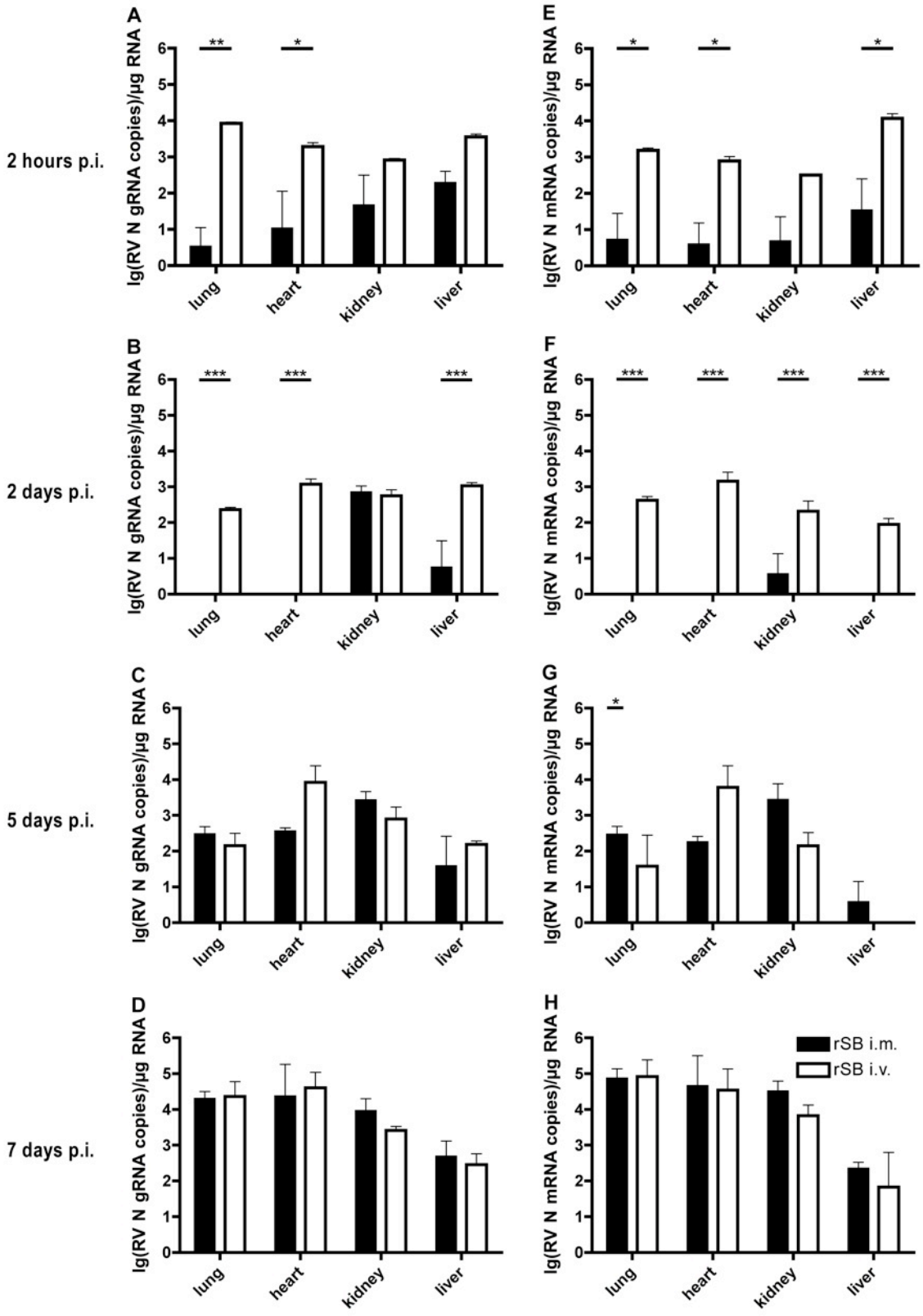

Fig. 15: Rabies virus in peripheral organs.
Twelve Swiss Webster mice were infected i.m. or i.v. with $5x10^6$ of rSB. Three mice per group were sacrificed after two hours (**A**, **E**) and two (**B**, **F**), five (**C**, **G**) and seven (**D**, **H**) days p.i. and RV N gRNA (**A** - **D**) and mRNA (**E** - **H**) copies were quantified by qPCR in total RNA from lungs, heart, kidneys and liver. Data are presented as lg of the mean RNA copy numbers (+ standard error) calculated for three mice per time point. Asterisks indicate significant differences in the virus load of a tissue in dependence of the infection route at the indicated time point (*, $p \leq 0.05$; **, $p \leq 0.01$; ***, $p \leq 0.001$).

After i.v. infection in contrast, RV N was found in all organs at every time point and the amounts of viral RNA were significantly higher especially in the lungs and in the heart two hours and two days after infection. In fact, the copy number of viral gRNA and mRNA at the early time points was constantly significantly dependent on the inoculation mode only for these two organs. In the progressed (five days p.i.) and final (seven days p.i.) stage of disease the viral distribution pattern in the periphery balanced between the i.m. and i.v. inoculated groups and variances in the results were mainly dependent on the type of organ (gRNA: $p \leq 0.01$; mRNA: $p \leq 0.001$), and not on the inoculation route.

Thus, looking at the distribution patterns, the viral load in the periphery after i.m. inoculation succeeded the progression of virus into the CNS: virus was consistently present in the peripheral organs in low concentrations only after high numbers of viral genomes in the brain were detectable (day five p.i.), and increased there over time until the final state of disease. Although mRNA could be demonstrated along with gRNA in most cases, the viral load in the periphery after i.v. inoculation grew only relatively slow over time. The steepest increase occurred between day five and day seven p.i., when the virus had reached about the same concentration in the brain as after i.m. inoculation at the fifth day of infection.

Another observation of note in this context is that the ratio between the negative and positive-stranded rSB RV N RNA was fairly equal in organs and not with the high excess (one to two lg levels) of mRNA as seen in neuronal tissue.

Since it could be demonstrated for DOG4 i.v. infected mice that viral RNA is detectable in total RNA of leukocytes up to several months after the inoculation, it was tested if this were true also for rSB infected mice. Thus, blood was obtained by heart puncture before sacrificing the mice and RNA was isolated from the cellular share after erythrocytes had been lysed and removed. As figure 16 shows, blood cells from rSB i.v. infected and even from i.m. inoculated mice also contained viral RNA, whereby significant differences between the groups existed, especially at the two early time points. The animals were not perfused with PBS or any other buffer before tissues for RNA isolation were taken out. Hence, in theory low copy numbers in tissues might result from contamination of the tissue RNA with blood RNA.

Assuming an average blood volume of 1.7 ml that is evenly distributed throughout the body, and an average body weight of 25 g for a mouse, about 7% of the mass of each sample can be attributed to whole blood. When calculating with the RNA yields per milligram solid

tissue respectively per milliliter blood that were obtained in this study, only 0.30% of the tissue total RNA originates from blood cells. That means from every thousand RV copies that are detected by quantitative RT-PCR in one microgram of total RNA, on average only three might derive from blood cell RNA that was co-isolated from the tissue. This value is actually much higher than in reality given the fact that most of the blood was withdrawn from the body before harvesting any solid tissue. Thus, those minute amounts were considered as irrelevant.

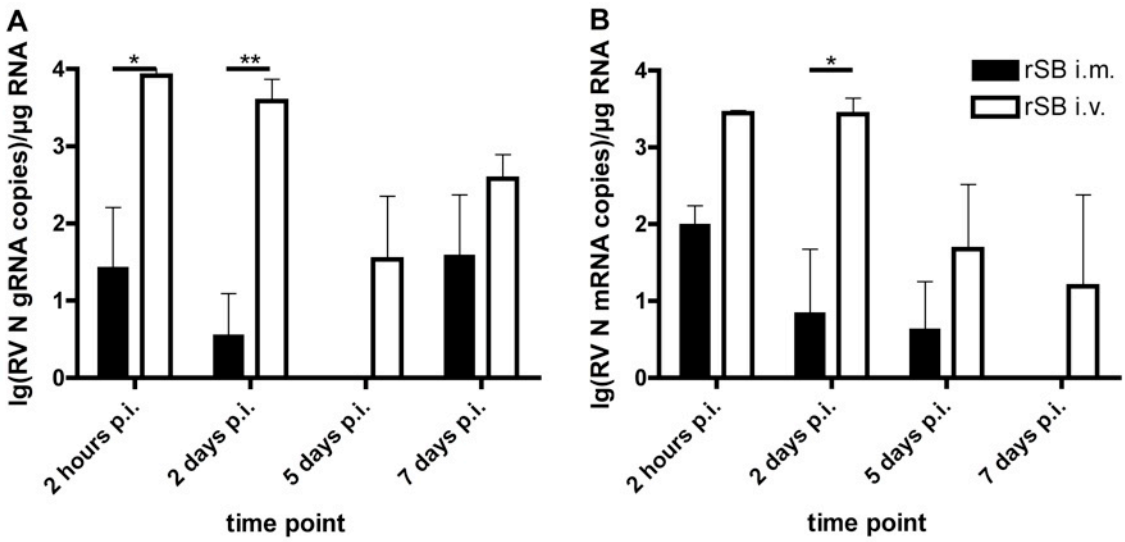

Fig. 16: Rabies virus viremia.
Twelve Swiss Webster mice were infected i.m. or i.v. with $5x10^6$ ffu of rSB. Three mice per group were sacrificed after two hours, two, five and seven days p.i. and RV N gRNA (**A**) and mRNA (**B**) copies were quantified by qPCR in total RNA from leukocytes. Data are presented as lg of the mean RNA copy numbers (+ standard error) calculated for three mice per time point. Asterisks indicate significant differences in the virus load in the blood in dependence on the infection route (**, $p \leq 0.01$; ***, $p \leq 0.001$).

6.4.3. Inoculum Size Dependent Presence of rSB in the CNS and at Peripheral Sites after Intravenous Inoculation

In 9.1 it was described that the outcome of an i.v. inoculation is dependent on the inoculum size. Sixty percent of mice infected with 10^5 ffu rSB survive, while an inoculation with 10^6 or more ffu leads to hundred percent lethality. Further, it was presented that peripheral organs are affected from the very beginning after i.v. inoculation with $5x10^6$ ffu rSB.

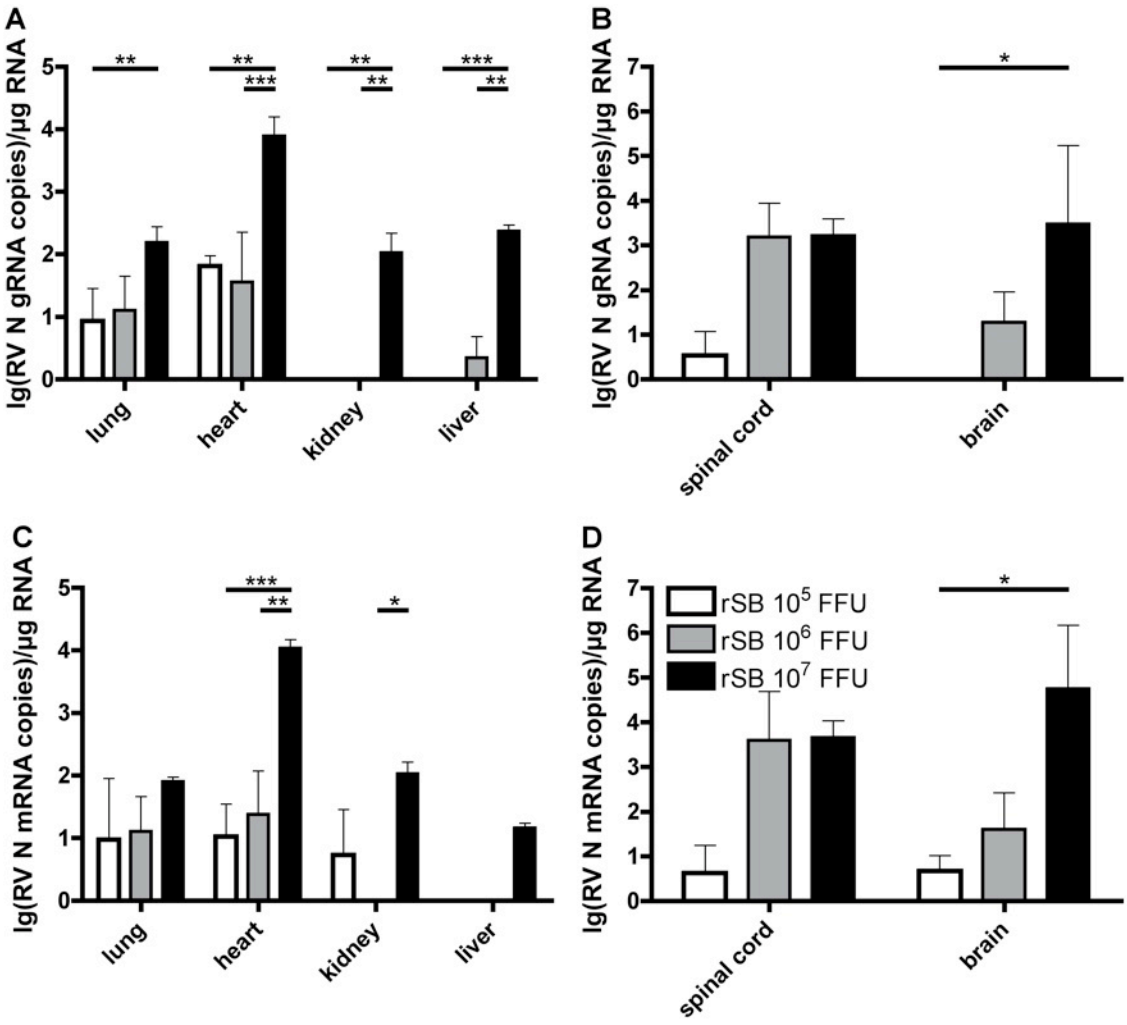

Fig. 17: Inoculum size dependent virus load in the CNS and peripheral organs.
Groups of three Swiss Webster mice were infected i.v. with 10^5, 10^6 or 10^7 ffu of rSB and sacrificed four days later. RV N gRNA (**A**, **B**) and mRNA (**C**, **D**) copies were quantified in total RNA from lungs, heart, kidneys and liver (**A**, **C**) as well as from spinal cord and brain (**B**, **D**). Data are presented as lg of the mean RNA copy numbers (+ standard error) calculated for three mice per inoculum size. Asterisks indicate significant differences in the virus load of a tissue in dependence on the inoculum size (*, $p \leq 0.05$; **, $p \leq 0.01$; ***, $p \leq 0.001$).

In order to analyze if a difference in virus loads of the CNS or peripheral organs is responsible for the decrease of mortality after i.v. inoculation with a lower amount of virions, three groups of mice were infected either with 10^5 (n = 3), 10^6 (n = 3), or 10^7 (n = 4) ffu rSB. The mice were sacrificed four days p.i., a time point at which none of them was showing any symptoms. Spinal cord, brain, lungs, heart, kidneys and liver were taken out for RNA isolation. One out of the four mice infected with the highest dose was chosen randomly to be kept as a positive control for the inoculation until the final stage of disease, which set in at the seventh day after infection. All RNA samples were subjected to reverse transcription and subsequent qPCR to quantify rSB gRNA and mRNA.

Overall, the amount of viral RV N gRNA as well as of mRNA in different peripheral tissues four days after i.v. inoculation depended significantly on the titer of the inoculum ($p \leq 0.001$) and the type of organ ($p \leq 0.001$), but no significant differences were detected between the groups that were infected with 10^5 or 10^6 ffu (Fig. 17 A, C).

In contrast, more prominent disparities existed between the two inoculums with higher virus titers. For the neuronal tissues like in the periphery the inoculum size affected the results significantly (gRNA, $p \leq 0.05$; mRNA, $p \leq 0.01$). The most remarkable difference between the groups infected with the two lower doses of rSB is apparent for the spinal cord, although it is not significant.

However, since the overall virus load in the periphery is about the same in both groups, it is most likely that rather the slower progress into the CNS is responsible for the higher percentage of survivorship in mice inoculated with 10^5 ffu than the virus load in the periphery.

Another interesting observation was that in all three groups the heart was the peripheral organ with the highest viral load, especially noticeable after the inoculation with 10^7 ffu. Indeed, a comparison between this group and the positive control animal that was inoculated with the same amount of particles, but sacrificed only in the final stage of disease, shows that the virus loads in spinal cord ($3.44x10^3$ versus $1.11x10^8$ genome copies per microgram of total RNA) and brain ($1.73x10^5$ vs. $5.78x10^7$) as well as in lungs ($2.23x10^2$ vs. $8.95x10^3$) and kidneys ($1.71x10^2$ vs. $1.19x10^4$) were 100 – 50,000 times lower, while the virus load in the heart ($1.30x10^4$ vs. $1.18x10^5$) at day four p.i. had already reached more than ten percent of its final level.

6.4.4. Virus Isolation from Peripheral Tissue

The evidence of viral gRNA and mRNA alone cannot be considered sufficient to prove that infectious particles are in fact generated and released. In order to analyze if indeed virions are detectable in the periphery and to confirm the assumption that organs are infected primarily and not only secondary by the transport of particles from the already completely affected CNS, 20%-organ homogenates were prepared for the inoculation of NA cells. Mice were infected i.m. or i.v. with 10^7 ffu of rSB and sacrificed four days after inoculation. All mice were free of symptoms at the time of tissue harvest.

It was not possible to detect infectious RV in NA cells that were incubated with homogenates from lungs, kidneys or liver. In contrast, from five out of six mice that were infected i.v. we were able to isolate infectious virus utilizing NA cells. Moreover, only two of the five mice, whose hearts were positive for infectious RV (Fig. 18 A, right), had also infectious particles in their brains at the same time (Fig. 18 B, right). After i.m. inoculation in contrast, it was not possible to isolate virus from the heart of any animal (Fig. 18 A, left), but in 50% of the brains infectious virus was present (Fig. 18 B, left).

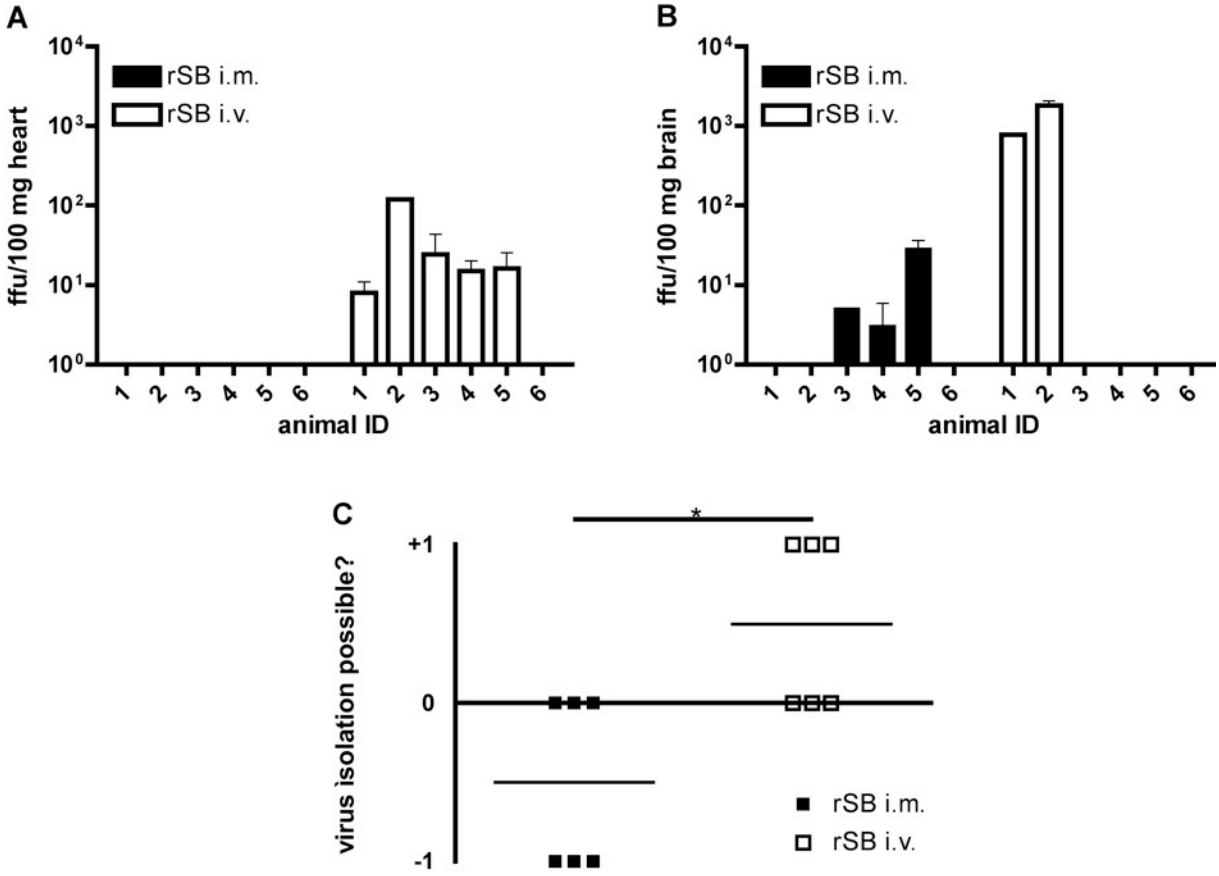

Fig. 18: Isolation of infectious particles from heart and brain tissue.
Six Swiss Webster mice were infected i.m. or i.v. with 10^7 ffu of rSB. All mice were sacrificed four days later and virus was isolated from hearts (**A**) and brains (**B**) by inoculating NA cells with 20%-organ homogenates. Data are presented as mean ffu per 100 mg tissue (+ standard error) for individual mice. **C**: The isolation of virus was rated as a qualitative event to see if a difference in the order of appearance of virus in brain and heart exists. A negative finding in a tissue was assigned the value zero, a positive finding in the brain ("B") the value "-1", in the heart ("H") "+1". The values were summed up for each individual mouse and the group means were tested for a significant difference with a two-sided t-test (*, $p \leq 0.05$).

To get a qualitative conclusion about the direction of viral migration (from the CNS to the periphery versus from the periphery into the CNS or independent infection of both) each mouse was rated with a simple point system: if no information about the time order of

infection could be drawn from the virus loads in brain and heart, for example if both tissues were either positive or negative for virus, the mouse was counted as “zero”. In contrast, if the brain was positive, but no virus was isolated from the heart, the animal was rated with “minus one”; and if the brain was virus free, while the heart contained infectious RV, “plus one” was assigned. Figure 18 C illustrates this approach. The two groups differed significantly in their rating ($p = 0.0101$), which supports indirectly the hypothesis that rSB infects peripheral organs directly, if it reaches the vascular system.

6.5. Identification of rSB Target Cells in Peripheral Organs on the Example of the Heart

In 9.4, molecular evidence for virus replication in various peripheral organs was presented. For the heart it was also shown that infectious virions are produced and released in the periphery and that rSB is able to infect organs directly without detouring over the CNS. The obvious question followed which structures exactly serve as host cells for rSB in the periphery. For the attempt to identify these targets, immunohistochemical analysis was performed, but restricted to cardiac tissue, since the heart seemed to be the organ that was most susceptive to RV infection in this setting.

For this approach, six six-to-eight-week old female Swiss Webster mice were infected either i.v. or i.m. with 10^7 ffu rSB. To assess possible differences in the replication sites between primary and secondary infection, the i.v. inoculated animals were sacrificed at day four p.i. when they were still free of symptoms, and tissue from the i.m. inoculated mice were collected at day six p.i. when most of them were in the final stage of disease. As target antigens for immunohistochemical staining served viral RNP, as well ChAT, TH and VAChT which were used to detect possible overlays of virus with autonomic ganglion cells and fibers or neuromuscular junctions. TH is synthesized in sympathetic second-order neurons; ChAT and VAChT mark autonomic first- and parasympathetic second-order neurons and their synaptic terminals as well as motor endplates. Also, sections were immunostained for CD3 to look for T cell infiltrations within the infected tissue, which were not found to be present in any of the analyzed hearts.

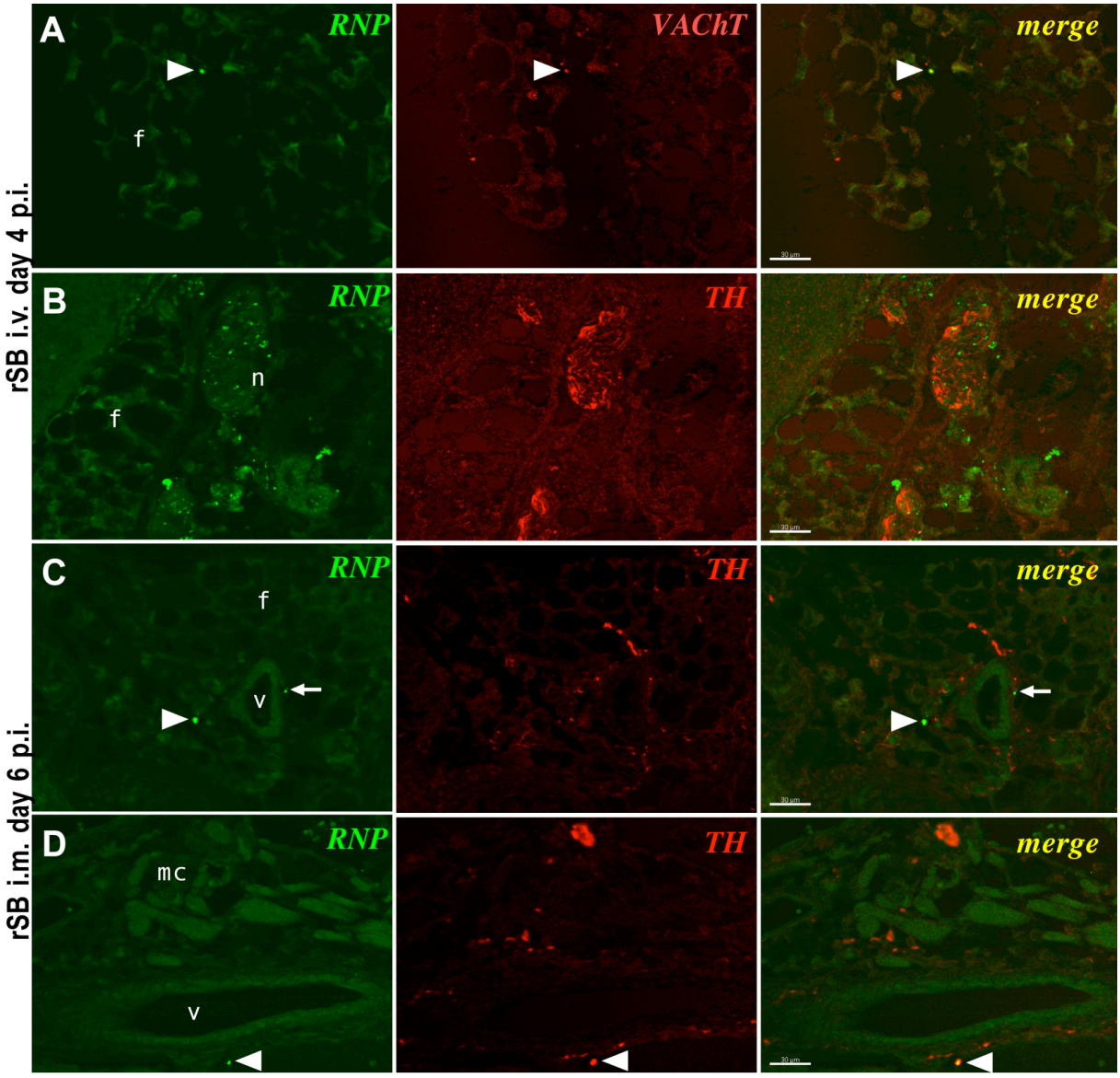

Fig. 19: Rabies virus positive nerve fibers in heart tissue.
Six Swiss Webster mice were inoculated i.v. (**A**, **B**) or i.m. (**C**, **D**) with 10^7 ffu of rSB and sacrificed four (i.v.) or six (i.m.) days later. Hearts were co-immunostained with primary antibodies against RNP (green, left column) and VAChT or TH (red, medium column). Co-localization of the two labeled antigens appear yellow (merge, right column). Abbreviations: f, fat cells; mc, myocardial fibers; n, nerve; v, vessel. Arrow heads point to single nerve fibers which are positive for both immunoreactivity against RNP and the second antigen, the arrow in **C** labels a fiber, that is positive for RNP, but not the co-stained antigen. White bars represent 30 µm.

In general, only relatively little immunoreactivity against RNP could be detected in the hearts, and the myocardium was negative for RV after both inoculation routes. The only structures where viral protein was verified were nerve fibers (Fig. 19) and the autonomic ganglion cells that lie in intramural clusters at the base of the cardiac atria (Fig. 20). Of the occasional events of RNP positive fibers in the hearts from rSB i.v. inoculated mice, figure 19 A shows the overlay of immunoreactivity with a VAChT fiber that crosses fat cells, and figure 19 B the presence of RNP in a nerve which also contained TH fibers.

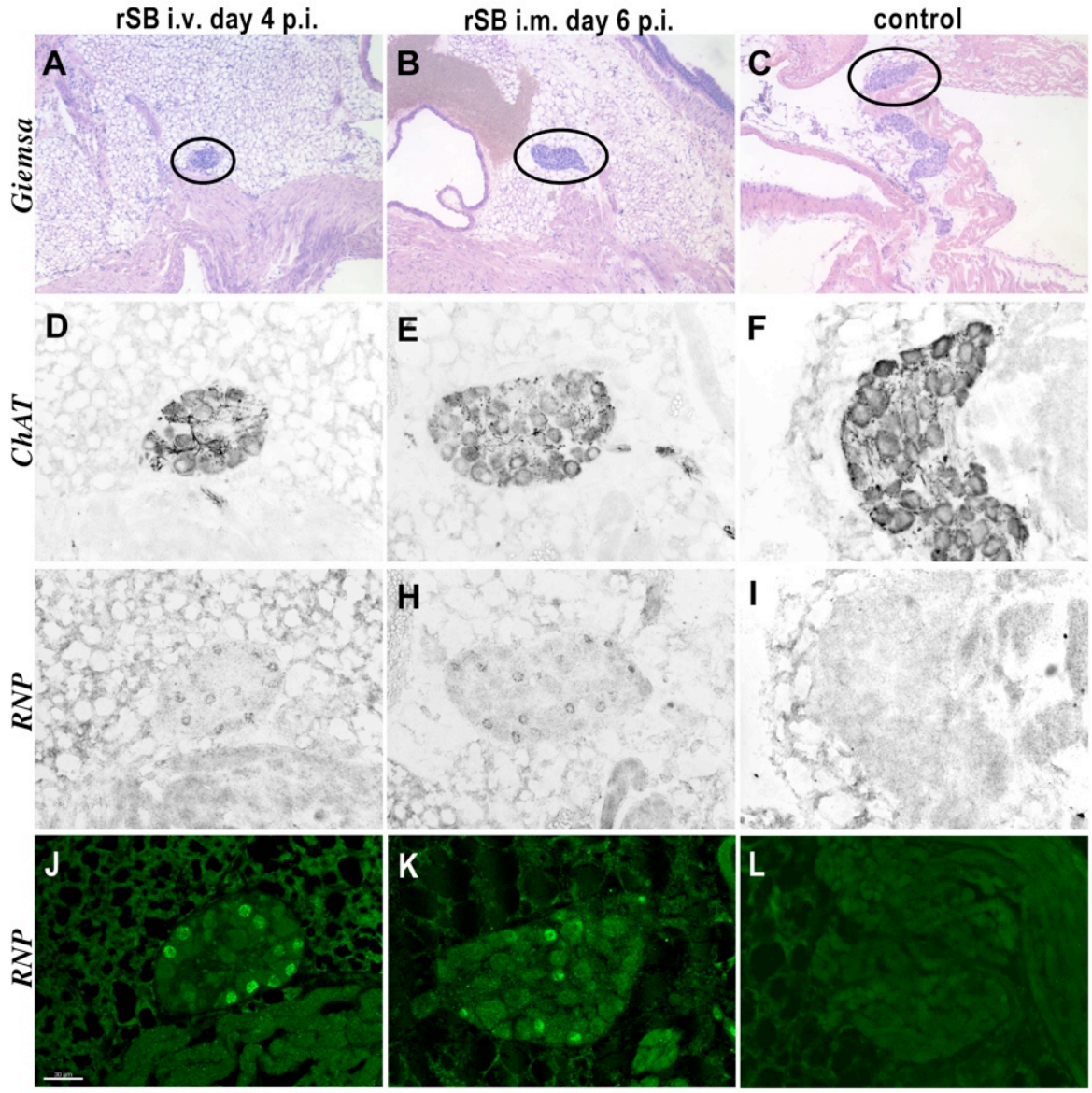

Fig. 20: Rabies virus positive neuronal cells in heart tissue.
Six Swiss Webster mice were inoculated i.v. (left column) or i.m. (middle column) with 10^7 ffu of rSB and sacrificed four (i.v.) or six (i.m.) days later. Hearts from these infected animals as well as from control mice were stained with Giemsa (upper row) in order to find regions with ganglia (encircled). Adjacent sections were enzymatically immunostained with primary antibodies against ChAT (second row) and RNP (third row). The bottom row shows fluorescence labeled immunostaining against RNP (white bar represents 30 µm).

In figures 19 C and D vessel associated RNP positive fibers with and without TH co-staining from a rSB i.m. infected heart are depicted. The enzymatic as well as the fluorescent immunohistochemical stainings against RNP revealed that the share of infected ganglion cells is about the same four days after i.v. (Fig. 20 G, J) respectively six days after i.m. inoculation (Fig. 20 H, K). Even in these neurons, the staining was rather sparse, but nevertheless present. Despite of the particular perinuclear staining pattern in the autonomic ganglion cells, which is peculiarly distinct from that of RV infected CNS neurons, RNP immunoreactivity was only

seen in infected animals and not in the heart ganglia of control mouse (Fig. 20 I, L) and thus must be considered as specific.

In summary, rSB is also neurotropic in the peripheral setting and was not detected in myocytes as well as endothelial cells or other non-neuronal cells or tissues. Also, there is no significant difference between viral loads in hearts from animals in the final stage of disease after i.m. infection (secondary infection) and viral loads in hearts from mice isolated early after after i.v. inoculation (primary infection). This is also congruent to the qPCR results regarding viral RNA levels in cardiac tissue.

6.6. Identification of the Main Viral Routes from the Periphery to the CNS after Intravenous or Intramuscular Inoculation

The immunohistochemical analysis of hearts from i.v. and i.m. infected mice led to the assumption that primary infection of peripheral neurons can indeed occur, but that these are probably no starting points for the progression of virions into the CNS. Nevertheless, the differential symptoms that mice develop following the two inoculation modi allowed the hypothesis that different nuclear areas are affected in the CNS and thus rSB enters it on different routes after i.m. or i.v. infection.

In order to verify this, twelve six-to-eight-weeks old female Swiss Webster mice were inoculated either i.v. or i.m. with 10^7 ffu rSB and spinal cords and brains were collected from four mice per group after two, four and seven days p.i. (i.v.) and two, four and six days p.i. respectively (i.m.). The tissues were prepared for immunohistochemical staining and frontal sections were analyzed with antibodies against RNP in comparison to sections from non-infected control mice. For a first screening, sections from all brains matched for the stereotaxic coordinates interaural 2.34 mm and bregma -1.46 mm were chosen (Fig. 21, red bar) using a sterotaxic mouse brain atlas for orientation [296]. This area comprises RV prone regions such as the hippocampus, thalamic and hypothalamic nuclei, basal ganglia, the amygdala, as well as primary and secondary somatosensory cortex.

Table 4 presents the morbidity status (from ‚-‘ no signs of illness to ‚+++++‘, morbid) and the virus load in the analyzed section plane for each animal (from ‚-‘ no RNP-immunoreactivity to ‚++++‘ many RNP immunoreactive neurons and fibers). For the i.m.

infected group the progress of the disease strongly correlated with the presence of virus: there was only viral antigen when the animals had first symptoms of loss of motor functions, namely performing negatively in the trunk curl test (i.m. morbidity status ++), and vice versa. The first region to appear rabies affected was the primary sensory cortex (animal b10), followed by the dorsomedial hypothalamic nucleus, the striatum and lateral and ventral posterior thalamic nuclei (animals b8 and b11). In the late stage (animal b12), the infection had spread to further cortical (secondary somatosensory cortex, retrospenial agranular and granular cortex, ectorhinal cortex) and hypothalamic areas (ventromedial and arcuate nucleus).

Table 4: Morbidity and virus load at different time points after i.m. or i.v. inoculation with rSB

rSB i.v.				rSB i.m.			
days p.i.	**animal**	**morbidity**	**virus load**	**days p.i.**	**animal**	**morbidity**	**virus load**
2	a1	-	-	2	b1	-	-
	a2	-	-		b2	-	-
	a3	-	-		b3	-	-
	a4	-	-		b4	-	-
4	***a5***	**-**	**++**	4	b5	-	-
	a6	**-**	**++**		b6	+	-
	a7	+	-		b7	+	-
	a8	+	-		***b8***	**++**	**++**
7	a9	++	-	6	b9	++	+
	a10	++	-		***b10***	**++**	**+**
	a11	**+++**	**-**		***b11***	**++**	**+++**
	a12	**++++**	**++**		***b12***	**+++**	**++++**

The analysis of the same section level from brains of i.v. infected animals resulted in a much more heterogeneous picture. There was no correlation between the presence of virus in the screened plane and the morbidity status of an animal. For example, animals a5 and a6 still behaved completely healthy while having already virus in several nuclei and in the neocortex. In contrast, mouse a11 showed strong signs of sickness, but virus was completely absent from the analyzed plane. Animal a12 was close to being morbid when sacrificed, although there was not more virus present than in the sections from the healthy mice a5 and a6. In those animals that showed immunoreactivity against RNP in the analyzed regions, hypothalamic areas (arcuate, supraoptic, dorsomedial nucleus) and the amygdala were especially prone to harbor viral antigen. Ventral thalamic regions, basal ganglia (striatum, globus pallidus) and cortical areas (primary and secondary somatosensory cortex) were also occasionally positive for virus. Based on this first screening, eight animals were chosen for further analysis (Table 4, bold italic).

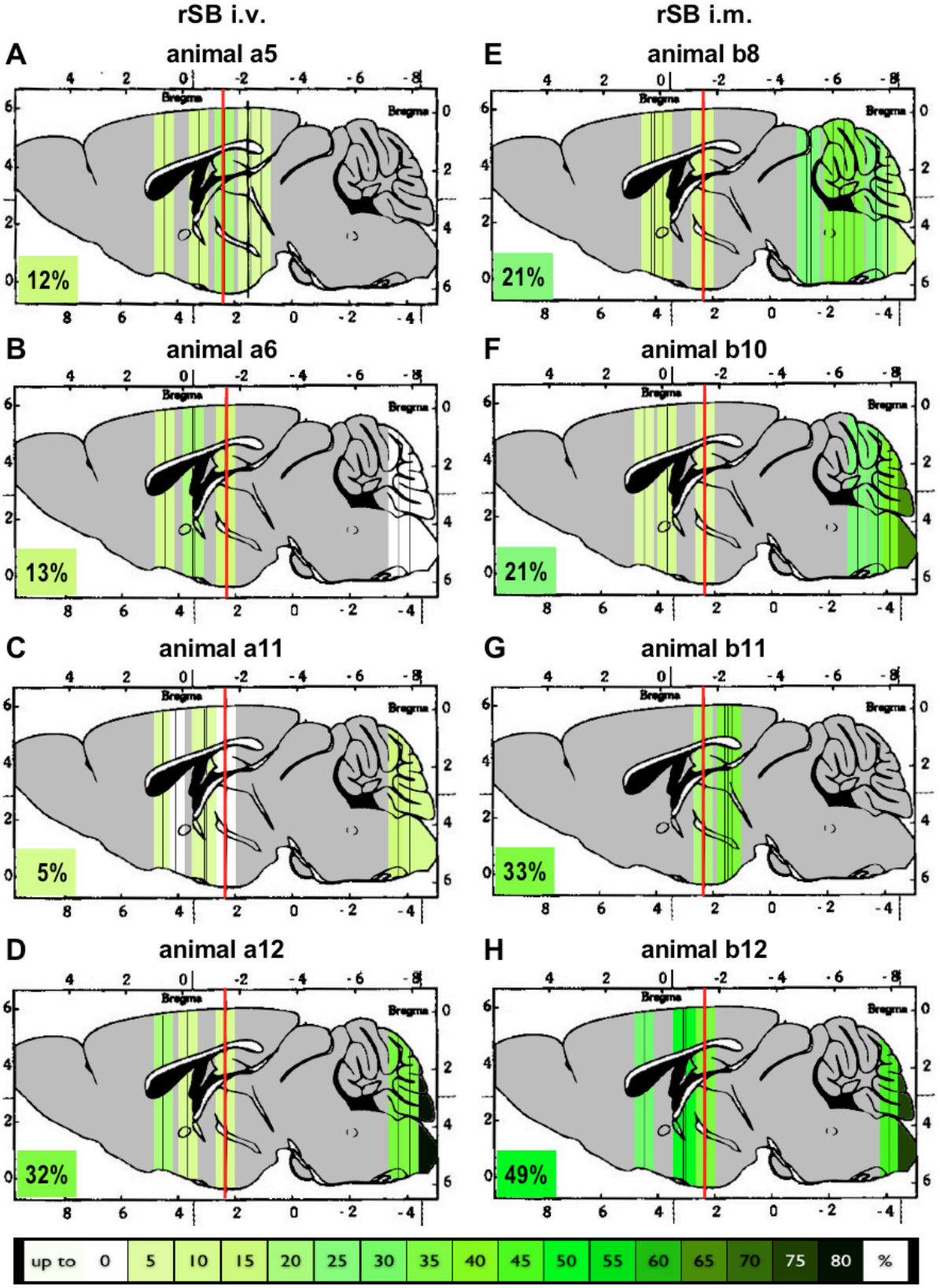

Fig. 21: Viral Progress into the CNS.
Color coded presentation of the percentage of virus infected nuclei, cortical areas and fiber tracts in frontal sections of mouse brains. Animal numbers relate to table 4. The red bar represents the section plane for the initial screening of all mouse brains (see text). Each vertical black bar represents another plane that was analyzed for the presence of viral antigen by immunohistochemistry of several sections. Distinct structures were identified and counted using a stereotaxic mouse brain atlas [296]. The color of each plane represents the percentage of virus positive structures (nuclei, fiber tracts, cortical areas) in each plane under investigation. Gray colored regions were not analyzed. The total percentage of RNP immunoreactive structures for each brain is noted in the left corner of each panel.

Figure 21 shows graphically the percentage of structures (nuclei, fiber tracts, cortical areas) that were RNP immunoreactive in each plane, whereby each plane is represented by a black bar and was analyzed by several sections. Cervical cord was also sectioned and stained with antibodies against RNP.

While for the i.m. infected animals the color coding visualizes that the virus progresses spatiotemporally wavelike from spinal cord and brain stem to the forebrain (Fig. 21 E - H), infection of the spinal cord or brain stem is not a prerequisite for infection of higher-order structures after i.v. inoculation (Fig. 21 B).

Detailed analysis of the affected CNS regions (see table 5 for complete list of immunohistochemical analyzed CNS structures) reveals that after i.m. inoculation virus first spreads through motor system pathways (Fig. 22 B): from the muscle it invades the spinal cord by the axons of motoneurons that lie in the Rexed laminae VIII and IX. *Via* the pyramidal tract it travels to the motocortex, from which it reaches premotocortical and primary somatosensory areas as well as the inferior olive, neurons in the reticular formation and Raphe nuclei. Originating from the olive, virus gets to the deep nuclei and the cortex of the cerebellum. *Via* the reticular formation, the basal ganglia become affected, and through the Raphe nuclei, RV reaches septal and hypothalamic nuclei as well as structures in the tegmentum of the midbrain.

During progression of the disease, various thalamic nuclei, further hypothalamic areas, limbic structures and other neocortical regions get infected. Virus is also found in additional spinal cord laminae, which it reaches by afferences to the ventral posterior nucleus of the thalamus (Rexed laminae I and II) as well as to the inferior olive and the cerebellar cortex (Rexed laminae III to VI).

In contrast to the bottom-to-top progression after i.m. inoculation, RV affected areas can be found in the brain of i.v. infected animals without showing immunoreactivity against RNP in the spinal cord or the brain stem (Fig. 22 A). Indeed, the hypothalamic paraventricular, supraoptic, preoptic, dorsomedial and arcuate nuclei as well as the lateral hypothalamic area were the main virus prone regions in the mice a5 and a6, which had already a moderate overall virus load, however showing no symptoms. In animal a6, virus had further proceeded to basal ganglia (striatum, globus pallidus) and other telencephalic nuclei (amygdala, nucleus

accumbens, septal nuclei), which all are accessible for the virus *via* their efferences to the affected hypothalamic nuclei.

The heavily symptomatic animals a11 and a12 showed a different viral distribution pattern which resembled much more those of the i.m. inoculated mice: in spinal cord, motor neurons in Rexed laminae VIII and IX were strongly affected and immunoreactivity against RNP could be observed also in the inferior olive, the reticular formation as well as in the premotor cortex and the cingulate gyrus. Additionally, in the brain of the more progressed animal a12, the primary motor and somatosensory cortex as well as cerebellum, basal ganglia and septal nuclei showed viral burden. Thalamic nuclei and Rexed laminae with efferences to these higher-order structures were positive for RNP, too. In contrast, the hypothalamus was not at all (a11) or much less affected (a12: only the preoptic and the dorsomedial hypothalamic nuclei) than in the mice a5 and a6.

Thus, although it was to be expected that all mice would have died with the same unspecific, motor function unrelated symptoms after i.v. inoculation as seen constantly in previous experiments, there are marked discrepancies between the distribution pattern of RNP positive areas in the CNS of mice in an early stage of the disease and in the progressed and late stages. Also in this context, it is surprising that infection of spinal motor neurons and motor cortical areas as well as other motor function related structures such as the inferior olive and the cerebellum seem not to be sufficient to elicit paralysis, since all these structures are affected in animal a12 and in part also in a11, but both mice did not show any signs of paralyzed limbs.

In addition, the assumption could be confirmed that the ganglion cells in the heart, representative for other peripheral neurons in organs, are not the origin of CNS infection after i.v. infection, at least in the timeframe that was analyzed in this study: since the cardiac neurons are innervated by neurons of the dorsal motor nucleus of vagus nerve and the nucleus ambiguus, this area should appear positive for RNP immunoreactivity if virus had travelled retrogradely from the periphery to the medulla oblongata *via* that route. However, from the three i.v. infected animals of which suitable sections could be analyzed (a6, a11, a12), none showed virus positive neurons in these nuclei.

Taken together these results show that the distribution pattern of RNP positive CNS structures after i.m. inoculation is explainable by the consecutive infection of neurons in

dependence on their connections to the motor neurons in the ventral horn of the spinal cord. In contrast, in i.v. infected mice, the forebrain can be affected independently from an infection of neurons in the spinal cord or the brain stem. In addition, retrograde transport of virus from peripheral organs also does not play a major role for the infection of the CNS after RV injection into the tail vein, if at all. The results also emphasize that the cause for a certain symptomatic occurrence is not easily explicable by the distribution pattern of affected CNS regions.

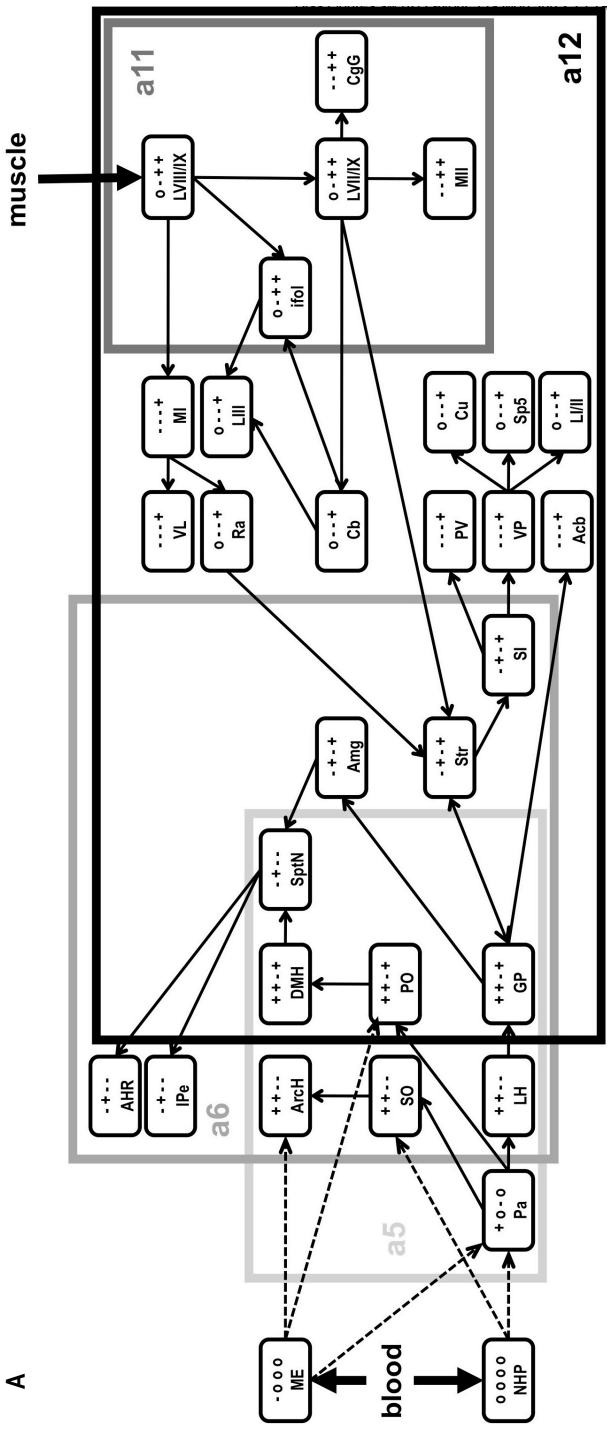

Fig. 22: Potential migration pathways of RV in the CNS after (A) i.v. or (B) i.m. inoculation.
See next page for details.

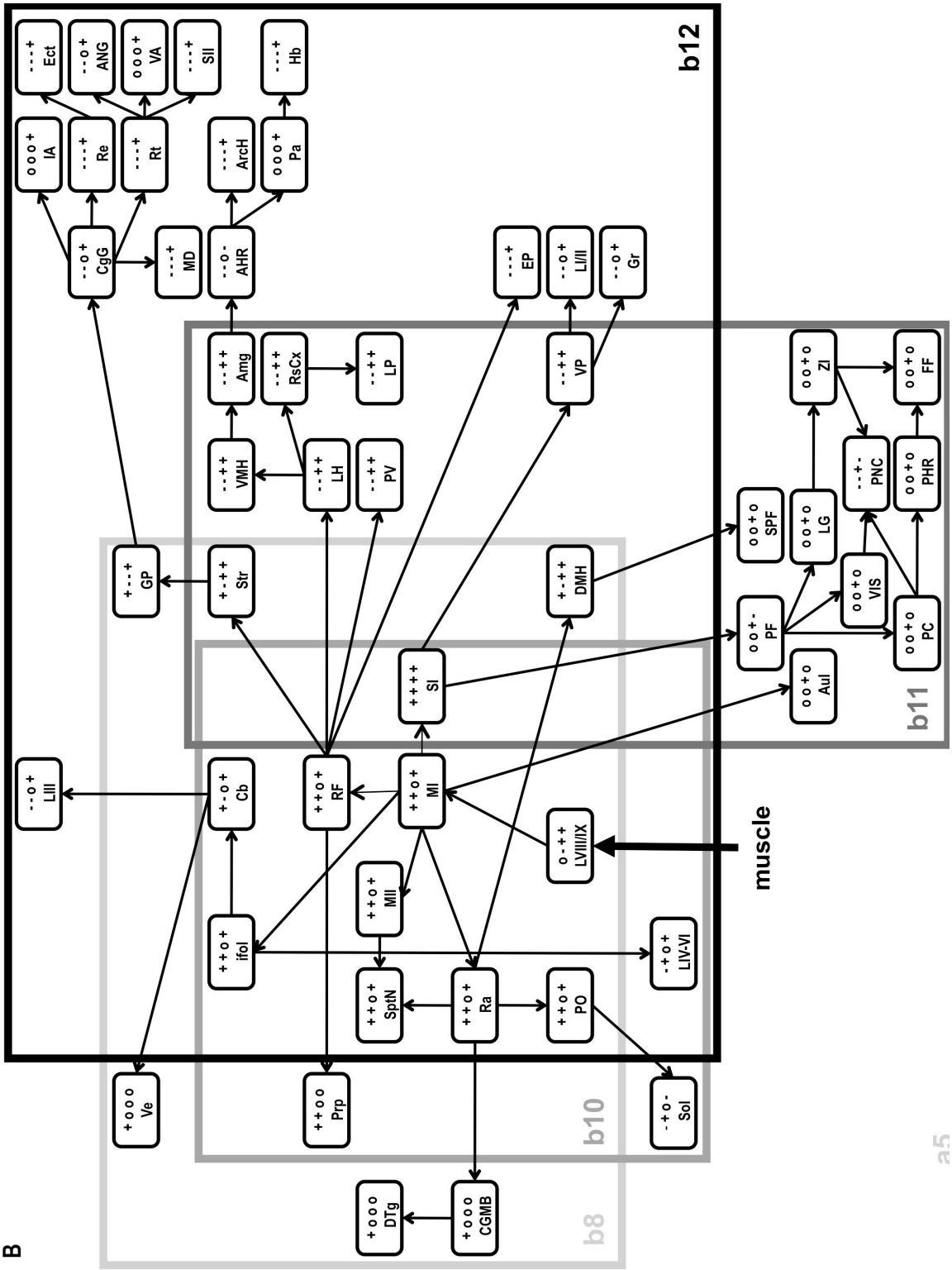

Fig. 22 continued:
Immunohistochemically stained sections of brains and spinal cords from animals a5, a6, a11, a12 (**A**) and b8, b10, b11 and b12 (**B**) were analyzed for the presence or absence of immunoreactivity against RNP in all structures displayed on the respective section plane (also compare figure 21 as well as table 4; see table 5 for abbreviations). Distinct structures were identified using a stereotaxic mouse brain atlas [296]. Potential migration pathways between RNP positive cortical areas and nuclei were composed manually using the BrainInfo database (http://braininfo.rprc.washington.edu/) for published efferent and afferent connections. Depicted connections were chosen by evaluating all possibilities regarding the best match for each animal as well as between the animals in dependence on time and morbidity. Key: **-**, structure was analyzed but negative for RNP immunoreactivity; **+**, structure was analyzed and positive for RNP immunoreactivity; **o**, structure was not analyzed; first to fourth position for animals (**A**) a5, a6, a11, a12 respectively (**B**) b8, b10, b11, b12. Black thick arrows in **A** and **B** mark the potential entries into the CNS.

Table 5: Immunohistochemically analyzed CNS structures with abbreviations.
Key: **-**, structure was analyzed but negative for RNP immunoreactivity; **+**, structure was analyzed and positive for RNP immunoreactivity; **+**, structure was analyzed and positive for RNP immunoreactivity but not included in figure 22; o, structure was not analyzed. Abbreviations in the „comment“ column: g, gray matter; w, white matter; SC, spinal cord; BS, brain stem; mo, medulla oblongata; ps, pons; mb, midbrain; CB, cerebellum; DE, diencephalon; et, epithalamus; th, thalamus; st, subthalamus; ht, hypothalamus; TE, telencephalon; fl, frontal lobe; pl, parietal lobe; ol, occipital lobe; ll, limbic lobe; bg, basal ganglia; st, septum.

abbre-viation	structure	a5	a6	a11	a12	b8	b10	b11	b12	comment
6	abducens nucleus	o	o	o	o	-	-	o	o	BS: ps; g
7	facial motor nucleus	o	o	o	o	-	-	o	o	BS: ps; g
10	dorsal motor nucleus of vagus nerve	o	-	-	-	-	+	o	-	BS: mo; g
12	hypoglossal nucleus	o	-	-	+	-	-	o	-	BS: mo; g
11n	accessory nerve	o	-	-	-	-	-	o	o	BS: mo; w
12n	hypoglossal nerve	o	-	-	-	-	-	o	-	BS: mo; w
2n	optic nerve	o	-	-	-	-	-	o	o	DE; w
4n	trochlear nerve	o	o	o	o	-	o	o	o	BS: mb; w
5n	facial nerve	o	o	o	o	-	-	o	o	BS: ps; w
8n	vestibulocochlear nerve	o	o	o	o	-	-	o	o	BS: ps; w
A1	noradrenergic group A1	o	-	-	-	-	-	o	-	BS: mo; g
A13	dopaminergic group A13	-	-	-	-	-	-	-	-	TE: fl; g
A5	noradrenergic group A5	o	o	o	o	-	-	o	o	BS: ps; g
AC	nucleus of anterior commissure	o	+	-	-	-	-	o	o	TE: st; g
ac	anterior commissure	-	-	-	-	-	-	o	-	TE; w
Acb	nucleus accumbens	-	-	-	+	-	-	o	-	TE; g
Acs5	accessory trigeminal nucleus	o	o	o	o	-	o	o	o	BS: ps; g
Acs7	accessory facial nucleus	o	o	o	o	-	-	o	o	BS: ps; g
AHR	anterior hypothalamic region	-	+	-	-	-	-	o	+	DE: ht; g
Amb	nucleus ambiguus	o	-	-	-	-	-	o	-	BS: mo; g
Amg	amygdala	-	+	-	+	-	-	+	+	TE; g
ANG	anterior nuclear group	-	-	-	-	-	-	o	+	DE: th; g
Ang	angular thalamic nucleus	-	-	-	-	-	-	-	-	DE: th; g
AP	area postrema	o	-	-	-	-	o	o	o	BS: mo; g
APS	anterior perforated substance	+	-	-	-	-	-	o	-	TE; g

abbre-viation	structure	a5	a6	a11	a12	b8	b10	b11	b12	comment
ArcH	arcuate nucleus of hypothalamus	+	+	-	-	-	-	-	+	DE: ht; g
asc	anterior spinocerebellar tract	o	-	+	+	+	+	o	+	SC; w
ast	anterior spinothalamic tract	o	-	-	-	-	+	o	+	SC; w
AuI	primary auditory cortex	-	o	o	o	o	o	+	o	TE: tl; g
AuII	secondary auditory cortex	-	o	o	o	o	o	-	o	TE: tl; g
BA	bed nucleus of accessory olfactory tract	-	o	-	o	o	o	o	-	TE; g
B	basal nucleus	-	-	-	-	-	-	o	-	TE; g
C1	adrenergic group C1	o	o	o	o	-	-	o	o	BS: mo; g
C3	adrenergic group C3	o	o	o	o	-	-	o	o	BS: mo; g
Cb	cerebellum	o	-	-	+	+	+	o	+	CB; g
CbCx	cerebellar cortex	o	-	-	+	+	-	o	+	CB; g
cc	corpus callosum	-	-	-	-	-	-	-	-	TE; w
CgG	cingulate gyrus	-	-	+	+	-	-	o	+	TE: ll; g
CGMB	central gray substance of midbrain	o	o	o	o	+	o	o	o	BS: mb; g
cing	cingulum	-	-	-	-	-	-	-	-	TE; w
Cir	circular nucleus	-	o	-	o	o	o	o	-	DE: ht; g
CL	central lateral nucleus	-	-	-	-	-	-	-	-	DE: th; g
Cl	claustrum	-	-	-	-	-	-	o	-	TE: bg; g
CM	central medial nucleus	-	-	-	-	-	-			
CnF	cuneiform nucleus	o	o	o	o	-	o			
Co	cochlear nuclei	o	o	o	o	-	-			
CP	cerebral peduncle	-	o	o	o	o	o			
cu	cuneate fasciculus	o	-	-	+	-	+			mo; w
Cu	cuneate nucleus	o	-	-	+	-	+	o	+	BS: mo; g
DMH	dorsomedial nucleus of hypothalamus	+	+	-	+	+	-	+	+	DE: ht; g
DRt	Koelliker-Fuse nucleus	o	o	o	o	-	o	o	o	BS: mo; g
Dt	dentate nucleus	o	o	o	o	+	-	o	o	CB; g
DTg	dorsal tegmental nucleus	o	o	o	o	+	o	o	o	BS: mb; g

abbre-viation	structure	a5	a6	a11	a12	b8	b10	b11	b12	comment
ex	external capsule	-	-	-	o	+	-	+	+	TE; w
Ect	ectorhinal cortex	-	-	-	-	-	-	-	+	TE; g
eml	external medullary lamina	-	o	o	o	o	o	-	o	DE: th; w
EP	endopiriform nucleus	-	-	-	-	-	-	-	+	TE: bg; g
exc	extreme capsule	o	-	-	-	-	-	o	o	TE; w
Fas	fastigial nucleus	o	o	o	o	+	+	o	o	CB; g
FF	fields of Forel	-	o	o	o	o	o	+	o	DE: st; w
FG	fasciolar gyrus	-	o	o	o	o	o	-	o	TE: ll; g
fi	fimbria of hippocampus	-	-	-	-	+	-	-	-	TE: ll; w
fx	fornix	-	-	-	-	-	-	-	-	TE; w
GH	gemini hypothalamic nucleus	-	o	o	o	o	o	-	o	DE: ht; g
GP	globus pallidus	+	+	-	+	+	-	-	+	TE: bg; g
gr	gracile fasciculus	o	-	+	+	-	-	o	+	SC; BS: mo; w
Gr	gracile nucleus	o	-	-	-	-	-	o	+	BS: mo; g
Hb	habenula	-	-	-	-	-	-	-	+	DE: et; g
hbc	habenular commissure	-	o	o	o	o	o	-	o	DE: et; w
hip	habenulo-interpeduncular tract	-	-	-	-	-	-	-	-	DE: et; BS: mb; w
IAT	interanterior thalamic nuclei	-	o	-	o	o	o	o	+	DE: th; g
IC	inferior colliculus	o	o	o	o	-	o	o	o	BS: mb; g
ic	internal capsule	-	-	-	+	-	-	+	+	TE; w
ICB	infracerebellar nucleus	o	o	o	o	-	-	o	o	CB; g
icp	inferior cerebellar peduncle	o	-	-	-	-	-	o	o	CB; w
ifol	inferior olive	o	-	+	+	+	+	o	+	BS: mo; g
IG	indusium griseum	-	-	-	-	-	-	-	+	TE: ll; g
IMA	intramedullary thalamic area	-	o	o	o	o	o	-	o	DE: th; g
IMT	intermedial thalamic nucleus	-	-	-	-	+	-	-	-	DE: th; g
In	nucleus intercalatus	o	-	-	-	-	-	o	o	BS: mo; g
In5	intertrigeminal nucleus	o	o	o	o	-	o	o	o	BS: ps; g
Ins	insula	-	-	-	-	-	-	o	-	TE; g
IP	interposed nucleus	o	o	o	o	+	+	o	o	CB; g

abbre-viation	structure	a5	a6	a11	a12	b8	b10	b11	b12	comment
IPe	intermediate periventricular nucleus	-	+	-	-	-	-	-	-	DE: ht; g
IS	inferior salivatory nucleus	o	o	o	o	-	-	o	o	BS: mo; g
LD	lateral dorsal nucleus	-	o	-	o	o	o	o	-	DE: th; g
LG	lateral geniculate nucleus	-	o	-	o	o	o	+	o	DE: th; g
LH	lateral hypothalamic area	+	+	o	o	o	o	+	+	DE: ht; g
LI, LII	Rexed laminae I, II	o	-	-	+	-	-	o	+	SC; g
LIV, LV, LVI	Rexed laminae IV, V, VI	o	-	-	-	-	+	o	+	SC; g
ll	lateral lemniscus	o	o	o	o	+	o	o	o	BS: ps; w
LOT	nucleus of lateral olfactory tract	-	o	-	o	o	o	o	-	TE; g
LP	lateral posterior nucleus	-	-	-	-	-	-	+	+	DE: th; g
lst	lateral spinothalamic tract	o	-	-	+	-	+	-	+	SC; w
LVII	Rexed lamina VII	o	-	-	+	-	+	o	-	SC; g
LVIII, IX	Rexed laminae VIII, IX	o	-	+	+	+	+	o	+	SC; g
LX	Rexed lamina X	o	-	-	+	-	+	o	+	SC; g
mcp	middle cerebellar peduncle	o	o	o	o	+	o	o	o	CB; w
MD	medial dorsal nucleus	-	-	-	-	-	-	-	+	DE: th; g
ME	median eminence	-	o	o	o	o	o	-	o	DE: ht; w
Me5	mesencephalic nucleus of trigeminal nerve	o	o	o	o	-	o	o	o	BS: mb; g
me5	mesencephalic tract of trigeminal nerve	o	o	o	o	-	o	o	o	BS: mb; w
mfb	medial forebrain bundle	+	+	-	-	-	-	+	+	DE: ht; w
MI	primary motor cortex	-	-	-	+	+	+	o	+	TE: fl; g
MII	supplementary motor cortex	-	-	+	+	+	+	o	+	TE: fl; g
ml	medial lemniscus	-	o	o	o	-	-	-	o	BS: mo, mb; DE; w
mlf	medial longitudinal fasciculus	o	-	-	+	+	+	o	-	BS; w
Mo5	motor nucleus of trigeminal nerve	o	o	o	o	-	o	o	o	BS: ps; g
MTG	middle temporal gyrus	-	o	o	o	o	o	o	o	TE: tl; g

abbre-viation	structure	a5	a6	a11	a12	b8	b10	b11	b12	comment
mthh	mammillothalamic tract of hypothalamus	-	-	-	-	-	-	+	-	DE: ht; w
NDB	nucleus of diagonal band	-	+	-	-	-	-	o	+	TE: st; g
NHP	neurohypophysis	o	o	o	o	o	o	o	o	DE; w
nsf	nigrostriatal fibers	-	-	-	-	-	-	-	-	BS: mb; DE; TE: bg; w
olf	olfactory tract	-	-	-	-	-	-	o	-	TE; w
opt	optic tract	-	-	-	-	-	-	-	-	DE; w
osp/ spo	olivospinal/spino-olivary tract	o	-	-	+	-	+	o	+	SC; BS: mo; w
Pa	paraventricular nucleus of hypothalamus	+	o	-	o	o	o	o	+	DE: ht; g
Pa5	paratrigeminal nucleus	o	-	-	-	-	-	o	-	BS: mo; g
PAR	parasubicular area	o	o	o	o	-	o	o	o	TE; g
PBN	nucleus parabrachialis	o	o	o	o	-	o	o	o	BS: ps; g
PC	paracentral nucleus	-	-	-	-	-	-	-	-	DE: th; g
pc	posterior commissure	-	o	o	o	o	o	-	o	BS: mb; w
Pe5	peritrigeminal zone	o	o	o	o	-	o	o	o	BS: ps; g
PF	parafascicular thalamic nucleus	-	o	o	o	o	o	+	-	DE: th; g
PHR	posterior hypothalamic region	-	o	o	o	o	o	+	o	DE: ht; g
Pi	pineal body	o	o	o	o	o	o	o	o	
PII	parietal association cortex	-	-	-	-	-	-	-	-	TE: pl; g
PNC	posterior nuclear complex	-	-	-	-	-	-	+	-	DE: th; g
PO	preoptic nuclei	+	+	-	+	+	+	o	+	DE: ht; g
PPA	prepyriform area	-	-	-	-	-	-	-	+	TE; g
PPY	parapyramidal nucleus	o	o	o	o	-	-	o	o	BS: mo; g
Pr5	principal sensory nucleus of trigeminal nerve	o	o	o	o	-	o	o	o	BS: ps; g
PRC	precommissural nucleus	o	o	o	o	o	o	+	o	BS: mb; g
PRh	perirhinal cortex	-	-	-	-	-	-	-	-	TE; g
Prp	nucleus prepositus	o	o	o	o	+	+	o	o	BS: mo; g
PRu	prerubral field	-	o	o	o	o	o	+	o	DE: st; g

abbre-viation	structure	a5	a6	a11	a12	b8	b10	b11	b12	comment
PS	parastrial nucleus	-	-	-	-	-	-	o	-	TE: st; g
psc	posterior spinocerebellar tract	o	-	-	+	-	-	o	+	SC; BS: mo; w
PSol	parasolitary nucleus	o	-	-	-	-	-	o	o	BS: mo; g
PSTN	parasubthalamic nucleus	-	o	o	o	o	o	+	o	DE: st; g
PT	paratenial nucleus	-	-	-	-	-	-	o	-	DE: th; g
PTA	nucleus of pretectal area	-	o	o	o	o	o	-	o	BS: mb; g
PV	paraventricular nucleus of thalamus	-	-	-	+	-	-	+	+	DE: th; g
py	pyramidal tract	o	-	-	+	+	+	o	+	SC; BS; w
Ra	raphe nuclei	o	-	-	+	+	+	-	+	BS; g
Re	reuniens nucleus	+	-	-	-	-	-	-	+	DE: th; g
RF	reticular formation	o	-	+	+	+	+	o	+	BS; g
Rh	rhomboidal nucleus	-	-	-	-	-	-	-	-	DE: th; g
rs	rubrospinal tract	o	-	-	-	-	-	o	-	SC; BS: mo; w
RsCx	retrosplenial cortex	-	-	-	-	-	-	+	+	TE; g
Rt	thalamic reticular nucleus	-	-	-	-	-	-	-	+	DE: th; g
rts	reticulospinal tract	o	-	-	+	-	+	o	+	BS: mo; w
SAG	sagulum	o	o	o	o	-	o	o	o	BS: ps; g
SCh	suprachiasmatic nucleus	-	-	-	-	-	-	o	-	DE: ht; g
SCO	subcommissural organ	-	o	o	o	o	o	-	o	BS: mb; g
scp	superior cerebellar peduncle	-	o	-	o	+	o	+	o	CB; w
SFi	septofimbrial nucleus	-	-	-	-	-	-	o	-	TE: st; g
SFO	subfornical organ	-	-	-	-	-	-	o	-	DE; g
SH	septohippocampal nucleus	-	-	-	-	-	-	o	-	TE: st; g
SI	primary somatosensory area	-	+	-	+	+	+	+	+	TE: pl; g
SII	secondary somatosensory area	+	-	-	-	-	-	-	+	TE: pl; g
SIn	substantia innominata	-	-	-	-	-	-	o	-	TE; g
SLg	sublingual nucleus	o	-	-	-	-	-	o	o	BS: mo; g
sm	stria medullaris of thalamus	-	-	-	-	-	-	-	-	DE: th; w
SM	submedial nucleus	-	-	-	-	-	-	-	-	DE: th; g

abbre-viation	structure	a5	a6	a11	a12	b8	b10	b11	b12	comment
SMT	submammillothalamic nucleus	-	o	o	o	o	o	-	o	DE: ht; g
SO	supraoptic nucleus	+	+	-	-	-	-	-	-	DE: ht; g
SoC	supraoptic crest	-	-	-	-	-	o	-	o	DE: ht; g
sol	solitary tract	o	-	-	-	-	-	o	-	SC; BS: mo; w
Sol	solitary nucleus	o	-	-	-	-	+	o	-	BS: mo; g
SOl	superior olive	o	o	o	o	-	o	o	o	BS: ps; g
Sp5	spinal trigeminal nucleus	o	-	-	+	+	+	o	+	BS: mo, ps; g
SPF	subparafascicular thalamic nucleus	-	o	o	o	o	o	-	o	DE: th; g
spt5	spinal trigeminal tract	o	-	-	-	+	-	o	-	BS: mo, ps; w
SptN	septal nuclei	+	+	-	+	+	+	o	+	TE: st; g
st	stria terminalis	-	-	-	-	-	-	-	+	TE; w
STh	subthalamic nucleus	-	o	o	o	o	o	-	o	DE: st; g
Str	striatum	-	+	-	+	+	-	+	+	TE: bg; g
StT	nucleus of stria terminalis	-	+	-	+	+	+	o	+	TE: st; g
SubC	nucleus subceruleus	o	o	o	o	-	o	o	o	BS: ps; g
SubG	subgeniculate nucleus	-	o	o	o	o	o	+	o	DE: th; g
SubI	subincertal nucleus	-	-	-	-	-	-	-	-	TE: fl; g
SUT	supratrigeminal nucleus	o	o	o	o	+	o	o	o	BS: ps; g
TM	tuberomammillary nucleus	-	o	o	o	o	o	-	o	DE: ht; g
TrH	terete hypothalamic nucleus	-	o	o	o	o	o	-	o	DE: ht; g
ts	tectospinal tract	o	-	-	+	+	+	-	+	SC; BS: mo; w
TS	triangular septal nucleus	+	o	-	o	o	o	o	-	TE: st; g
tz	trapezoid body	o	o	o	o	-	o	o	o	BS: ps; w
VA	ventral anterior nucleus	-	o	-	o	o	o	o	+	DE: th; g
Ve	vestibular nuclei	o	o	o	o	+	o	o	o	BS: mo; g
VI	striate area 17	-	o	o	o	o	o	-	o	TE: ol; g
VIS	visual cortex	-	o	o	o	o	o	+	o	TE: ol; g
VL	ventral lateral nucleus	-	-	-	+	-	-	-	-	DE: th; g

abbre-viation	structure	a5	a6	a11	a12	b8	b10	b11	b12	comment
VM	ventromedial thalamic nucleus	+	-	-	-	-	-	-	-	DE: th; g
VMH	ventromedial nucleus of hypothalamus	-	-	-	-	-	-	+	+	DE: ht; g
VP	ventral posterior nucleus	-	-	-	+	-	-	+	+	DE: th; g
vs	vestibulospinal tract	o	-	-	+	-	-	o	-	SC; BS: mo; w
VTA	ventral tegmental area	o	o	o	o	-	o	o	o	BS: mb; g
X	nucleus X	o	o	o	o	-	o	o	o	BS: mo; g
Xi	xiphoid thalamic nucleus	-	o	-	o	o	o	o	-	DE: th; g
Y	nucleus Y	o	o	o	o	-	o	o	o	BS: mo; g
ZI	zona incerta	-	o	-	o	o	o	+	o	TE: fl; g
ZL	zona limitans	-	-	-	-	-	-	o	-	TE: st; g

7. Discussion

7.1. The Rationale for the Selection of DOG4 and rSB as Model Rabies Virus Strains

The present study was carried out with two RV strains of GT I, namely a canine wildtype isolate DOG4 and the recombinant rSB, who is a clone of the bat-derived wildtype isolate SHBRV18.

Most previous studies of RV pathogenesis used laboratory strains like CVS and its variants, for example non-pathogenic derivatives of the SAD strain. On the other hand, street RV isolates from skunks and dogs that are not systematically characterized are used. This makes it difficult to compare results and to validate their relevance for the pathogenesis of those strains that have the largest impact on human health. Therefore, the selection of model strains for the present work was considered important.

Globally, human rabies is most often contracted through encounters with rabid dogs. Thus, canine RV strains should be of greatest interest if studying the disease in the laboratory. In addition, since bat-related rabies is emerging on five continents, the responsible strains may not be disregarded. Taking these considerations into account, it was decided to include a dog-derived classical as well as a bat-derived non-classical RV in the experiments.

Most molecular studies and experimental *in vivo* experiments with aerial RV have been carried out with GT I strains, and only recently attention in this regard is paid more and more also to GT V and VI (EBLV 1 and 2). From the GT I RV bat strains, isolates from silver-haired bats (SHBRV) are of special interest, since they are responsible for seventy-five percent of bat-related human rabies cases in the United States of America [133].

One report that compared a SHBRV isolate with the Mexican dog/coyote RV strain (COSRV) revealed that the bat-derived strain was in advantage in producing infectious particles in fibroblasts and epithelial cells. It also was less temperature sensitive than the canine strain. However, it showed a reduced neurovirulence in mice if administered i.m., while it was similar effective after intracranial or intradermal inoculation [275]. Thus, though

belonging to the same GT and being endemic in the same geographical region, SHBRV and COSRV differ greatly in their features [275].

Dietzschold *et al*. [101] compared in an extensive study eleven SHBRV and eight dog-derived isolates (DRV). They confirmed and broadened the findings made by Morimoto and coworkers regarding the lower temperature sensitivity of SHBRV and the susceptibility of non-neuronal cells to this virus, which was on average tenfold higher. Although the SHBRV RV G sequences were less genetically diverse among the different isolates than those of the canine-derived RV G proteins, the results for the grade of neurotropism varied more than for the DRV variants. Also, their pathogenicity, which was overall not significantly different from the DRV strains, exhibited a strong negative correlation to the level of temperature sensitivity. Among the examined isolates were also the human brain isolates DOG4 and SHBRV18, which share only 89.6% homology in the amino acid sequence of the variable regions in the central domain of the G protein (aa 176 to 337). Regarding the neuronal specificity, both strains lie closely to their group averages, which is also true for the pathogenicity and temperature sensitivity of DOG4. In Dietzschold's experiments, SHBRV18 was more sensitive for temperature and not as pathogenic in mice as the average of the bat-derived RV group. However, it grew well in cell culture, which led to its selection for further studies (personal communication with B. Dietzschold) such as the generation of a recombinant virus based on its nucleotide sequence in order to elucidate which genomic elements contribute to the neuroinvasiveness of street RV [110]. The resulting recombinant SHBRV18 (SB0; here: rSB) behaved indistinguishable from its template strain in *in vivo* and *in vitro* experiments [110].

Thus, for the conduction of the present study, DOG4 and rSB were considered as suitable representatives of the two GT I RV groups that cause the most human fatalities, since they are both well characterized *in vitro* as well as *in vivo*.

7.2. The Relevance of Intravenous Inoculation for Naturally Occurring Rabies Virus Infections

Experimental RV *in vivo* infections are usually initiated by i.m., intranasal (i.n.) or i.c. inoculation, and lead to different outcomes depending on the strain that is administered.

Within these three modi the administration of virus into a muscle is likely to imitate best the most often naturally occurring infection route.

Beside an intradermal component, the natural i.m. inoculation always consists also of a vascular part due to the rapture of vessels caused by the bite of the rabid animal for example, by which the disease is transmitted. The well documented neurotropism and neuroinvasiveness of RV usually lead to a broad infection of the brain, originating from the sensory and motor nerve fibers that densely innervate muscle tissue. It is not known how many virions are actually transmitted through a bite. However, it is most likely that the amount of virions that is retained within the tissue at the inoculation site outnumbers by far the share that is distributed incidentally throughout the organism by lymphatic or blood vessels, what was also shown in this study (Fig. 12 and 16). Consequently, the resulting onset and symptoms of the disease are determined by the rapid entry into and migration within the neural network, which covers all other events that might be initiated in the periphery by vascularly distributed virions. These, however, could play a role if only few particles are transmitted, either because the bite incident occurred when the virus has not reached its maximum concentration in the saliva yet, or because the intrusion of virions was minimally invasive as it often seems to be the case with bat-related rabies.

In order to maximize the share of virus that is distributed in the organism by the vascular system, the infection of animals by injection of virus into one of the tail veins was chosen. Subsequently, this reduces the numbers of virions that finally get to possibly susceptible cells in the periphery. In this way, the natural situation is mimicked, whereas the massive invasion of the nervous system emanating from one site is avoided. In addition, these conditions were considered a good way to clarify if infection of organs can occur before the virus has reached the CNS and migrates back from there to the periphery. In this way, organs might present a possible site for the harboring of virus during the long incubation periods that are sometimes observed [258, 343].

7.3. Usefulness of the TaqMan® Technique for the Absolute Quantification of Viral RNA

The direct fluorescent antibody test (FAT) on unfixed brain samples – collected *ante* or *post mortem* – is still the gold standard for confirming the diagnosis of RV infection since its

development in the late 1950 [322]. The detection of viral RNA by RT-PCR came up only in the early 1990 [105, 202, 258, 323] and has been proven to be much more sensitive than the conventional techniques [94], but also more prone to false-positive results, which still prevents it to replace FAT as trusted method of first choice in rabies diagnosis. Nevertheless, the PCR technique is under constant improvement and refinement for its use in that area [237, 280, 299], since the possibility to detect the presence of RV in *ante mortem* collected samples like saliva or liquor [90, 290] is only one of its advantages over FAT.

Beside rabies diagnosis, modified PCR methods such as the combination of hemi-nested primers and subsequent Southern blot hybridization [158] or restriction fragment length polymorphism analysis after a strain-specific RT-PCR [181] are of special interest when it comes to the discrimination of different lyssavirus genotypes or RV and RRV strains. The use of specific oligonucleotide probes in PCR enzyme linked immunosorbent assays [45] or the direct application of genotype-specific TaqMan® probes [44] proved also to be helpful in this question. The technique to add fluorogenic oligonucleotides to a PCR which provide information about the current amount of contained template molecules during the reaction by exploiting the 5' exonuclease activity of the Taq DNA polymerase and the fluorescence resonance energy transfer between a fluorescence molecule at the 3' end and a quencher at the 5' end of the probe, came up first in the early nineties [172, 222, 242]. Adaptations of this real-time PCR method were soon developed for the quantification of specific templates such as viral genomes [276].

For the present study it was also chosen to design strain specific TaqMan® RT-PCR assays in order to quantify the viral load in tissues, since they are more accurate and robust while less time consuming than alternative procedures such as including intercalating fluorescing DNA dyes like Syber Green into the PCR reactions. Highly specific hybridization between probe and template may be of advantage if discriminating different but still similar templates. On the other hand however, it means that sequence specificity of the designed primers as well as the fluorescence and quencher labeled TaqMan® probes is a prerequisite, since mismatches, especially in the central part of an oligonucleotide, lead to false-negative results and reduce PCR efficiency. This would be detrimental, particularly when this method is not used for qualitative conclusions but for quantification [122, 137, 177, 306].

In consequence, separate sets of primers and probes had to be designed for DOG4 and rSB and an own standard curve for every set of oligonucleotides to be generated in order to get reliable PCR efficiencies which allowed for the most accurate calculation of template molecules. Efficiencies between ninety and hundred percent are usually accepted. In this study, the conditions of the four oligonucleotide sets that were used produced efficiencies between ninety-two and hundred percent and were able to reliably quantify as low as hundred initial template copies.

Absolute quantification by a standard curve based on amplifications of known amounts of starting molecules was preferred to the common strategy to relate the Ct values of the gene of interest in one sample to the Ct values obtained by the amplification of one or more housekeeping genes in the same sample, because it was previously shown that RV influences the gene transcription of its host cell and thus is likely to falsify the results by altering the amounts of housekeeping genes, especially during the late stages of the infection [122, 137, 306]. Total RNA from tissues was reverse-transcribed using the gene-specific reverse primer of the suitable qPCR oligonucleotide set instead of random oligonucleotides or oligo(dT) primers to maximize sensitivity and specificity of the reverse transcription reaction. Consistency of the reaction efficiency was confirmed for each primer by comparison of the performance of multiple cDNA samples derived from the same RNA.

In order to distinguish between negative- and positive-stranded viral RNA, the primers for the detection of gRNA were designed to amplify an amplicon that spans the leader – RV N gene border, while the primer pairs for positive sense RNA hybridized within the sequence of RV N. During the replication of RV, not only negative-stranded gRNA molecules and viral mRNA are generated but although positive-stranded intermediate gRNA which are also recognized by the primers and probes for RV N mRNA. These sense genomes are randomly incorporated into budding virions and lead to non-infectious particles [114]. Finke and Conzelmann reported a ratio of forty-nine to one between budded SAD L19 virions with the correct genome orientation and those with an inverted sequence and found this relation also inside the cell. Own experiments with the primers and probes for rSB gRNA and mRNA revealed a ratio of eighteen to one in RNA isolated from purified virions. This has to be kept in mind when evaluating the qPCR results obtained for the various tissue RNA. The alternative use of oligo(dT) primers in reverse transcription would have been no guarantee to circumvent this issue, since the RV genome possesses stretches of uracils between the

transcription frames of genes that usually serve as template for the L protein to generate a poly(A) tail at the 3' end of nascent viral mRNAs. However, oligo(dT) primers could bind to those sequences, too, and lead to the same or even a larger error, since oligo-uracil stretches exist in every IGR.

The qPCR assay designed for this study proved to be a reliable, consistent and sensitive method to absolutely quantify RV gRNA and mRNA in various tissues. Its use was already transferred and adapted to other RV strains and published [108, 352].

7.4. Implications of the Long-term Persistence of DOG4 in the CNS of Healthy Mice

In contrast to Dietzschold's report [101] the recombinant clone of SHBRV18 was as pathogenic as DOG4, causing ninety to hundred percent lethality in mice when inoculated into the gastrocnemius muscle. In fact, mice died even faster than after infection with the canine strain: fifty percent of rSB inoculated mice were dead on average after 7.5 days versus 10.5 days following DOG4 injection with the same amount of ffu (Fig. 6 B, 8 and 11 B). The reason for this discrepancy may lie in the inoculum size, but this cannot be compared since Dietzschold *et al.* used the fifty percent lethal dose value obtained in *in vivo* experiments with mice as basis and the present study referred to ffu detected in a cell culture system.

The difference between rSB and DOG4 was even more striking after administration into one of the tail veins. While rSB caused death in consistently hundred percent of the mice when infected with 10^6 or more ffu, DOG4 failed totally in establishing a symptomatic infection, although mice reacted on the inoculation with a slight weight loss between day six and ten (Fig. 11 A). Thus, in contrast to rSB, the change of inoculation route rendered the infection with a usually lethal dose of DOG4 completely harmless for mice. Surprisingly, qPCR revealed the persistence of viral RNA in the CNS of i.v. infected mice for at least thirty-five weeks (Fig. 11 C, D), although at relatively low and decreasing levels.

The presence of RV in apparently healthy animals has been reported before. Several cases have been described, for example by Fekadu and Aghomo who were able to isolate RV from saliva and brain of naturally infected asymptomatic dogs [4], or from the saliva of a dog that recovered from the disease [111]. The fact that no viral antigen could be detected in brain

and spinal cord by immunohistochemistry is probably due to a sensitivity discrepancy between the two methods. This was also observed previously in studies with Sindbis virus, a neurotropic pathogen with a positive sense single-stranded RNA genome that causes acute encephalitis in mice which is usually cleared within eight days: virus isolation from the brain failed as soon as eight days after infection [144], viral protein was not detectable by immunohistochemistry later than two weeks and RNA by *in situ* hybridization later than twenty days after inoculation [186, 229], while demonstration of viral RNA by RT-PCR was successful as late as twenty-four weeks after infection [371].

The attempt to isolate virus from the brains of two DOG4 i.v. infected mice thirty-five weeks after the inoculation was probably unsuccessful because VNA were still present in the homogenate with which the NA cells were inoculated [184]. The VNA serum titers were high throughout the observation period of more than eight months (Fig. 11 E). This favors the categorization of this state as latent RV infection with a constant production of small amounts of proteins that provide an ongoing stimulus for the immune system, rather than as an abortive infection with residual RNP in the CNS [145]. Such a low productive rate as it is seen here suggests a mechanism to escape the immune response by controlled downregulation of viral gene expression [267]. On the other hand, VNA are able to directly restrict viral gene expression instead of mediating cytotoxic destruction of virally infected cells. This might provide an alternative explanation for the gradual decline of viral RNA over time that was observed in the present study, too [8, 100, 123, 124, 229].

For the clearance of apathogenic RV from the CNS the B cell response is the main requirement, while cytotoxic CD8 T cells are not mandatory [125, 297, 302, 340]. The restricted impact of the cellular adaptive immune response against virus-infected neurons might be caused by an ineffective major histocompatibility complex (MHC-) I mediated antigen presentation, since MHC-I are only displayed by electrically silent neurons under interferon gamma stimulation [253, 283, 369]. Thus, VNA are the main effectors against RV [174] and are able to prevent rabies if given as PEP before the onset of symptoms [14] or even to clear the infection in experimental set-ups with apathogenic variants. Hereby, VNA can reach the CNS either by crossing the blood-brain-barrier, which develops an enhanced permeability caused by pro-inflammatory processes [298], or they are produced intrathecally by invading memory B cells or plasma blasts/cells [264].

One decisive prerequisite for a timely and sufficient activation of the immune system is, however, that the virus is long enough in the periphery at sites where it cannot escape innate and cellular immunity. The findings of this study indicate that the restricted tropism of DOG4 is a main difference to rSB. Whereas rSB can directly invade cells in the periphery, for example ganglionic cells in the heart, and evade immunological surveillance mechanisms of the host organism, i.v. injected DOG4 fails to do so. Consequently, the host is able to generate a sufficiently high VNA titer and to start proinflammatory processes that lead to the sequestering of virions and the restriction of their cell-to-cell spread as well as their replication in the CNS [100]. The striking disparity between the survivorship of mice after i.v. inoculation with DOG4 or rSB (Fig. 8) as well as the strain dependent distribution of viral antigen in the CNS (Fig. 9 and 10) suggest that these results are a matter of tropism which is mainly up to RV G [110, 273]. Direct proof of this assumption in the context of the present study remains to be shown since the recovery of a chimeric rSB with a DOG4 G gene instead of its generic one has repeatedly failed.

While it usually does not present a particular problem to exchange certain genes [273] or add additional reading frames [107, 108] in apathogenic RV strains like the recombinant variants of SAD B19, wildtype RV strains appear to be especially sensitive to genome manipulation. For rSB, neither the introduction of an additional open reading frame (ORF) such as that for GFP (personal communication with B. Dietzschold), nor the exchange of the RV G gene as tried in this study yielded infectious virus particles.

As described in the introduction, the gene order in the RV genome is responsible for the number of mRNA copies that are produced from each gene. Also, the IGR play a major role in the regulation of gene expression [116]. Wildtype strains tightly regulate their gene expression. For example, the less RV G is produced and displayed on the cell surface, the more pathogenic the virus is [274]. Similar sensitive correlations might exist for the other four genes. A shift in the relation of the quantities of the single gene products and the displacement of IGR from their natural context by the introduction of an additional foreign gene might disrupt the integrity of that virus and prevent the production of infectious progeny.

Another cause of failure to generate rSB-DOG4 might lie in the inability of DOG4 G to interact properly with rSB M. The interaction between RV M and RV G is essential for the assembly of virus at the cell surface [263]. Since the G proteins of rSB and DOG4 differ from

each other remarkably [101], their physical cooperation with RV M proteins of the other strain might be impossible. This is supported by the report of Pulmanausahakul and coworkers [307], which observed an increased pathogenicity as well as a more efficient cell-to-cell spread of SN virus containing both rSB M and G instead of its own genes or only one of the two rSB genes. This emphasizes the importance of an optimal interaction between RV M and G that might have not been provided in the rSB-DOG4 virions.

From the presented data it cannot be excluded that the persistent DOG4 RNA in the CNS is able to be reactivated and to cause a fulminant encephalitis when the humoral anti-RV response is decreased as it could be shown with persistent Sindbis virus [228]. Experiments in transgenic mice deficient in the production of antibodies could elucidate this issue and provide more insight into the hypothesis that the i.v. injection of a canine RV strain might represent a suitable model to study long-term incubation periods in rabies.

7.5. The Impact of Persistent Rabies Virus Viremia

After DOG4 i.v. (Fig. 11 C, D) as well as rSB i.v. and i.m. inoculation (Fig. 15 A, B), leukocytes isolated at different time points by qPCR tested positive for RV gRNA and mRNA. Discrepancies between the detection of gRNA and mRNA that were occasionally observed can be probably attributed to the fact that the quantified amounts were often at the lower sensitivity limit of the assay.

Many viruses, like for example hepatitis B virus, measles virus or human immunodeficiency virus, use the hematogenous route to spread within an organism, either only after replication at the entry site or to get access to remote susceptible host cells directly after inoculation. In general, RV is not thought to belong to this group of viruses. Nevertheless, several investigators could show over the past decades that viremia occasionally occurs during rabies [21, 22, 243] and that animals indeed can be infected by getting in contact with blood from a rabid vector [41, 61]. However, infectivity of blood-borne RV is often restricted by antibodies that bind to RV and neutralize it, thus leading to negative results of functional tests [24, 143, 327].

In the most recent study with a qualitative TaqMan® one-step RT-PCR assay, with which murine blood was examined for the presence of RV [243], viral RNA was only detected

one hour to two days after i.m. inoculation and in the later state of the disease. In accordance with these findings, viral gRNA was substantiated after i.m. injection of rSB at two hours and two days p.i., which can be rationally explained by leakage of inoculum fluid into circulation due to injured blood vessels in the course of the infection procedure. Lodmell and his coworkers extracted RNA from whole blood and not, as in the present study, from purified leukocytes. In addition, they did not differentiate between gRNA and mRNA. The results presented here reveal however that RV might not be carried only freely by the bloodstream, but that it indeed resides in leukocytes and is able to replicate within them, as it was shown previously for *in vitro* infected immune cells [233, 310, 354]. Not surprisingly, the amounts of viral RNA to be verified in blood cells after i.v. inoculation were greater than after the classical infection route. This can be easily explained by the elevated ratio between the number of virions in the bloodstream and susceptible cells compared to i.m. injection.

In contrast to Lodmell's report, viral RNA was detected at all time points under investigation and not only in the symptomatic stages of the disease. After DOG4 i.v. inoculation, RV was even substantiated in rather constant amounts over the whole observation period of more than eight months, although mice never showed any signs for a manifested CNS infection. Thus, Lodmell's explanation for the detection of RV in blood after the onset of paralysis, namely the escape of degraded viral particles or possibly infectious virions into the bloodstream due to cell destruction in the CNS and other tissues, cannot satisfactorily explicate these findings, since apoptosis and necrosis are poorly seen in wildtype RV infections. The assay that the researchers used cannot be reconstructed because they did not clarify if they infected the mice with the same bat isolate which they took as template for the design of the primers and the dual-labeled probe. Since TaqMan® assays are sensitive for nucleotide mismatching, the PCR efficiency might not have been optimal. This might have led to a detection limit higher than in the study presented here. Moreover, direct comparison is not possible, for Lodmell and coworkers only reported the amount of total RNA that they subjected to the assay, but not absolute viral copy numbers.

There was a marked drop of viral content in the blood cell RNA from day two to day five after rSB i.v. inoculation (Fig. 16). Thoulouze *et al*. [354, 356] stated that RV elicits apoptosis in lymphocytes. They compared the effects in immune cells that were infected either with an attenuated or a highly neurovirulent laboratory RV strain and found that the ability to induce apoptosis correlated inversely with the neurotropism of a strain. The rSB

virus is highly pathogenic, but also better capable of infecting non-neuronal cells *in vitro* than DOG4, for example [101]. Thus, the reduction of viral RNA from day two on might be explainable by the induction of apoptosis in blood cells that are overladen with rSB material, while those with a still low virus load survive and serve as host cells further on. With regard to the number of viral genomes per microgram total RNA, not many infected cells persist and the transcription rate is rather low. The invasion of lymphocytes by RV could be explained by the fact that lymphocytes also express an α-bungarotoxin sensitive nAChR variant which might serve as an entry key for RV [204, 382]. Although the infection of nucleated blood cells is likely to be rather accidental *in vivo*, it could nevertheless play a role in long-term incubations, since RV is able to persist at relatively stable amounts at least up to eight months in the blood of healthy appearing mice as the DOG4 i.v. data show (Fig. 11 C).

7.6. Rabies Virus at the Inoculation Site

Replication of RV in muscle tissue at the inoculation site is still a controversial topic. As stated in the introduction, there are at least as many findings in favor for it than observations that argue against it. The present study was not primarily designed to provide new insights into that topic which would support either the one or the other point of view. Rather, examinations of the inoculation sites were undertaken because it was important to answer the question if most of the i.v. administered inoculum was removed by the bloodstream as intended, or if the majority of virions were trapped around the injection site as with i.m. inoculation.

As shown in figure 12 A, significantly less virions were retained in the tail compared to muscle tissue after i.m. inoculation, although a considerable number of viral genomes could still be substantiated. Since the standard error for the qPCR results at two hours p.i. is rather small, it is assumed that in each mouse about the same amount of virions was evenly distributed by the bloodstream throughout the body. While the number of gRNA molecules in tail tissue stays relatively stable for the first five days p.i. around 10^4 copies per microgram total RNA, there is a marked drop of viral genomes in the muscle of more than one lg level from the day of inoculation to the second day. This observation might be explained either by degradation of input virions or their migration within nerve fibers from the site of inoculation to the perikaryon of the first-order neuron.

The quantification results for rSB mRNA in the tail (Fig. 12 B) indicate that there must be susceptible cells at this site which allow the virus to replicate. Enframed by skin with hair follicles, the murine tail contains, beside nerve fibers and blood vessels, chondroid tissue, bone, tendon and muscle. Thus, a variety of cells have to be considered, such as myocytes, fibroblasts and keratinocytes. All three cell types have proven to be susceptible for RV: street RV can amplify in myotubes [361], rSB grows excellently in BSR cells, a fibroblast cell line [101, 275], and virus has also been detected in epidermal cells as well as in hair follicles of the skin [25, 189]. Keratinocytes might be a target for RV because they express an α-bungarotoxin sensitive nAChR [141].

Viral mRNA could also be quantified at the muscular injection site at all time points under investigation. The significantly steeper replication rate in muscle tissue, assessed by the slope of the regression line for the mRNA levels from day two to five p.i., indicates that there are likely to be different conditions for viral replication in the tail. The most prevalently represented cells in muscle tissue are obviously myocytes. Thus, these might be the sites at which the virus resides and finds favorable conditions – that means suitable host cell factors – for its replication.

However, looking at the findings in muscle fibers from mice that were infected with a GFP expressing RV (Fig. 12 C), the site of replication appears very restricted. The GFP pattern strongly resembles that of motor endplates. The genomes of the recombinant virus is altered in this way that the gene for GFP is an indicator for the transcription of the viral genome. The nascent GFP itself is not attached in any way to the viral proteins, thus it can diffuse independently from the virus within the cell. In this respect it is surprising that the GFP is not distributed more randomly in the myocyte cytoplasm. Altogether the possibility has to be considered that not the muscle cell is actually the site of viral amplification but the attached nerve fiber. Although still widely ignored by neurobiology textbooks evidences for an axonal protein synthesis machinery have accumulated over the last decades [135, 208, 300]. The presence of polysomes, translational initiation factors, rRNA, tRNA and aminoacyl-tRNA synthetases [180, 404] have been verified along the axon [48] as well as in axon terminals and synaptic domains [91, 196, 252]. It is suggested that the on-site translation of mRNA, which is selectively transported into the neurite [375, 389], plays intrinsically a decisive role in growth cone guidance [238] and axon regeneration [370, 390, 404], axon viability [170] and long-term potentiation/depression [40, 136, 403]. Therefore the expression

of viral proteins in nerve terminals instead of myocytes might be possible and the distinct replication patterns at the inoculation site after i.m. and i.v. injection could be based on the different density of innervation in muscle and tail, being in favor for the former.

The question of RV replication at the inoculation site would be easily answered with a recombinant virus whose genome lacks the RV G gene but expresses a fluorescent protein, as they were previously described. Such G deficient viruses were shown to fail in transsynaptic spread, thus only replicating in the first cell that they get access to [106]. The ongoing expression of the fluorescent protein leads to a strong labeling of the infected cell [384]. In this way it would become clear if RV in general or which particular RV strains replicate in non-neuronal structures at the inoculation site, or whether only nerve fibers are affected or both occurs concomitantly. Comparison between different homogeneously transcomplemented RV G deficient virus strains and a RV strain that is heterogeneously transcomplemented with G proteins from different strains would reveal hereby if possible differences are based on the cell tropism mediating RV G only, or if also the interaction between cellular and viral proteins play a role in this context.

7.7. Further Insight into the Independency of Symptoms from the Localization of Rabies Virus within the CNS

For long, researchers have tried to relate the two variants of human rabies, the paralytic and the furious form, to specific infection parameters such as the virus strain, the inoculation site or the transmitting vector [168]. So far, none of these variables proved to be responsible for the distinct symptom patterns rabies can become manifest in. Best example for the independence of disease signs from virus genetics and transmitting animal species is the report of a dog infecting two persons, one of which developed the encephalitic form of rabies, while the other patient became paralytic [164]. Previous immunohistological analyses suggested that neither the localization nor the amount of viral antigen in the CNS correlated to the appearance of different clinical signs [357]. Irrespective of the specification of the disease, spinal cord, brain stem, thalamus, hypothalamus and the basal ganglia are the preferential sites for virus replication in man [167].

7.7.1. Rabies Virus Migration Pattern after Intramuscular Inoculation

Experimental RV inoculation with DOG4 or rSB into a limb muscle of a mouse leads to paralysis in hundred percent of the morbid cases. A furious manifestation of symptoms or a disease manifestation without early motor deficits have not been observed with these two virus strains. Nevertheless, as shown in sagittal sections of spinal cord and brain (Fig. 9 and 10), virus load and distribution within the CNS at terminal stages were rather different between rSB and DOG4. Neurons of the dorsal as well as the ventral part of the spinal cord were heavily affected by DOG4, whereas rSB was detected only moderately in the ventral zones. This suggests that the backward spread from the brain to the spinal cord via afferent pathways might start earlier or be more pronounced for the canine strain. Also, this observation contradicts the proposition of others that bat-derived strains prefer sensory pathways for the invasion of the spinal cord in contrast to dog-related strains [162, 275]. In this case, after rSB inoculation, the dorsally located, mainly sensory neurons should have been more than or at least as heavily affected as the anterior motor cells. Moreover, while DOG4 on the level of the brain mainly concentrated in the midbrain tegmentum, rSB was most prominent in the cerebellum. Both structures relate to motor functions. Keeping in mind however that after rSB i.v. infection virus was also found there, while none of the mice did become paralyzed, an obvious functional connection remains elusive.

In this study, a very detailed immunohistochemical analysis was undertaken to localize RV antigen in the CNS dependent on time and disease progress after i.v. or i.m. inoculation with rSB. Only few studies are published which trace RV systematically, often restricted to the specification of brain superstructures or to the analysis of the brain stem. One report exists with a qualitative and quantitative comparison of virus distribution patterns in skunks after inoculation with either CVS (i.n.) or a street RV strain (i.m. or i.n.) [339]. The animals developed paralytic (CVS) or furious (street RV) rabies. They were sacrificed at the appearance of symptoms and their brains were serially sectioned from the spinal cord to the olfactory lobe and subsequently immunostained for RV antigen. Surprisingly, the authors stated that the distribution of RV antigen in those animals that were infected with street RV was the same regardless of the infection route. Also, the comparison of the fifty-one analyzed areas between the two different virus strains after i.n. inoculation resulted only in few marked differences: there was more street RV than CVS antigen in motor cranial nerve nuclei (hypoglossal nucleus, facial nucleus, motor nucleus of the trigeminal nerve) as well as in the

red nucleus and the midbrain raphe nuclei. On the other hand, CVS antigen was more prominent than street RV in cerebellar Purkinje cells, the epithalamic habenular nuclei, the neocortex and the olfactory lobe. A correlation between these few differences and the aggressive behavior of the street RV infected animals on the one side, and the motor deficits of the CVS inoculated skunks on the other is not easy to draw. Moreover, only one time point and stage of disease was analyzed which did not allow for the attempt to elucidate the possible pathways of virus propagation into and within the CNS. The fact that there were basically no differences in the dissemination patterns after i.m. and i.n. inoculation with street RV would be interesting to investigate in further detail.

In another study using brains from skunks which were in an early asymptomatic stage of the disease, Charlton and coworkers [70] found the reticular formation to be a very important transit zone for viral spread after i.m. inoculation with street RV. From the different amounts of viral antigen in the examined skunk brains they draw the conclusion that in the earliest stage RV was restricted to motor related areas such as the primary motor cortex in the frontal telencephalic lobe and the red nucleus in the midbrain. Furthermore, RV occurred in the inferior olive as well as in the lateral vestibular nucleus and the cerebellar nucleus interpositus. Later, virus spread to the ventral posterior complex of the thalamus which relays sensory information from the spinal cord and the dorsal column nuclei (gracile and cuneate nucleus) in the medulla oblongata. These two zones were also to be found positive for viral antigen. The described spatiotemporal pattern suggests viral invasion from the spinal cord to the brain through pyramidal and extrapyramidal efferent pathways to brain stem (red nucleus, reticular formation, vestibular nucleus, inferior olive) and neocortex (primary motocortex) and the further dissemination from cortical areas to sensory system structures (ventral posterior complex of thalamus, dorsal column nuclei) *via* afferent connections.

In the present study now, similar but more detailed findings were made in mice inoculated i.m. with rSB and sacrificed at different stages of the disease. On average more than eighty CNS structures from the spinal cord to the forebrain were analyzed on various levels with several serial frontal sections each. Other studies in mice, comparable in this detail, do not exist. Taking only those connections between different nuclei and cortical areas into account for which a published reference exists in the BrainInfo database (http://braininfo.rprc.washington.edu) it was possible to conclusively retrace the potential invasion and migration pathways of RV after i.m. inoculation (Fig. 22 B). Hereby, almost all RNP

positive structures as well as individualities between the animals could be factored in if taking the motor neurons in the ventral horn of the spinal cord as only source for the invasion of RV into the CNS (Fig. 22 B, red arrow). Of course, numerous further interconnections between analyzed regions exist by which RV might have been also transported and disseminated. These were skipped only for the matter of reducing complexity.

As in Charlton‘s skunk brain study, the first RV immunoreactive areas in the murine CNS were mainly motor related structures in the brain stem (reticular formation, vestibular nucleus, inferior olive), the cerebellum (cortex and deep nuclei), the cortex (primary and secondary/supplementary motor cortex) and basal ganglia (striatum, globus pallidus) (Fig. 22 B, b8). This makes it tempting, again, to assign the first mild motor symptoms the mouse showed in that stage of the disease to the viral burden in these structures as causative, especially since no motor dysfunctions were observed in animals where virus had not arrived at the forebrain yet (table 4). Thus, the presence of RV in motoneurons, the spinal cord cell population which were solely RNP immunoreactive in this stage, or in higher motor centers is not sufficient to elicit paralysis. Moreover, viral RNA can be already detected in the brain much earlier than any clinical sign appears (Fig. 13, 2 hours/days p.i.). Also, at least for rSB, the results contradict the hypothesis that sensory and motor pathways are used concomitantly for the retrogradely directed progression of virus from the periphery into the CNS.

7.7.2. Direct Invasion of the CNS by rSB after Intravenous Inoculation through Secretory Circumventricular Organs

The analysis of migration pathways after i.m. inoculation with regard to the symptomatic progress of the disease gets more elucidating if taking the results for the i.v. infected group into account in parallel. In contrast to DOG4, rSB was lethal for mice if administered *via* the bloodstream. Although this inoculation route led to a slightly delayed disease onset in comparison to i.m. infected animals, it was nevertheless more effective. Furthermore, the clinical symptoms for rabies were completely different. For the i.v. inoculation, the mice became never paralyzed, but developed rather heavy general signs of sickness. In his early report from 1965, Johnson [198] described the symptoms of mice infected i.c. with CVS as follows: „[…] *the mice remained well for 4 to 5 days after which their fur became ruffled and activity decreased. Over the following 24 to 48 hours the mice became increasingly docile and hypoactive, their legs often were extended or abducted,*

respiration became labored […]. *When moved, the mice were grossly unsteady* […] *and when lifted by the tail a fine tremor of the whole body was often seen, but no convulsions. The mice remained in this moribund state for 1 to 5 days and often appeared dead until moved.*“. This description fits very accurately the symptomatic appearance of i.v. infected mice in this study.

Our suspicion that i.v. inoculation leads to a direct invasion of the brain by rSB is supported by the fact that not only negative- but also positive-stranded viral RNA can be reliably detected there by qPCR as early as two hours after i.v. injection. However, localization of RNP on the protein level was successful only after four days (table 4). Johnson reported the infection of ependymal cells lining the ventricles as well as closely situated neurons. This observation could not been made in this study in any of the infected animals. Thus, the entrance of rSB *via* cerebral liquor, which is transsudated into the ventricles from vessels of the choroid plexus, and the transit into neuronal tissue *via* ependymal cells is not very likely in this case.

With regard to an experiment presented recently by Kumar *et al.* [215,], direct viral invasion through blood vessels might be proposed. Kumar and his colleagues managed to transvascularly deliver nucleic acids into neurons by using a part of the RV glycoprotein as vehicle. They designed this approach assuming that the twenty-nine amino acids long stretch of the RV G which binds to nAChR would be sufficient to overcome the blood-brain-barrier. Indeed, they were able to specifically transduce neurons by i.v. application of various small interfering RNA bound to the RV-derived vehicle. This might be also possible with whole infectious particles if the mechanism the researchers conclude from their study is really based on transcytosis mediated by nAChR that is found widespreadly on epithelial cells of brain capillaries [139]. However, the findings by immunohistochemical analysis of tissue from i.v. infected mice in the present study do not suggest in any way that RV is able to cross the blood-brain-barrier throughout the brain. This would have substantiated in a rather randomly distribution of viral antigen, which is not seen in the detailed analyses.

The third possibility for a potential invasion strategy of RV into the CNS after i.v. administration is the transit *via* circumventricular organs (CVO). These are clusters of neurons whose processes communicate directly with liquor and blood through an open blood-brain-barrier. CVO are extensively vascularized by capillaries with fenestrated endothelium. Their function is to sense many different circulating substances like glucose or cytokines in

the blood in order to initiate a central reaction to them and adapt brain functions to changing conditions in the periphery. On the other hand, the CNS also releases brain-derived mediators into the blood at these sites. Thus, CVO act as an interface between the peripheral circulation and the brain.

In mammals, eight CVO are known which can be grouped into those that are mainly sensory and also contain neuronal cell bodies, and those which consist principally of neurosecretory fibers. Sometimes the choroid plexus in the ventricles are also added to the list of CVO. The area postrema in the midline near the fourth ventricle as well as the organum vascularis laminae terminalis (supraoptic crest) and the subfornical organ close to the third ventricle form the group of classical sensory CVO. All have been analyzed for RNP immunoreactivity, but neurons as well as fibers have never shown to contain any viral antigen in any of the brains.

From the group of secretory CVO, which consist mainly of axons and glial cells, only the subcommissural organ (SCO) and the median eminence (ME) were examined. Both were free of immunoreactive antigen. The SCO takes a special position among the CVO anyway, since its capillaries are not fenestrated [320]. Thus, RV invasion at this site would not have been advantaged over the direct uptake at any site of the brain with a normal blood-brain-barrier. The remaining three CVO, the pineal gland (PG), the neurohypophysis (NPH) and the intermediate lobe of the pituitary gland, were not available for immunohistochemical staining. Like the SCO, the PG is not a classical CVO since it functions rather in an endocrine than neurosecretory way and does not essentially rely on neuronal input for signaling. It also does not transfer any information from the blood to the CNS [199]. Therefore, CNS invasion by RV through cells of the PG can be considered rather unlikely. This assumption is supported by the finding that the suprachiasmatic nucleus from which the PG receives input for the coordination of the circadian rhythm was negative in all four i.v. infected animals.

However, also not proven directly, the intrusion of rSB from vessels into the CNS retrogradely through neurosecretory fibers of the ME and the NPH is strongly implied if a close look is taken at the nuclei that bore RV antigen in the brains of two mice sacrificed four days after infection (Fig. 22 A, a5/6). In the mouse a5, hypothalamic neurons were involved almost exclusively, among them both principal nuclei that project axons to the NPH, namely the paraventricular and supraoptic nucleus. Moreover, the preoptic nuclei which release

hormones for the regulation of the secretory function of the anterior pituitary gland into the bloodstream within the region of the median eminence contained RNP immunoreactive neurons. The arcuate nucleus that is considered to form a functional complex together with the ME [402] was also positive in immunostainings for viral antigen. All other regions of the brain found to harbor RNP - mainly additional hypothalamic areas, septal nuclei and basal ganglia - can be explained by the network that exists between them and the nuclei linked to NHP and ME. The picture for animal a6 is essentially the same.

Although the hypothalamus holds essential roles in all autonomic and homeostatic tasks such as food uptake, salt and water balance, sexual behavior, circadian rhythm, body temperature and many more, and is an integrative center for the vegetative nervous system, specific signs of any disturbances of these functions related to the viral burden was not observed in mice in that stage of disease, only later on.

7.7.3. Independence of Motor Dysfunctions from Viral Burden in Function-Related CNS Areas

Conflictingly, mouse a11 which exhibited already the typical signs of i.v. transmitted rabies disease did not harbor any RV antigen in any of the analyzed hypothalamic nuclei. It was surprising that only seven CNS structures out of a total of one hundred and thirty-two analyzed nuclei, cortical areas and fiber tracts showed immunoreactivity against RNP (Fig. 22 A, a11). All of those are mainly motor related and the migration pattern strongly reminds of an i.m. infected mouse in an early stage of disease similar to animal b10, with the exception of an earlier involvement of the cingulate gyrus. The same picture holds true for the i.v. inoculated moribund mouse a12, whose pattern of infected structures resembles that of b12. The only nuclei that were exclusively RNP positive in the late stage of disease after i.v. inoculation were the nucleus accumbens and the ventral lateral nucleus of thalamus, while in the i.m. infected mouse several more thalamic and hypothalamic nuclei contained immunoreactive neurons in comparison to a12.

These findings support and broaden the observations made by others, that the cause of distinct symptoms in rabies is not to reveal within the CNS. At least, neither destruction nor neurophysiologic disturbance of motility-related neurons can be attributed to paresis since the histologic appearance of infected neurons, the overall viral load (Fig. 13, 7 days p.i.) as well as the distribution of virus (Fig. 22 A, a11/12 and B, b11/12) do not reveal any essential

distinctions in the CNS of moribund mice after i.v. or i.m. inoculation with rSB, although cardinal symptoms differ greatly. These findings are in contrast to those in mice infected with CVS in which the onset of paresis paralleled with necrosis of spinal cord motor neurons [292]. This suggests that the mechanisms causing motor dysfunction and death might be different for infections with either wildtype or laboratory RV strains.

7.8. Immunologic Determinants of Symptoms and Outcome in Murine Rabies Virus Infection

Previous studies searched for alternative explanations for the RV-induced paralysis in man and animal and claimed to have found them in the peripheral immune reactions as well as in the loss of integrity of peripheral nerves. Mitrabhakdi and colleagues [270] reported that in humans with paralytic rabies in contrast to those with a furious manifestation anterior horn cells were completely intact. However, peripheral nerves exhibited substantial demyelination and often also axon damage which was not seen in the encephalitic form. Similar was already stated by Chopra *et al.* more than twenty years earlier [78]. The demyelination and axon degeneration might be caused by the cellular and humoral anti-rabies response since paralysis cannot be observed in peripherally inoculated mice which are either generally immune suppressed by cyclophosphamide or lack T-cells due to their genetic background [184]. While mice infected peripherally with a dog-derived RV isolate did not show symptoms during immune suppression in spite of viral antigen in the CNS, the removal of immune suppression or the administration of RV antiserum to immunosuppressed animals was sufficient to provoke paralysis [344]. Transfer of T cells was required to have the same effect for athymic mice infected with a bat-derived RV isolate [349]. The observation that immunoglobulins and complement are found to deposit on RV containing axons [335] as well as the report of paralytic complications during the treatment of an encephalitic patient with anti-rabies immunoglobulin [166] argue for a decisive role of the immune response in the pathology of RV-induced paralysis.

Another indication is that in inadequately vaccinated humans and animals the phenomenon of ‘early death‘ can be observed: people and mice die faster than unimmunized controls [47, 303, 336]. Thus, whereas an early and strong antibody reaction or the timely passive immunization with RV antiserum protects, an only late or too weak response is

detrimental for the host [173, 244]. Insights into the question which immune effectors are held to be mainly responsible for the nerve damage are divided, though. VNA titers are about the same in the paralytic and encephalitic form, and most patients that present with paralysis lack RV specific cytotoxic T cell responses [164].

In the present study, the VNA titers were only insignificantly higher in mice infected i.v. with 10^6 ffu compared to i.m. inoculated animals. The differences between the corresponding mice infected with only 10^5 ffu were greater, but in both groups less antibodies were produced than after administration of the larger inoculum (Fig. 6 C). The on average higher titers after i.v. infection are likely to be the consequence of the longer incubation time and disease progress, as well as the ubiquitary distribution of RV *via* the vascular and lymphatic system resulting in an prolonged and extended exposure to immune effectors.

This more widespread dissemination of viral antigen and the replication of virus at many sites in the periphery (Fig. 14) might be the key for understanding the different symptoms of i.m. and i.v. inoculated mice, independent from RV localization within the CNS. While after i.m. administration of rSB the peripheral VNA and complement mediated response remains restricted to the nerve fibers RV uses for retrograde invasion into the CNS, the reaction in i.v. infected mice is targeted at viral antigen presented from multiple cells distributed in the whole organism causing multiorgan failure and leading to death. A decisive role of cytotoxic T cells hereby is rather unlikely since neither in the CNS of mice inoculated i.m. or i.v. with rSB, nor in the heart, which was investigated as a representative for peripheral organs, infiltration of $CD3^+$ cells occurred. This harmonizes with previous observations in which motor dysfunction was found to be dependent on the presence of $CD4^+$ T cells, VNA and viral antigen [344, 379]. Wiktor as well as Hirai and coworker even stated the suppression of the cytotoxic T cell response especially if mice were inoculated with a street RV [171, 385]. Baloul *et al.* found the upregulation of Fas ligand (FasL) in infected neurons and the induction of apoptosis in invading T cells caused by their binding to FasL as the mechanism for the inability of the cellular immune response to contribute to the control of the RV infection [28].

The hypothesis that the development of distinct symptoms and outcomes originates from the interplay of virus antigen localization and VNA presence in dependence of their timely action, the involved virus strain and its inoculation site might be a good explanatory

model for the rabies disease variants in mice presented here and elsewhere [125, 184, 292, 344, 379, 385]: peripherally inoculated wildtype isolates and cultivated strains such as rSB and DOG4 which are characterized by a rather high neuroinvasiveness [29, 331] manage to ascend to the spinal cord within peripheral nerves before this could have been prevented by innate or adaptive immune reactions. Nevertheless, in the course of the disease an antibody response is generated. This is most likely due to residual virus at the inoculation site (Fig. 12), but it could also be the result of the presentation of CNS-derived viral antigen in the cervical lymph nodes [92, 152]. Subsequently, the VNA target infected nerves and lead to demyelination and axon loss causing motor weakness and finally paresis in the inoculated limb [234]. When the virus has replicated in the CNS and starts to spread back into the periphery by viscero- and somatosensory fibers, other nerves as well as peripheral organs become further targets for the detrimental VNA response [282] which might cause paresis in additional limbs as well as the deterioration of the general health condition leading finally to death. After i.c. or i.n. inoculation, paralysis is usually not seen, because virus does not emigrate from the CNS anterogradely to the periphery, leaving motor fibers untroubled by the VNA attacks. A preferential centrifugal spread within somatosensory fibers, however, might explain the observation of paresis after i.c. inoculation with certain strains, since RV reaching muscle spindles *via* this route could infect adjacent motor fibers on second order [134, 385].

In contrast to wildtype strains, attenuated viruses often cause only local but irreversible paralysis with (e.g. PV) [125] or without (e.g. ERA) [379, 385] ascendence into the brain, or do not elicit any symptoms at all (e.g. HEP) [385]. Mice usually survive peripheral inoculation with those RV, whereby VNA titers are comparable with animals after infection with street RV [385] and also between asymptomatic and paralytic mice inoculated with the same strain [125]. The reason for the protective role of antibodies in these cases is probably due to the fact that attenuated RV strains are less neuroinvasive which means that more virus remains longer exposed to immune cells and factors at the inoculation site. Also, while the speed with which virions are transported within nerve fibers is the same for attenuated and pathogenic viruses (both types of RV use the same cell machinery), the former do not spread as effectively than the latter [185]. This and the phenomenon that they are often more antigenic by inducing apoptosis or leading to necrosis in infected cells might favor the generation of a timely and rather strong immune reaction, while the targets for the effectors

are still locally restricted and minimal [125, 184, 188, 200, 274, 308]. Thus, damage to the host‘s nervous system is kept marginally and virus can be cleared.

The production of VNA after inoculation with rSB in this study was measurable from day five p.i. on, which parallels the onset of disease after application of virions into a muscle as well as into a tail vein (Fig. 6 A and 14). The larger the inoculum was, the higher were the VNA titers reached in the terminal stage of the disease (Fig. 6 C). Also, higher titers were generally observed after i.v. inoculation (Fig. 6 C and 14 A). This corresponds well with the outcome of disease in the experimental groups: the more virions are injected into the organism and the more widespreadly they are disseminated in the body, the more the immune system gets exposed and the more effectively it can react upon the antigens and lead to a strong VNA response. Although i.v. inoculated rSB infects the brain directly (Fig. 13, Fig. 21, Fig 22 A) and replicates also at various sites in the periphery (Fig. 15), the disease progress is slightly slower, respectively much slower and not lethal, depending on the dose in comparison to i.m. infection (Fig. 6 B). This effect might be explained by the dilution of the inoculum within the blood after i.v. inoculation. Although susceptible cells at various sites are potentially reached within the organism, only few virions are likely to get really access. The multiplication of virions therefore starts from a relatively small basis. In contrast, after inoculation into the muscle, the inoculum remains rather concentrated (Fig. 12 A, B) within an environment highly favorable for virus invasion. Thus, the higher efficiency for viral spread and multiplication leads to a faster distribution of virus within the CNS (Fig. 21, left column versus right column). In the end, the time lost during the ascendence from the spinal cord to the brain after i.m. inoculation and the disadvantage of a low amount of CNS invading virions after i.v. injection level out and the same virus loads in brain and spinal cord are reached in the terminal stages of both groups (Fig. 13).

The detrimental effects that cause the distinct symptoms, however, remain concentrated to the sites where virus-harboring cells in the periphery were exposed to the immune system from early on: peripheral nerves on the one site, infected peripheral organs on the other. While the massive invasion of organs by late centrifugal spread after i.m. inoculation might have a decisive effect on the health condition of the rabid mice, the late appearance of RV antigen in motor neurons after i.v. injection, as observed in animals a11 and 12 (Fig. 22 A) might not be sufficient to elicit paralysis. In addition it cannot be clarified, if rSB reached them centrifugally from the brain, which seems to be unlikely given the prerequisite of retrograde

transport. Or if the virus load in the ventral horn of the spinal cord late in infection results from a delayed invasion *via* muscle fibers.

In contrast to rSB, DOG4 lost its pathogenicity if injected into a tail vein. Most likely due to a more restricted neurotropism in comparison to rSB [101, 275], the dilution of the inoculum in the bloodstream and the enhanced exposure to immune mediators similar to rSB i.v. inoculation, an early and strong VNA titer is generated that is able to restrict the ascending CNS infection, control viral replication and protect the host from a lethal outcome for a long time in spite of persistent viral presence (Fig. 11).

In summary, while the production of VNA is rather similar between the experimental groups, the effectiveness of VNA regarding host protection and virus control is dependent on the neurotropism and neuroinvasiveness of the infecting RV strain. Although rSB and DOG4 are similar neuroinvasive after inoculation into muscle, the broader neurotropism of rSB is advantageous for its infectiousness following distribution *via* the vascular route in comparison to DOG4. Hereby, the action of VNA against peripherally distributed antigen rather than the localization of RV within the CNS determines the manifestation of distinct symptoms.

7.9. New Findings on the Primary and Secondary Infection of Peripheral Organs - an Explanatory Model for the Route of Rabies Virus Infection after Organ and Tissue Transplantation

The observation that RV spreads centrifugally from the CNS to various peripheral organs during the late phase of the disease is rather common, in humans as well as in laboratory animals [102, 189, 197, 237, 243]. Jogai as well as Jackson and their colleagues which performed immunohistochemical studies on tissue from rabies infected humans found viral antigen in nerve plexus of multiple organs such as the submucosal and myenteric plexus of the gastrointestinal tract. The adrenal medulla was usually affected, too. In the pancreas, Jackson detected RV sometimes in islet cells, whereas Jogai only stated exocrine acinus cells to be infected. They also presented diverting results for the heart: while Jackson claimed to have stained viral antigen within cardiomyocytes, the other study could only see it in epicardial nerve twigs.

The only peripheral RV target tissue that has been tried to infect directly is the submandibular gland [69], where the virus can be found in the late stages of the disease [176, 189, 236]. The attempt, however, failed. Rather, the virus migrated from the gland *via* the sympathetic neural network centripetally into the CNS and only after having reached the medulla oblongata around the twelfth day after inoculation, virus was released as infectious particles from the salivary glands.

In the present study it was shown for the first time that RV - depending on the strain - can infect organs in the periphery directly without having to pass the CNS and to spread back centrifugally (Fig. 18). While RNA could be substantiated in all organs under investigation from as early as two hours p.i. (Fig. 15 A, E), the isolation of infectious particles at an asymptomatic stage of disease after i.v. inoculation was possible only from the heart. This was also the organ which had constant and increasing presence of viral gRNA, whereas the levels in the other organs were rather variable or decreasing over time (Fig. 15). Also, the enlargement of the i.v. inoculum in terms of virion number had the most marked effect on the virus load of the heart (Fig. 17). However, the conditions for rSB replication in the periphery do not seem very favorable given the low ratio of mRNA and gRNA copy numbers, which might result from the phenotypical nature of the cells in which virus resides in the organs.

Immunohistochemical analyses of the heart as representative for the peripheral organs showed that exclusively neurons get infected. Neither cardiomyocytes nor any type of connective tissue cells were found to be positive for RV antigen in any of the six examined hearts from i.v. infected mice.

The question arises what the difference constitutes between the heart and the other organs that leads to a better yield of infectious particles from the heart although all organs are infected. Moreover, if only neurons are susceptible, what then is the reason for the relatively low replication rates in contrast to neurons within the CNS where mRNA levels of viral genes are usually one to two logs higher than the number of gRNA present (Fig. 13).

7.9.1. Innervation Patterns of Organs Relevant for Rabies Virus Infection

All ganglionic cells within organs belong to the parasympathetic network. They present the second-order neurons which receive input from vagal nuclei in the brain stem (dorsal motor nucleus of the vagal nerve, nucleus ambiguus) or from the intermediolateral column of

the sacral spinal cord. The organs under investigation are all supplied by the former. The postganglionic fibers then reach out into the organ parenchyma to innervate mainly smooth muscle cells and glandular structures. Their main neurotransmitter is acetylcholine, but they are also rich in all kinds of neuropeptides and even monoaminergic transmitters have been found.

Ganglion cells of the liver which was the organ with the lowest susceptibility for an infection by rSB sit primarily within the hilar region and in larger portal fields [316]. In rodents, postganglionic parasympathetic fibers from these ganglia as well as sympathetic fibers originating from the coeliac ganglion are restricted to the Glisson triads, the hepatic arterial and the portal venous vasculature and do not reach into the parenchyma [13]. Central input mainly comes from the lateral and ventromedial hypothalamic nuclei for the parasympathetic respectively the sympathetic visceromotor network [207, 373]. The liver is also supplied by sensory nerve fibers which make it reactive to mechanical and thermal [2] as well as osmotic [3] and chemical [142, 324] stimuli. Viscerosensory fibers serve as sensors for circulating cytokines and metabolites such as glucose and lipids. They conduct information *via* the nodose ganglia to the nucleus of the solitary tract in the brain stem [251, 287], whereas protopathic stimuli reach higher-order CNS structures by neurons within the lower thoracic dorsal root ganglia [373]. The termination of fibers of either nature on hepatocytes and within the Disse space is still unsettled [209, 251, 316]. The fact that there is no continuous endothelium at this site would favor the uptake of virions from the bloodstream in case of adjacent susceptible fibers or cells.

For long, the kidneys were thought to be innervated only by sensory and postganglionic sympathetic fibers [36] with a predominantly efferent input only for arterial blood vessels containing smooth muscle cells as well as the juxtaglomerular apparatus [99]. Although activated by mechanical and chemical stimuli [211, 277, 313, 314], the frequency of afferent fibers was found to be considerably diminished in relation to the number of visceromotor fibers, mainly restricted to the renal pelvic region [113]. Similar to the hepatic sensory innervation, dorsal root ganglion cells relay sensory information either directly to the gracile nucleus [337] or the information is transferred to spinoreticular or spinothalamic neurons within the dorsal horn of the spinal cord [12]. Viscerosensory afferences connected to neurons from the nodose ganglia are relayed to the solitary nucleus [337]. The presence of parasympathetic fibers and neurons was doubted since findings were inconsistent [260, 269,

288, 358, 380]. In newer studies [239-241] it was revealed that ganglionic cells indeed exist but very few only. Liu and colleagues counted on average twelve somata per rat kidney, mainly in the pelvic wall, at the renal hilus and along interlobar vasculature. Morphologically and neurochemically rather heterogeneous, they form clusters, but are found often isolated, too. This and their small number probably resulted in the conflicting reports regarding their existence in the past.

Pulmonary collections of parasympathetic neurons are mainly airway ganglia since they are disseminated throughout the proximal bronchial tube walls much like neuronal cells of the enteric plexus [149, 317]. They are involved in the regulation of the bronchial caliber leading to the contraction of smooth muscle cells *via* nicotinic neurotransmission. Some larger clusters of neurons can be found, too. Baluk *et al.* for example described a constant ganglion of about two hundred neurons associated with the pulmonary vein at the tracheal bifurcation in mouse [31]. As in the other organs, first-order neurons for the parasympathetic innervation of the lung sit in the dorsal motor nucleus of the vagal nerve as well as in the nucleus ambiguus [42]. Fibers from the cervical ganglia of the sympathetic trunk run in association with bronchial blood vessels for which they provide motor input, and also innervate submucosal glands. Only mechano- and chemosensitive C-fibers are not only in the airways, but expand also into the lung parenchyma. Most of those glutamatergic afferences derive from vegetative neurons in the nodose and jugular ganglia and project to the solitary nucleus [51]. The smaller share comes from the cervical dorsal root ganglia, running together with sympathetic fibers.

The heart, finally, is the organ under investigation with the most defined collection of ganglionic cells. Ai and coworkers found about eighteen neuronal clusters in individual mouse hearts [6]. In mammals, globular as well as plain intramural ganglia [295] can be found mainly on the dorsal surface of the atria in three distinct zones which are interconnected by nerves: near the sinoatrial node, the atrioventricular node and the lower pulmonary vein [6]. They consist of a heterogeneous populations of one hundred to two hundred bipolar, unipolar and multipolar somata with differing dimensions and shapes [35]. These neurons are thought to present not only postganglionic parasympathetic neurons, but also sensory and inter-neurons [17, 18, 74, 398]. Nevertheless, as seen in own immunohistochemical analyses (Fig. 19 D - E), all cardiac neurons are positive for ChAT [223, 257], although some have aminergic and neuropeptidergic neurotransmitter in addition

[223, 271, 272, 338, 348]. The postganglionic axons of the cardiac neurons form close contacts with cardiomyocytes and conducting muscle fibers and send also terminals into connective tissue [74]. They are thought to relay cardioinhibitory modulations with respect to heart rate, atrioventricular conduction and myocardium contractility [73]. In laboratory rodents, more than fifty percent of the parasympathetic input to the cardiac ganglia can be traced back to the nucleus ambiguus [6] which targets mainly nicotinic neurons [73], while only twelve to eighteen percent derive from the dorsal motor nucleus of the vagal nerve [75], connecting to cells with muscarinic acetylcholine receptors [73]. As for the lung, sympathetic innervation of the heart arises from the cervicothoracic chain ganglia.

7.9.2. Quantity of Ganglion Cells and their Accessibility to Rabies Virus from the Vascular System Matter

The susceptibility of different organs to rSB is likely to depend strongly on the number of neurons within an organ as well as their accessibility. Liver and kidney contain only very few neurons and only at very distinct sites. Moreover, although they are very well vascularized and in spite of the relatively open blood - tissue barrier in the liver, only few virions seem to manage the invasion of these organs. Most presumably this can be attributed to the rather sparse or non-existing parasympathetic innervation in these areas.

Lung and heart both contain numerous ganglionic cells, thus rSB would come across enough potentially susceptible neuronal cells to produce progeny. However, while the cardiac postganglionic fibers reach out to the cardiac parenchyma and presumably also into the atrial lumina to sensor chemical and mechanical stimuli, the pulmonary ganglion related fibers are more associated with bronchial airways. Thus, the likelihood for an uptake of virions by them and is - again - rather small.

In all organs, invasion of the neural network could have been also occurred by sympathetic fibers, especially because they provide vessels with visceromotor innervation. Indeed, as shown for the heart in figure 19, RNP immunoreactivity was detected not only in cholinergic, but also in fibers positive for tyrosine hydroxylase, presumably sympathetic axons. Although not seen very often, such co-localizations were preferentially observed in axons adjacent to small vessels. Since this study was principally conducted to identify cells within organs that serve as primary targets for infection by RV, sympathetic ganglia have not been analyzed.

7.9.3. *Autonomic Ganglion Cells: not the Best Nursery for Rabies Virus Progeny*

The number of RNP positive neurons in cardiac ganglia four days after i.v. injection differed not significantly from what was found seven days after i.m. inoculation (Fig. 20 G, H, J, K). This is consistent also with the results on the RNA level (Fig. 15). Nevertheless, the amount of virions that could be isolated from mice were minimal in both groups, suggesting suboptimal conditions in peripheral neurons for the production of virus progeny.

This assumption is supported by the rather unusual staining pattern in comparison to the staining within CNS neurons, as well as the small share of infected ganglion cells. Jogai *et al.* observed, too, that RV antigen in extracranial organs was present rather as fine to coarse granules than blob-like masses as seen in the CNS [197]. The RNP staining in the cardiac ganglia (Fig. 20 G, H, J, K) was mainly concentrated around the nuclei of the neurons. A similar finding was reported by Ni and colleagues after infection of BHK-21 cells with the HEP strain. They interpreted the perinuclear viral material as immature envelope proteins contained within the endoplasmic reticulum due to unregulated synthesis of RV G leading finally to cytopathic effects [285]. This cannot be taken as an explanation for the staining pattern seen in this study, since the antibody that was used is directed against RNP and not RV G. Also, the infected ganglionic cells did not show signs of cell lysis. However, the unusual aggregation of viral product might be the result of the failure in correct assembly of new virions, maybe due to a missing host cell factor. An early report by Tsiang exists [364] in which he stated that autonomic ganglia are susceptible to RV, but the infected cells do not produce infectious particles efficiently. This describes very well the findings made for the cardiac ganglia in the present study: rSB infects cardiac ganglia and other organs on a direct pathway independent from the invasion into the CNS and replicates there, but at much lower rates and even much less productive than in central neurons.

It is not surprising from this perspective that the ability to directly invade peripheral autonomic neurons was only seen for rSB, but not for DOG4. The bat-derived strain is much more adaptive to different cellular environments than the canine virus. This becomes already evident when cultivating the two strains in *in vitro* systems. While rSB grows also very efficiently on fibroblast cell lines, DOG4 relies strictly on cells with neuronal character. Although ganglia cells are neuronal, of course, the fact of their inaccessibility for DOG4

together with its inability to invade the brain effectively from the periphery on other ways than *via* the common motor and sensory routes suggests that the canine strain is adjusted to certain neuronal host cells which provide an essential environment that cannot be established by other neurons. On the other hand, the susceptibility of peripheral ganglionic cells and the low rate of virus production there might present good conditions for bat-related strains to use such sites as harbors for long-term persistence.

7.9.4. Closed Gateways: no Transition of Rabies Virus from Peripheral Organs into the CNS on Nerval Pathways

The virus load itself does not seem to elicit any organ related symptoms, and without the massive inoculum that was used in this study for the i.v. injections the virus might have remained hidden from immune system behind the special immune status of neurons. In the short time the experimental infection lasted virus did not detectably ascend from the peripheral organs to the CNS after i.v. inoculation: the ventromedial hypothalamic area where the higher-order neurons for the sympathetic network lie was negative in all four brains analyzed (Fig. 22 A). The same is true for the dorsal motor nucleus of the vagal nerve and the nucleus ambiguus, both containing first-order neurons for the visceromotor efferences to the peripheral organs.

During the late state of the disease, virus rather takes somatosensory routes *via* the reticular formation or the thalamus directly to the dorsal horn of the spinal cord in order to emigrate from the CNS to the periphery. This conclusion is based on the observation that the gracile nucleus as well as the solitary nucleus which relays viscerosensible informations were negative for virus in all brains under investigation. The ventral posterior thalamus as well as the reticular formation and the dorsal horn of the spinal cord, however, contained virus-infected neurons in the progressed state of disease. After i.m. inoculation both visceromotor nuclei of the vagal nerve did not show any immunoreactivity for RNP except in one case (table 5, 10, b10).

In contrast, both hypothalamic areas mainly related to the vegetative nervous system, the ventromedial and lateral areas, were virus positive in the late stage of the disease (Fig. 22 B). The evasion by sympathetic and/or parasympathetic pathways, however, would contradict the strictly retrograde transport of RV within neuronal processes and thus is excluded from the possible pathways out of the CNS. Similar to the situation in the late phase of the disease after

i.v. inoculation, the pattern of nuclei containing RNP immunoreactive neurons rather suggests the outflow of virions from the CNS into the periphery on pathways belonging to the somatosensory system, although the usage of viscerosensory fibers cannot be excluded completely since the solitary nucleus was positive for RNP in one case.

Taken together these results suggest that, although rSB infects cardiac neurons and presumably also ganglion cells within other organs directly after distribution through the vascular system, this environment is not optimal for an efficient production of infectious progeny. Also, the invasion of the CNS by visceroefferent fibers that connect to those host cells seems to be very restricted. The infection of the CNS is realized on alternative pathways, either *via* the NPH and the ME-arcuate-complex or through access by motor fibers. In late stages of the rabies infection, virus evades the CNS regardless of the infection route preferentially through somatosensory fibers and reaches peripheral organs at a rather fast pace. Hereby, infection of neuronal cell bodies by the CNS derived virions might occur since cardiac ganglions harbored immunoreactive RNP comparable to i.v. infected animals.

Given the fact that after organ transplantation the donor organ is cut off from extrinsic autonomic input [20] as well as from sensory systems for many months, it seems rather unlikely that RV would have spread from the nerve plexus to the CNS on nerval pathways. The findings here that, even when functional connections from the infected intrinsic neurons to the CNS exist, rSB was not able to use them for the ascendence to higher-order structures, argue against such a possibility. Rather, the leakage of virus from injured sensory fibers into the bloodstream of the organ recipient during the surgical procedure and the resulting invasion of the CNS either directly or by nerve fibers terminating at other sites sounds like a more conclusive explanation for the transmission of rabies disease by organ transplantation.

Alternatively to the short-term release of virus, few infectious particles might be released from ganglion cells within organs by natural budding or during gradual loss of neurons due to the lack of nerval input. The medically induced immunosuppression of the organ recipients would favor the unresisted distribution of only few virions *via* the vascular route which otherwise might elicit a strong antibody response as seen in the experimental animals in this study.

7.10. Concluding Remarks and Outlook

It could be shown that the canine RV strain DOG4 fails while the recombinant virus rSB that is based on the bat-derived isolate SHBRV18 is able to infect organs directly and independently from the virus located in the CNS *via* non-neuronal pathways. Thus, the distinct differences in the tropism of DOG4 and rSB might explain the special features rabies that is caused by bats manifests. The investigation of the presence of viral antigen within autonomic ganglia in the periphery should become a standard if dead bats are examined, especially if the CNS is negative for RV. This would provide insight if peripheral organs are a common site for the harbor of RV in asymptomatic bats. The examination of leukocytes with sensitive methods such as qPCR should be included, too, since the finding of viral replication in blood cells during *in vivo* infection needs further confirmation.

While rSB elicits a lethal infection in mice regardless of the route on which the virus is brought into the organism, inoculation with DOG4 into a tail vein produces only a prolonged, probably VNA controlled, latent CNS infection. The experiment should be repeated in variably immunosuppressed animals to define the exact role the immune system is playing in the control of the RV infection. Other bat-derived and canine RV strains as well as isolates from other vectors should be tested for infectiousness *via* the vascular route to establish if the distribution of virus by blood might present a common feature of certain groups of strains.

The study evinced that, although bat-derived strains have a broader cell tropism in *in vitro* experiments, rSB could only be found in the periphery in neuronal cells. At least on the protein level it was never detected in any other cell type such as fibroblast or myocytes. However, the failure of DOG4 to infect peripheral neurons independent from the virus load in the brain and the distinct distributions of DOG4 and rSB in the CNS as well as the finding that not all cardiac neurons exhibit viral antigen strongly suggests the existence of a strain dependent preference for phenotypically different neurons. The search for a common denominator of all neurons that get infected by a certain RV in discrimination of those neurons that never become affected, whether it be a cytoplasmic host cell factor or a distinct molecule in the membrane, has not really taken off yet.

Finally, the examination of the routes on which rSB enters the CNS after i.m. or i.v. inoculation, and the identification of the nuclei and cortical areas it affects confirmed the observation made by others that neither the extent of viral burden nor its localization

determines the symptomatic manifestation of the rabies infection. Rather, the VNA-mediated immunity is likely to hold a very important role in this regard. Beside this, the study showed for the first time that rSB is able to invade the brain directly without passing the spinal cord, most likely *via* neurosecretory fibers on the base of the diencephalon. Together with the findings that viral RNA can be substantiated in the blood as well as that rSB seems not to have open access to fibers that connect to intrinsic neurons in organs the assumption is supported that RV contained in transplanted organs is rather brought to the CNS *via* the bloodstream than through nerves. The fact that transplanted tissue is deprived from extrinsic innervation for many months is in favor for this conclusion.

8. Abbreviations

Prefixes:

k	10^3
m	10^{-3}
µ	10^{-6}
n	10^{-9}

Physical abbreviations:

°C	degree Celcius
Da	Dalton
g	gram(s)
x g	centrifugal force
h	hour(s)
l	liter
M	mol per liter
min	minute(s)
sec	second(s)
%	percent

Organizations:

CDC	Centers for Disease Control and Prevention (http://www.cdc.gov)
WHO	World Health Organization (http://www.who.int/en)

Abbreviations for CNS structures:

see table 5

Other abbreviations:

aa	amino acid(s)
ABLV	Australian bat lyssavirus
AD	*anno domini* [Latin]
ANOVA	analysis of variance
BC	before Christ
BHK	baby hamster kidney
bp	base pair(s)
BSA	bovine serum albumin
cDNA	complementary desoxyribonucleic acid(s)
ChAT	choline acetyl transferase
CNS	central nervous system
CO_2	carbon dioxide
COSRV	Mexican dog/coyote street rabies virus
Ct	threshold cycle(s)
CVO	circumventricular organ(s)
CVS	challenge standard virus
DAB	3,3-diaminobenzidine
dATP	deoxyadenosine triphosphate(s)
dCTP	deoxycytidine triphosphate(s)
ddH_2O	double distilled water
dGTP	deoxyguanosine triphosphate(s)
DMEM	Dulbecco's minimal essential medium
DNA	desoxyribonucleic acid
DPBS	Dulbecco’s phosphate buffered saline
DRV	dog-derived rabies virus
dTTP	deoxythimidine triphosphate(s)
DUV	Duvenhague virus
EBLV	European bat lyssavirus
EDTA	ethylenediamine tetraacetic acid
FAM	6-carboxyfluorescent
FasL	Fas ligand
FAT	fluorescent antibody test
FBS	fetal bovin serum
FITC	fluorescein isothiocyanate
ffu	focus forming unit(s)
GBS	Guillain-Barré syndrome
GFP	green fluorescent protein
gRNA	genomic ribonucleic acid
GT	genotype(s)
HBSS	Hank’s balanced salt solution
i.c.	intracerebral, intracerebrally
IGR	intergenic region
i.m.	intramuscular, intramuscularly
i.n.	intranasal, intranasally
IU	international unit(s)
i.v.	intravenous, intravenously
kb	kilobase(s)
LB	lysogeny broth
LBV	Lagos bat virus

LC8	light chain 8
lg	decadic logarithm
MHC-I	major histocompatibility complex I
moi	multiplicity of infection
MOKV	Mokola virus
mRNA	messenger ribonucleic acid(s)
NA	neuroblastoma
nAChR	nicotinic acetylcholine receptor
NCAM	neural cell adhesion molecule
nt	nucleotide(s)
p75NTR	low-affinity neurotrophin receptor p75
PBS	phosphate buffered saline
PCR	polymerase chain reaction
PEP	post-exposure prophylaxis
p.i.	*post infectionem* [Latin]
qPCR	quantitative polymerase chain reaction
RFFIT	rapid fluorescent focus inhibition test
RNA	ribonucleic acid(s)
RNP	ribonucleoprotein(s)
RPMI	Roswell Park Memorial Institute medium
RRV	rabies virus related virus(es)
rSB	recombinant silver-haired bat rabies virus 18
RT	reverse transcription
RT-PCR	reverse transcription polymerase chain reaction
RV	rabies virus(es)
SAD	Street Alabama Dufferin
SHBRV	silver-haired bat rabies virus
T_a	annealing temperature
TAE	tris acetate ethylenediamine tetraacetic acid
TAMRA	6-carboxy-tetramethyl-rhodamine
TH	tyrosine hydroxylase
T_m	melting temperature
UV	ultraviolet
VAChT	vesicular acetylcholine transporter
VNA	virus neutralizing antibodies
VSV	vesicular stomatitis virus
ZNS	*Zentralnervensystem* [German]

9. Bibliography

1. **Abraham G and Banerjee AK**. The nature of the RNA products synthesized in vitro by subviral components of vesicular stomatitis virus. **Virology** (**1976**)71:230-241.
2. **Adachi A and Niijima A**. Thermosensitive afferent fibers in the hepatic branch of the vagus nerve in the guinea pig. **Journal of the autonomic nervous system** (**1982**)5:101-109.
3. **Adachi A, Niijima A and Jacobs HL**. An hepatic osmoreceptor mechanism in the rat: electrophysiological and behavioral studies. **The American journal of physiology** (**1976**)231:1043-1049.
4. **Aghomo H and Rupprecht CE**. Further studies on rabies virus isolated from healthy dogs in Nigeria. **Veterinary Microbiology** (**1990**)22:17-22.
5. **Aguilar-Sétien A, Brochier B, Tordo N, de Paz O, Desmettre P, Péharpré D and Pastoret P-P**. Experimental rabies infection and oral vaccination in vampire bats (*Desmodus rotundus*). **Vaccine** (**1998**)16:1122-1126.
6. **Ai J, Epstein PN, Gozal D, Yang B, Wurster R and Cheng ZJ**. Morphology and topography of nucleus ambiguus projections to cardiac ganglia in rats and mice. **Neuroscience** (**2007**)149:845-860.
7. **Albertini AA, Wernimont AK, Muziol T, Ravelli RB, Clapier CR, Schoehn G, Weissenhorn W and Ruigrok RW**. Crystal Structure of the Rabies Virus Nucleoprotein-RNA Complex. **Science** (**2006**)313:360-363.
8. **Alexandersen S, Larsen S, Cohn A, Uttenthal A, Race R, Aasted B, Hansen M and Bloom M**. Passive transfer of antiviral antibodies restricts replication of Aleutian mink disease parvovirus in vivo. **Journal of virology** (**1989**)63:9-17.
9. **Alvarez L, Fajardo R, Lopez E, Pedroza R, Hemachudha T, Kamolvarin N, Cortes G and Baer G**. Partial recovery from rabies in a nine-year-old boy. **The Pediatric infectious disease journal** (**1994**)13:1154-1155.
10. **Amengual B, Bourhy H, López-Roig M and Serra-Cobo J**. Temporal dynamics of European bat lyssavirus type 1 and survival of Myotis myotis bats in natural colonies. **PLoS ONE** (**2007**)2:e566.
11. **Amengual B, Whitby J, King A, Serra-Cobo J and Bourhy H**. Evolution of European bat lyssaviruses. **The Journal of general virology** (**1997**)78:2319-2328.
12. **Ammons WS**. Renal afferent input to thoracolumbar spinal neurons of the cat. **The American journal of physiology** (**1986**)250:R435-443.
13. **Anil MH and Forbes JM**. Neural control and neurosensory functions of the liver. **The Proceedings of the Nutrition Society** (**1987**)46:125-133.
14. **Anonymous**. WHO Expert Committee on rabies. **World Health Organization Technical Report Series** (**1992**)824:1-84.
15. **Anonymous**. Rabies infections in organ donor and transplant recipients in Germany, p. 8-9. In Plötzsch C (ed.), Rabies-Bulletin-Europe, vol. 29. WHO Collaborating Centre for Rabies Surveillance and Research, Wusterhausen, Germany (**2005**).
16. **Arai YT, Kuzmin IV, Kameoka Y and Botvinkin AD**. New lyssavirus genotype from the Lesser mouse-eared bat (Myotis blythi), Kyrghyzstan. **Emerging infectious diseases** (**2003**)9:333-337.
17. **Armour JA and Hopkins DA**. Activity of canine in situ left atrial ganglion neurons. **The American journal of physiology** (**1990**)259:H1207-1215.
18. **Armour JA and Hopkins DA**. Activity of in vivo canine ventricular neurons. **The American journal of physiology** (**1990**)258:H326-336.
19. **Arnheiter H, Davis NL, Wertz GW, Schubert M and Lazzarini RA**. Role of the nucleocapsid protein in regulating vesicular stomatitis virus RNA synthesis. **Cell** (**1985**)41:259-267.
20. **Arrowood JA, Minisi AJ, Goudreau E, Davis AB and King AL**. Absence of parasympathetic control of heart rate after human orthotopic cardiac transplantation. **Circulation** (**1997**)96:3492-3498.
21. **Atanasiu P, Gamet A, Tsiang H, Dragonas P and Lépine P**. [New data on the routes of alimination of rabies virus in infected animals]. **Comptes rendus hebdomadaires des séances de l'Académie des sciences. Série D: Sciences naturelles** (**1970**)271:2434-2436.
22. **Aubert M, Blancou J, Barrat J, Artois M and Barrat M**. [Transmissibility and pathogenicity in the red fox of two rabies viruses isolated at a 10 year interval]. **Annales de recherches vétérinaires. Annals of veterinary research** (**1991**)22:77-93.

23. **Badrane H, Bahloul C, Perrin P and Tordo N**. Evidence of two lyssavirus phylogroups with distinct pathogenicity and immunogenicity. **Journal of virology** (**2001**)75:3268-3276.
24. **Baer G, Shanthaveerappa T and Bourne G**. Studies on the pathogenesis of fixed rabies virus in rats. **Bulletin of the World Health Organization** (**1965**)33:783-794.
25. **Balachandran A and Charlton K**. Experimental rabies infection of non-nervous tissues in skunks (Mephitis mephitis) and foxes (Vulpes vulpes). **Veterinary pathology** (**1994**)31:93-102.
26. **Ball LA, Pringle CR, Flanagan EB, Perepelitsa VP and Wertz GW**. Phenotypic consequences of rearranging the P, M, and G genes of vesicular stomatitis virus. **Journal of virology** (**1999**)73:4705-4712.
27. **Ball LA and White C**. Order of transcription of genes of vesicular stomatitis virus. **Proceedings of the National Academy of Sciences of the United States of America** (**1976**)73:442-446.
28. **Baloul L, Camelo S and Lafon M**. Up-regulation of Fas ligand (FasL) in the central nervous system: a mechanism of immune evasion by rabies virus. **Journal of neurovirology** (**2004**)10:372-382.
29. **Baloul L and Lafon M**. Apoptosis and rabies virus neuroinvasion. **Biochimie** (**2003**)85:777-788.
30. **Baltimore D, Huang AS and Stampfer M**. Ribonucleic acid synthesis of vesicular stomatitis virus, II. An RNA polymerase in the virion. **Proceedings of the National Academy of Sciences of the United States of America** (**1970**)66:572-576.
31. **Baluk P and Gabella G**. Fine structure of the autonomic ganglia of the mouse pulmonary vein. **Journal of neurocytology** (**1987**)16:169-184.
32. **Banerjee AK**. In vitro synthesis of RNA that contains polyadenylate by virion-associated RNA polymerase of vesicular stomatitis virus. **Proceedings of the National Academy of Sciences of the United States of America** (**1973**)70:3566-3570.
33. **Banerjee AK**. Transcription and replication of rhabdoviruses. **Microbiological reviews** (**1987**)51:66-87.
34. **Banerjee AK and Chattopadhyay D**. Structure and function of the RNA polymerase of vesicular stomatitis virus. **Advances in virus research** (**1990**)38:99-124.
35. **Baptista CA and Kirby ML**. The cardiac ganglia: cellular and molecular aspects. **The Kaohsiung journal of medical sciences** (**1997**)13:42-54.
36. **Barajas L, Liu L and Powers K**. Anatomy of the renal innervation: intrarenal aspects and ganglia of origin. **Canadian journal of physiology and pharmacology** (**1992**)70:735-749.
37. **Baratawidjaja R, Morrissey L and Labzoffsky N**. Demonstration of vaccinia, lymphocytic choriomeningitis and rabies viruses in the leucocytes of experimentally infected animals. **Archiv für die gesamte Virusforschung** (**1965**)17:273-279.
38. **Barge A, Gagnon J, Chaffotte A, Timmins P, Langowski J, Ruigrok RW and Gaudin Y**. Rod-like shape of vesicular stomatitis virus matrix protein. **Virology** (**1996**)219:465-470.
39. **Barge A, Gaudin Y, Coulon P and Ruigrok RW**. Vesicular stomatitis virus M protein may be inside the ribonucleocapsid coil. **Journal of virology** (**1993**)67:7246-7253.
40. **Beaumont V, Zhong N, Fletcher R, Froemke RC and Zucker RS**. Phosphorylation and local presynaptic protein synthesis in calcium- and calcineurin-dependent induction of crayfish long-term facilitation. **Neuron** (**2001**)32:489-501.
41. **Becker P and Zunker M**. [Different behaviour of street rabies and virus fixé strains in parabiotic rats]. **Zentralblatt für Bakteriologie. 1. Abt. Originale. A: Medizinische Mikrobiologie, Infektionskrankheiten und Parasitologie** (**1980**)247:290-295.
42. **Belvisi MG**. Overview of the innervation of the lung. **Current opinion in pharmacology** (**2002**)2:211-215.
43. **Birnboim H and Doly J**. A rapid alkaline extraction procedure for screening recombinant plasmid DNA. **Nucleic acids research** (**1979**)7:1513-1523.
44. **Black EM, Lowings JP, Smith J, Heaton PR and McElhinney LM**. A rapid RT-PCR method to differentiate six established genotypes of rabies and rabies-related viruses using TaqMan™ technology. **Journal of virological methods** (**2002**)105:25-25.
45. **Black EM, McElhinney LM, Lowings JP, Smith J, Johnstone P and Heaton PR**. Molecular methods to distinguish between classical rabies and the rabies-related European bat lyssaviruses. **Journal of virological methods** (**2000**)87:123-131.
46. **Blaisdell J**. The deadly bite of ancient animals: written evidence for rabies, or the lack thereof, in the ancient Egyptian and Mesopotamian texts. **Veterinary history** (**1994**)8:22-28.

47. **Blancou J, Andral B and Andral L**. A model in mice for the study of the early death phenomenon after vaccination and challenge with rabies virus. **The Journal of general virology** (**1980**)50:433-435.
48. **Bleher R and Martin R**. Ribosomes in the squid giant axon. **Neuroscience** (**2001**)107:527-534.
49. **Blumberg BM, Giorgi C and Kolakofsky D**. N protein of vesicular stomatitis virus selectively encapsidates leader RNA in vitro. **Cell** (**1983**)32:559-567.
50. **Blumberg BM and Kolakofsky D**. Intracellular vesicular stomatitis virus leader RNAs are found in nucleocapsid structures. **Journal of virology** (**1981**)40:568-576.
51. **Bonham AC, Chen CY, Sekizawa S and Joad JP**. Plasticity in the nucleus tractus solitarius and its influence on lung and airway reflexes. **Journal of applied physiology (Bethesda, Md : 1985)** (**2006**)101:322-327.
52. **Bose S, Mathur M, Bates P, Joshi N and Banerjee AK**. Requirement for cyclophilin A for the replication of vesicular stomatitis virus New Jersey serotype. **The Journal of general virology** (**2003**)84:1687-1699.
53. **Bourhy H, Dacheux L, Strady C and Mailles A**. Rabies in Europe in 2005. **Euro surveillance : bulletin européen sur les maladies transmissibles = European communicable disease bulletin** (**2005**)10:213-216.
54. **Bourhy H, Kissi B, Lafon M, Sacramento D and Tordo N**. Antigenic and molecular characterization of bat rabies virus in Europe. **Journal of clinical microbiology** (**1992**)30:2419-2426.
55. **Bourhy H, Kissi B and Tordo N**. Molecular diversity of the lyssavirus genus. **Virology** (**1993**)194:70-81.
56. **Bracci L, Antoni G, Cusi M, Lozzi L, Niccolai N, Petreni S, Rustici M, Santucci A, Soldani P, Valensin P and al. e**. Antipeptide monoclonal antibodies inhibit the binding of rabies virus glycoprotein and alpha-bungarotoxin to the nicotinic acetylcholine receptor. **Molecular immunology** (**1988**)25:881-888.
57. **Brookes SM, Parsons G, Johnson N, McElhinney LM and Fooks AR**. Rabies human diploid cell vaccine elicits cross-neutralising and cross-protecting immune responses against European and Australian bat lyssaviruses. **Vaccine** (**2005**)23:4101-4109.
58. **Brüggmann D, Lips K, Pfeil U, Haberberger R and Kummer W**. Multiple nicotinic acetylcholine receptor alpha-subunits are expressed in the arterial system of the rat. **Histochemistry and cell biology** (**2002**)118:441-447.
59. **Buchholz UJ, Finke S and Conzelmann K-K**. Generation of bovine respiratory syncytial virus (BRSV) from cDNA: BRSV NS2 is not essential for vrus replication in tissue culture, and the human RSV leader region acts as a functional BRSV genome promoter. **Journal of virology** (**1999**)73:251-259.
60. **Bulenga G and Heaney T**. Post-exposure local treatment of mice infected with rabies with two axonal flow inhibitors, colchicine and vinblastine. **The Journal of general virology** (**1978**)39:381-385.
61. **Burne J**. Viraemia in rabies. **Lancet** (**1970**)1:195-196.
62. **Burrage T, Tignor GH and Smith AL**. Immunoelectron microscopic localization of rabies virus antigen in central nervous system and peripheral tissue using low-temberature embedding and protein A-gold. **Journal of virological methods** (**1983**)7:337-350.
63. **Burrage T, Tignor GH and Smith AL**. Rabies virus binding at neuromuscular junctions. **Virus research** (**1985**)2:273-289.
64. **Calisher CH, Childs JE, Field HE, Holmes KV and Schountz T**. Bats: important reservoir hosts of emerging viruses. **Clinical microbiology reviews** (**2006**)19:531-545.
65. **Carroll AR and Wagner RR**. Role of the membrane (M) protein in endogenous inhibition of in vitro transcription by vesicular stomatitis virus. **Journal of virology** (**1979**)29:134-142.
66. **CDC**. Human-to-human transmission of rabies via corneal transplant. France. **MMWR. Morbidity and mortality weekly report** (**1980**)29:25-26.
67. **CDC**. Human Rabies --- Indiana and California, 2006. **MMWR. Morbidity and mortality weekly report** (**2007**)56:361-365.
68. **Charlton K and Casey G**. Experimental rabies in skunks: immunofluorescence light and electron microscopic studies. **Laboratory investigation; a journal of technical methods and pathology** (**1979**)41:36-44.
69. **Charlton K, Casey G and Campell J**. Experimental rabies in skunks: mechanisms of infection of the salivary glands. **Canadian journal of comparative medicine (Gardenvale, Québec)** (**1983**)47:363-369.
70. **Charlton K, Casey G, Wandeler A and Nadin-Davis S**. Early events in rabies

virus infection of the central nervous system in skunks (Mephitis mephitis). **Acta neuropathologica** (**1996**)91:89-98.

71. **Charlton K, Casey G and Webster W**. Rabies virus in the salivary glands and nasal mucosa of naturally infected skunks. **Canadian journal of comparative medicine (Gardenvale, Québec)** (**1984**)48:338-339.
72. **Charlton K, Nadin-Davis S, Casey G and Wandeler A**. The long incubation period in rabies: delayed progression of infection in muscle at the site of exposure. **Acta neuropathologica** (**1997**)94:73-77.
73. **Cheng Z and Powley TL**. Nucleus ambiguus projections to cardiac ganglia of rat atria: an anterograde tracing study. **The Journal of comparative neurology** (**2000**)424:588-606.
74. **Cheng Z, Powley TL, Schwaber JS and Doyle FJ**. Vagal afferent innervation of the atria of the rat heart reconstructed with confocal microscopy. **The Journal of comparative neurology** (**1997**)381:1-17.
75. **Cheng Z, Powley TL, Schwaber JS and Doyle FJ**. Projections of the dorsal motor nucleus of the vagus to cardiac ganglia of rat atria: an anterograde tracing study. **The Journal of comparative neurology** (**1999**)410:320-341.
76. **Chong LD and Rose JK**. Membrane association of functional vesicular stomatitis virus matrix protein in vivo. **Journal of virology** (**1993**)67:407-414.
77. **Chong LD and Rose JK**. Interactions of normal and mutant vesicular stomatitis virus matrix proteins with the plasma membrane and nucleocapsids. **Journal of virology** (**1994**)68:441-447.
78. **Chopra JS, Banerjee AK, Murthy JM and Pal SR**. Paralytic rabies: a clinico-pathological study. **Brain : a journal of neurology** (**1980**)103:789-802.
79. **Cliquet F and Picard-Meyer E**. Rabies and rabies-related viruses: a modern perspective on an ancient disease. **Revue scientifique et technique (International Office of Epizootics)** (**2004**)23:625-642.
80. **Colonno RJ and Banerjee AK**. A unique RNA species involved in initiation of vesicular stomatitis virus RNA transcription in vitro. **Cell** (**1976**)8:197-204.
81. **Colonno RJ and Banerjee AK**. Mapping and initiation studies on the leader RNA of vesicular stomatitis virus. **Virology** (**1977**)77:260-268.
82. **Combard A and Printz Ané C**. Inhibition of vesicular stomatitis virus transcriptase complex by the virion envelope M protein. **Biochemical and biophysical research communications** (**1979**)88:117-123.
83. **Conomy JP, Leibowitz A, McCombs W and Stinson J**. Ariborne rabies encephalitis: demonstration of rabies virus in the human central nervous system. **Neurology** (**1977**)27:67-69.
84. **Constantine DG**. Geographic translocation of bats: known and potential problems. **Emerging infectious diseases** (**2003**)9:17-21.
85. **Conti C, Superti F and Tsiang H**. Membrane carbohydrate requirement for rabies virus binding to chicken embryo related cells. **Intervirology** (**1986**)26:164-168.
86. **Conzelmann K-K**. Genetic manipulation of non-segmented negative-strand RNA viruses. **The Journal of general virology** (**1996**)77:381-389.
87. **Conzelmann K-K, Cox JH, Schneider L and Thiel H**. Molecular cloning and complete nucleotide sequence of the attenuated rabies virus SAD B19. **Virology** (**1990**)175:485-499.
88. **Coulon P, Derbin C, Kucera P, Lafay F, Prehaud C and Flamand A**. Invasion of the peripheral nervous systems of adult mice by the CVS strain of rabies virus and Its avirulent derivative AvO1. **Journal of virology** (**1989**)62:3550-3554.
89. **Craven RC, Harty RN, Paragas J, Palese P and Wills JW**. Late domain function identified in the vesicular stomatitis virus M protein by use of rhabdovirus-retrovirus chimeras. **Journal of virology** (**1999**)73:3359-3365.
90. **Crepin P, Audry L, Rotivel Y, Gacoin A, Caroff C and Bourhy H**. Intravitam Diagnosis of Human Rabies by PCR Using Saliva and Cerebrospinal Fluid. **Journal of clinical microbiology** (**1998**)36:1117-1121.
91. **Crispino M, Kaplan BB, Martin R, Alvarez J, Chun J, Benech J and Giuditta A**. Active polysomes are present in the large presynaptic endings of the synaptosomal fraction from squid brain. **The Journal of neuroscience : the official journal of the Society for Neuroscience** (**1997**)17:7694-7702.
92. **Cserr HF, Harling-Berg CJ and Knopf PM**. Drainage of brain extracellular fluid into blood and deep cervical lymph and its immunological significance. **Brain pathology (Zurich, Switzerland)** (**1992**)2:269-276.
93. **Das T, Mathur M, Gupta AK, Janssen GM and Banerjee AK**. RNA polymerase of vesicular stomatitis virus specifically associates with translation elongation

factor-1 alpha beta gamma for its activity. **Proceedings of the National Academy of Sciences of the United States of America** (**1998**)95:1449-1454.

94. **David D, Yakobson B, Rotenberg D, Dveres N, Davidson I and Stram Y**. Rabies virus detection by RT-PCR in decomposed naturally infected brains. **Vet Microbiol** (**2002**)87:111-118.
95. **Davis NL, Arnheiter H and Wertz GW**. Vesicular stomatitis virus N and NS proteins form multiple complexes. **Journal of virology** (**1986**)59:751-754.
96. **De BP and Banerjee AK**. Specific interactions of vesicular stomatitis virus L and NS proteins with heterologous genome ribonucleoprotein template lead to mRNA synthesis in vitro. **Journal of virology** (**1984**)51:628-634.
97. **De BP and Banerjee AK**. Role of cellular kinases in the gene expression of non-segmented negative strand RNA viruses. **Biological chemistry** (**1997**)378:489-493.
98. **De BP, Thornton GB, Luk D and Banerjee AK**. Purified matrix protein of vesicular stomatitis virus blocks viral transcription in vitro. **Proceedings of the National Academy of Sciences of the United States of America** (**1982**)79:7137-7141.
99. **Dieterich HJ**. Electron microscopic studies of the innervation of the rat kidney. **Zeitschrift für Anatomie und Entwicklungsgeschichte** (**1974**)145:169-186.
100. **Dietzschold B, Kao M, Zheng Y, Chen Z, Maul G, Fu ZF, Rupprecht CE and Koprowski H**. Delineation of putative mechanisms involved in antibody-mediated clearance of rabies virus from the central nervous system. **Proceedings of the National Academy of Sciences of the United States of America** (**1992**)89:7252-7256.
101. **Dietzschold B, Morimoto K, Hooper DC, Smith JS, Rupprecht CE and Koprowski H**. Genotypic and phenotypic diversity of rabies virus variants involved in human rabies: implications for postexposure prophylaxis. **Journal of human virology** (**2000**)3:50-57.
102. **Dutta M, Saha V and Sarkar P**. Detection of rabies virus in different tissues of experimentally infected mice at preclinical and postclinical stages of the disease. **Indian J Exp Biol** (**1992**)30:877-880.
103. **Ehrenfeld E**. Polyadenylation of vesicular stomatitis virus mRNA. **Journal of virology** (**1974**)13:1055-1060.
104. **Emerson S and Yu Y**. Both NS and L proteins are required for in vitro RNA synthesis by vesicular stomatitis virus. **Journal of virology** (**1975**)15:1348-1356.
105. **Ermine A, Larzul D, Ceccaldi P-E, Guesdon J and Tsiang H**. Polymerase chain reaction amplification of rabies virus nucleic acids from total mouse brain RNA. **Molecular and cellular probes** (**1990**)4:189-191.
106. **Etessami R, Conzelmann K-K, Fadak-Ghotbi B, Natelson B, Tsiang H and Ceccaldi P-E**. Spread and pathogenic characteristics of a G-deficient rabies virus recombinant: an in vitro and in vivo study. **Journal of General Virology** (**2000**)81:2147-2153.
107. **Faber M, Bette M, Preuss MA, Pulmanausahakul R, Rehnelt J, Schnell MJ, Dietzschold B and Weihe E**. Overexpression of Tumor Necrosis Factor Alpha by a Recombinant Rabies Virus Attenuates Replication in Neurons and Prevents Lethal Infection in Mice. **Journal of virology** (**2005**)79:15405-15416.
108. **Faber M, Faber M-L, Li J, Preuss MA, Schnell MJ and Dietzschold B**. Dominance of a Nonpathogenic Glycoprotein Gene over a Pathogenic Glycoprotein Gene in Rabies Virus. **Journal of virology** (**2007**)81:7041-7047.
109. **Faber M, Pulmanausahakul R, Hodawadekar SS, Spitsin S, McGettigan JP, Schnell MJ and Dietzschold B**. Overexpression of the rabies virus glycoprotein results in enhancement of apoptosis and antiviral immune response. **Journal of virology** (**2002**)76:3374-3381.
110. **Faber M, Pulmanausahakul R, Nagao K, Prosniak M, Rice AB, Koprowski H, Schnell MJ and Dietzschold B**. Identification of viral genomic elements responsible for rabies virus neuroinvasiveness. **Proceedings of the National Academy of Sciences of the United States of America** (**2004**)101:16328-16332.
111. **Fekadu M, Shaddock J, Chandler F and Baer G**. Rabies virus in the tonsils of a carrier dog. **Archives of virology** (**1983**)78:37-47.
112. **Fekadu M, Shaddock J, Chandler F and Sanderlin D**. Pathogenesis of rabies virus from a Danish bat (Eptesicus serotinus): neuronal changes suggestive of spongiosis. **Archives of virology** (**1988**)99:187-203.
113. **Ferguson M and Bell C**. Ultrastructural localization and characterization of sensory nerves in the rat kidney. **The**

Journal of comparative neurology (**1988**)274:9-16.

114. **Finke S and Conzelmann K-K**. Ambisense gene expression from recombinant rabies virus: random packaging of positive- and negative-strand ribonucleoprotein complexes into rabies virions. **Journal of virology** (**1997**)71:7281-7288.
115. **Finke S and Conzelmann K-K**. Dissociation of rabies virus matrix protein functions in regulation of viral RNA synthesis and virus assembly. **Journal of virology** (**2003**)77:12074-12082.
116. **Finke S, Cox JH and Conzelmann K-K**. Differential transcription attenuation of rabies virus genes by intergenic regions: generation of recombinant viruses overexpressing the polymerase gene. **Journal of virology** (**2000**)74:7261-7269.
117. **Finke S, Müller-Waldeck R and Conzelmann K-K**. Rabies virus matrix protein regulates the balance of virus transcription and replication. **The Journal of general virology** (**2003**)84:1613-1621.
118. **Fishbein DB and Robinson LE**. Rabies. **The New England journal of medicine** (**1993**)329:1632-1638.
119. **Flanagan EB, Ball LA and Wertz GW**. Moving the glycoprotein gene of vesicular stomatitis virus to promoter-proximal positions accelerates and enhances the protective immune response. **Journal of virology** (**2000**)74:7895-7902.
120. **Fraser G, Hooper P, Lunt RA, Gould AR, Gleeson L, Hyatt AD, Russell G and Kattenbelt JA**. Encephalitis caused by a Lyssavirus in fruit bats in Australia. **Emerging infectious diseases** (**1996**)2:327-331.
121. **Fu ZF and Jackson AC**. Neuronal dysfunction and death in rabies virus infection. **Journal of neurovirology** (**2005**)11:101-106.
122. **Fu ZF, Weihe E, Zheng Y, Schaefer MK-H, Sheng H, Corisdeo S, Rauscher F, 3rd, Koprowski H and Dietzschold B**. Differential effects of rabies and borna disease viruses on immediate-early- and late-response gene expression in brain tissues. **Journal of virology** (**1993**)67:6674-6681.
123. **Fujinami R and Oldstone M**. Antiviral antibody reacting on the plasma membrane alters measles virus expression inside the cell. **Nature** (**1979**)279:529-530.
124. **Fujinami R and Oldstone M**. Alterations in expression of measles virus polypeptides by antibody: molecular events in antibody-induced antigenic modulation. **Journal of immunology (Baltimore, Md. : 1950)** (**1980**)125:78-85.
125. **Galelli A, Baloul L and Lafon M**. Abortive rabies virus central nervous infection is controlled by T lymphocyte local recruitment and induction of apoptosis. **Journal of neurovirology** (**2000**)6:359-372.
126. **Gastka M, Horvath J and Lentz TL**. Rabies virus binding to the nicotinic acetylcholine receptor alpha subunit demonstrated by virus overlay protein binding assay. **The Journal of general virology** (**1996**)77:2437-2440.
127. **Gaudier M, Gaudin Y and Knossow M**. Crystal structure of vesicular stomatitis virus matrix protein. **The EMBO journal** (**2002**)21:2886-2892.
128. **Gaudin Y, Ruigrok RW, Knossow M and Flamand A**. Low-pH conformational changes of rabies virus glycoprotein and their role in membrane fusion. **Journal of virology** (**1993**)67:1365-1372.
129. **Gaudin Y, Ruigrok RW, Tuffereau C, Knossow M and Flamand A**. Rabies virus glycoprotein is a trimer. **Virology** (**1992**)187:627-632.
130. **Gaudin Y, Tuffereau C, Durrer P, Flamand A and Ruigrok RW**. Biological function of the low-pH, fusion-inactive conformation of rabies virus glycoprotein (G): G is transported in a fusion-inactive state-like conformation. **Journal of virology** (**1995**)69:5528-5534.
131. **Gaudin Y, Tuffereau C, Segretain D, Knossow M and Flamand A**. Reversible conformational changes and fusion activity of rabies virus glycoprotein. **Journal of virology** (**1991**)65:4853-4859.
132. **Ghatak S, Banerjee R, Agarwal R and Kapoor K**. Zoonoses and bats: a look from human health viewpoint. **The Journal of communicable diseases** (**2000**)32:40-48.
133. **Gibbons RV**. Cryptogenic rabies, bats, and the question of aerosol transmission. **Annals of emergency medicine** (**2002**)39:528-536.
134. **Gillet J, Derer P and Tsiang H**. Axonal transport of rabies virus in the central nervous system of the rat. **Journal of neuropathology and experimental neurology** (**1986**)45:619-634.
135. **Giuditta A, Kaplan BB, van Minnen J, Alvarez J and Koenig E**. Axonal and presynaptic protein synthesis: new insights into the biology of the neuron. **TRENDS in Neuroscience** (**2002**)25:400-404.

136. **Giustetto M, Hegde AN, Si K, Casadio A, Inokuchi K, Pei W, Kandel ER and Schwartz JH**. Axonal transport of eukaryotic translation elongation factor 1{alpha} mRNA couples transcription in the nucleus to long-term facilitation at the synapse. **Proceedings of the National Academy of Sciences of the United States of America** (**2003**)100:13680-13685.
137. **Glodowski DR, Petersen JM and Dahlberg JE**. Complex nuclear localization signals in the matrix protein of vesicular stomatitis virus. **The Journal of biological chemistry** (**2002**)277:46864-46870.
138. **Gode G and Bhide N**. Two rabies deaths after corneal grafts from one donor. **Lancet** (**1988**)2:791.
139. **Gotti C and Clementi F**. Neuronal nicotinic receptors: from structure to pathology. **Progress in Neurobiology** (**2004**)74:363-396.
140. **Gould AR, Hyatt AD, Lunt R, Kattenbelt JA, Hengstberger S and Blacksell S**. Characterisation of a novel lyssavirus isolated from Pteropid bats in Australia. **Virus research** (**1998**)54:165-187.
141. **Grando SA, Horton RM, Pereira EF, Diethelm-Okita BM, George PM, Albuquerque EX and Conti-Fine BM**. A Nicotinic Acetylcholine Receptor Regulating Cell Adhesion and Motility Is Expressed in Human Keratinocytes. **J Investig Dermatol** (**1995**)105:774-781.
142. **Granneman J and Friedman MI**. Hepatic modulation of insulin-induced gastric acid secretion and EMG activity in rats. **The American journal of physiology** (**1980**)238:R346-352.
143. **Gribencha S and Barinsky I**. Viraemia in rabies. **Acta virologica** (**1982**)26:301.
144. **Griffin DE and Johnson RT**. Role of the immune response in recovery from Sindbis virus encephalitis in mice. **Journal of immunology (Baltimore, Md. : 1950)** (**1977**)118:1070-1075.
145. **Griffin DE, Levine B, Tyor W, Ubol S and Despres P**. The role of antibody in recovery from alphavirus encephalitis. **Immunological reviews** (**1997**)159:155-161.
146. **Grimm R**. The history of the eradication of rabies in most European countries. **Historia medicinae veterinariae** (**2002**)27:295-301.
147. **Gupta AK, Mathur M and Banerjee AK**. Unique capping activity of the recombinant RNA polymerase (L) of vesicular stomatitis virus: association of cellular capping enzyme with the L protein. **Biochemical and biophysical research communications** (**2002**)293:264-268.
148. **Gupta AK, Shaji D and Banerjee AK**. Identification of a novel tripartite complex involved in replication of vesicular stomatitis virus genome RNA. **Journal of virology** (**2003**)77:732-738.
149. **Hahn HL**. Role of the parasympathetic nervous system and of cholinergic mechanisms in bronchial hyperreactivity. **Bulletin européen de physiopathologie respiratoire** (**1986**)22 Suppl 7:112-142.
150. **Hanham CA, Zhao F and Tignor GH**. Evidence from the anti-idiotypic network that the acetylcholine receptor is a rabies virus receptor. **Journal of virology** (**1993**)67:530-542.
151. **Hanna JN, Carney IK, Smith GA, Tannenberg AE, Deverill JE, Botha JA, Serafin IL, Harrower BJ, Fitzpatrick PF and Searle JW**. Australian bat lyssavirus infection: a second human case, with a long incubation period. **The Medical journal of Australia** (**2000**)172:597-599.
152. **Harling-Berg C, Knopf PM, Merriam J and Cserr HF**. Role of cervical lymph nodes in the systemic humoral immune response to human serum albumin microinfused into rat cerebrospinal fluid. **Journal of Neuroimmunology** (**1989**)25:185-193.
153. **Harmon SA, Robinson EN and Summers DF**. Ultrastructural localization of L and NS enzyme subunits on vesicular stomatitis virus RNPs using gold sphere-staphylococcal protein A-monospecific IgG conjugates. **Virology** (**1985**)142:406-410.
154. **Harrison A and Murphy F**. Lyssavirus infection of muscle spindles and motor end plates in striated muscle of hamsters. **Archives of virology** (**1978**)57:167-175.
155. **Harty RN, Brown ME, McGettigan JP, Wang G, Jayakar HR, Huibregtse JM, Whitt MA and Schnell MJ**. Rhabdoviruses and the cellular ubiquitin-proteasome system: a budding interaction. **Journal of virology** (**2001**)75:10623-10629.
156. **Harty RN, Paragas J, Sudol M and Palese P**. A proline-rich motif within the matrix protein of vesicular stomatitis virus and rabies virus interacts with WW domains of cellular proteins: implications for viral budding. **Journal of virology** (**1999**)73:2921-2929.
157. **Hattwick M, Weiss T, Stechschulte C, Baer G and Gregg M**. Recovery from rabies. A case report. **Annals of internal medicine** (**1972**)76:931-942.
158. **Heaton PR, Johnstone P, McElhinney LM, Cowley R, O'Sullivan E and**

Whitby JE. Heminested PCR Assay for Detection of Six Genotypes of Rabes and Rabies-Related Viruses. **Journal of clinical microbiology** (**1997**)35:2762-2766.

159. **Hefti E and Bishop DH**. The 5' sequences of VSV transcription product RNA (+/- SAM). **Biochemical and biophysical research communications** (**1976**)68:393-400.
160. **Hellenbrand W, Meyer C, Rasch G, Steffens I and Ammon A**. Cases of rabies in Germany following organ transplantation. **Euro surveillance : bulletin européen sur les maladies transmissibles = European communicable disease bulletin** (**2005**)10:E050224.050226.
161. **Helmick C**. The epidemiology of human rabies postexposure prophylaxis 1980-1981. **JAMA : the journal of the American Medical Association** (**1983**)250:1990-1996.
162. **Hemachudha T**. Rabies, p. 401-444. In Davis L and Kennedy P (ed.), Infectious diseases of the nervous system. Butterworth-Heinemann, Oxford (**2000**).
163. **Hemachudha T, Laothamatas J and Rupprecht CE**. Human rabies: a disease of complex neuropathogenetic mechanisms and diagnostic challenges. **Lancet neurology** (**2002**)1:101-109.
164. **Hemachudha T, Phanuphak P, Sriwanthana B, Manutsathit S, Phanthumchinda K, Siriprasomsup W, Ukachoke C, Rasameechan S and Kaoroptham S**. Immunologic study of human encephalitic and paralytic rabies. Preliminary report of 16 patients. **The American journal of medicine** (**1988**)84:673-677.
165. **Hemachudha T, Sunsaneewitayakul B, Desudchit T, Suankratay C, Sittipunt C, Wacharapluesadee S, Khawplod P, Wilde H and Jackson AC**. Failure of therapeutic coma and ketamine for therapy of human rabies. **Journal of neurovirology** (**2006**)12:407-409.
166. **Hemachudha T, Sunsaneewitayakul B, Mitrabhakdi E, Suankratay C, Laothamathas J, Wacharapluesadee S, Khawplod P and Wilde H**. Paralytic complications following intravenous rabies immune globulin treatment in a patient with furious rabies. **International journal of infectious diseases : IJID : official publication of the International Society for Infectious Diseases** (**2003**)7:76-77.
167. **Hemachudha T, Wacharapluesadee S, Laothamatas J and Wilde H**. Rabies. **Current neurology and neuroscience reports** (**2006**)6:460-468.
168. **Hemachudha T, Wacharapluesadee S, Lumlertdaecha B, Orciari LA, Rupprecht CE, La-Ongpant M, Juntrakul S and Denduangboripant J**. Sequence analysis of rabies virus in humans exhibiting encephalitic or paralytic rabies. **The Journal of infectious diseases** (**2003**)188:960-966.
169. **Hemachudha T, Wacharapluesadee S, Mitrabhakdi E, Wilde H, Morimoto K and Lewis RA**. Pathophysiology of human paralytic rabies. **Journal of neurovirology** (**2005**)11:93-100.
170. **Hillefors M, Gioio A, Mameza M and Kaplan BB**. Axon viability and mitochondrial function are dependent on local protein synthesis in sympathetic neurons. **Cellular and molecular neurobiology** (**2007**)27:701-716.
171. **Hirai K, Kawano H, Mifune K, Fujii H, Nishizono A, Shichijo A and Mannen K**. Suppression of cell-mediated immunity by street rabies virus infection. **Microbiology and immunology** (**1992**)36:1277-1290.
172. **Holland PM, Abramson RD, Watson R and Gelfand DH**. Detection of specific polymerase chain reaction product by utilizing the 5'-->3' exonuclease activity of *Thermus aquaticus* DNA polymerase. **Proceedings of the National Academy of Sciences of the United States of America** (**1991**)88:7276-7280.
173. **Hooper DC**. The role of immune responses in the pathogenesis of rabies. **Journal of neurovirology** (**2005**)11:88-92.
174. **Hooper DC, Morimoto K, Bette M, Weihe E, Koprowski H and Dietzschold B**. Collaboration of antibody and inflammation in clearance of rabies virus from the central nervous system. **Journal of virology** (**1998**)72:3711-3719.
175. **Houff S, Burton R, Wilson R, Henson T, London W, Baer G, Anderson L, Winkler W, Madden D and Sever J**. Human-to-human transmission of rabies virus by corneal transplant. **The New England journal of medicine** (**1979**)300:603-604.
176. **Howard D**. Rabies virus titer from tissues of naturally infected skunks (Mephitis mephitis). **American journal of veterinary research** (**1981**)42:1595-1597.
177. **Hughes G, Smith JS, Hanlon CA and Rupprecht CE**. Evaluation of a TaqMan PCR Assay To Detect Rabies Virus RNA: Influence of Sequence Variation and Application to Quantification of Viral Loads. **Journal of clinical microbiology** (**2004**)42:299-306.

178. **Hummeler K, Tomassini N, Sokol F, Kuwert E and Koprowski H**. Morphology of the nucleoprotein component of rabies virus. **Journal of virology** (**1968**)2:1191-1199.
179. **Hwang LN, Englund N, Das T, Banerjee AK and Pattnaik AK**. Optimal replication activity of vesicular stomatitis virus RNA polymerase requires phosphorylation of a residue(s) at carboxy-terminal domain II of Its accessory subunit, phosphoprotein P. **Journal of virology** (**1999**)73:5613-5620.
180. **Ingoglia N, Giuditta A, Zanakis M, Babigian A, Tasaki I, Chakraborty G and Sturman J**. Incorporation of 3H-amino acids into proteins in a partially purified fraction of axoplasm: evidence for transfer RNA-mediated, post-translational protein modification in squid giant axons. **The Journal of neuroscience : the official journal of the Society for Neuroscience** (**1983**)3:2463-2473.
181. **Ito M, Itou T, Shoji Y, Sakai T, Ito FH, Arai YT, Takasaki T and Kurane I**. Discrimination between dog-related and vampire bat-related rabies viruses in Brazil by strain-specific reverse transcriptase-polymerase chain reaction and restriction fragment length polymorphism analysis. **Journal of Clinical Virology** (**2003**)26:317-330.
182. **Ito Y, Nishizono A, Mannen K, Hiramatsu K and Mifune K**. Rabies virus M protein expressed inEscherichia coli and its regulatory role in virion-associated transcriptase activity. **Archives of virology** (**1996**)141:671-683.
183. **Iverson LE and Rose JK**. Localized attenuation and discontinuous synthesis during vesicular stomatitis virus transcription. **Cell** (**1981**)23:477-484.
184. **Iwasaki Y, Gerhard W and Clark HF**. Role of Host Immune Response in the Development of Either Encephalitic or Paralytic Disease After Experimental Rabies Infection in Mice. **Infection and Immunity** (**1977**)18:220-225.
185. **Jackson AC**. Biological basis of rabies virus neurovirulence in mice: comparative pathogenesis study using the immunoperoxidase technique. **Journal of virology** (**1991**)65:537-540.
186. **Jackson AC, Moench T, Griffin DE and Johnson RT**. The pathogenesis of spinal cord involvement in the encephalomyelitis of mice caused by neuroadapted Sindbis virus infection. **Laboratory investigation; a journal of technical methods and pathology** (**1987**)56:418-423.
187. **Jackson AC and Park H**. Experimental rabies virus infection of p75 neurotrophin receptor-deficient mice. **Acta neuropathologica** (**1999**)98:641-644.
188. **Jackson AC and Rossiter JP**. Apoptosis plays an important role in experimental rabies virus infection. **Journal of virology** (**1997**)71:5603-5607.
189. **Jackson AC, Ye H, Phelan C, Ridaura-Sanz C, Zheng Q, Li Z, Wan X and Lopez-Corella E**. Extraneural organ involvement in human rabies. **Laboratory investigation; a journal of technical methods and pathology** (**1999**)79:945-951.
190. **Jacob Y, Badrane H, Ceccaldi P-E and Tordo N**. Cytoplasmic dynein LC8 interacts with lyssavirus phosphoprotein. **Journal of virology** (**2000**)74:10217-10222.
191. **Javadi MA, Fayaz A, Mirdehghan SA and Ainollahi B**. Transmission of rabies by corneal graft. **Cornea** (**1996**)15:431-433.
192. **Jayakar HR, Jeetendra E and Whitt MA**. Rhabdovirus assembly and budding. **Virus research** (**2004**)106:117-132.
193. **Jayakar HR, Murti KG and Whitt MA**. Mutations in the PPPY motif of vesicular stomatitis virus matrix protein reduce virus budding by inhibiting a late step in virion release. **Journal of virology** (**2000**)74:9818-9827.
194. **Jeetendra E, Ghosh K, Odell D, Li J, Ghosh HP and Whitt MA**. The membrane-proximal region of vesicular stomatitis virus glycoprotein G ectodomain is critical for fusion and virus infectivity. **Journal of virology** (**2003**)77:12807-12818.
195. **Jeetendra E, Robison CS, Albritton LM and Whitt MA**. The membrane-proximal domain of vesicular stomatitis virus G protein functions as a membrane fusion potentiator and can induce hemifusion. **Journal of virology** (**2002**)76:12300-12311.
196. **Jiménez C, Eyman M, Scotto Lavina Z, Gioio A, Li K, van der Schors R, Geraerts W, Giuditta A, Kaplan BB and van Minnen J**. Protein sythesis in synaptosomes: a proteomics analysis. **Journal of neurochemistry** (**2002**)81:735-744.
197. **Jogai S, Radotra B and Banerjee AK**. Rabies viral antigen in extracranial organs. A post-mortem study. **Neuropathology and applied neurobiology** (**2002**)28:334-338.
198. **Johnson RT**. Experimental rabies: studies of cellular vulnerability and pathogenesis using fluorescent antibody

staining. **Journal of neuropathology and experimental neurology** (**1965**)24:6622-6674.

199. **Joly JS, Os√≥rio J, Alunni A, Auger H, Kano S and R√©taux S**. Windows of the brain: towards a developmental biology of circumventricular and other neurohemal organs. **Seminars in cell & developmental biology** (**2007**)18:512-524.
200. **Juntrakul S, Ruangvejvorachai P, Shuangshoti S, Wacharapluesadee S and Hemachudha T**. Mechanisms of escape phenomenon of spinal cord and brainstrem in human rabies. **BMC Infectious Deseases** (**2005**)5:104.
201. **Justice PA, Sun W, Li Y, Ye Z, Grigera PR and Wagner RR**. Membrane vesiculation function and exocytosis of wild-type and mutant matrix proteins of vesicular stomatitis virus. **Journal of virology** (**1995**)69:3156-3160.
202. **Kamolvarin N, Tirawatnpong T, Rattanasiwamoke R, Tirawatnpong S, Panpanich T and Hemachudha T**. Diagnosis of rabies by polymerase chain reaction with nested primers. **The Journal of infectious diseases** (**1993**)167:207-210.
203. **Kawai A, Toriumi H, Tochikura TS, Takahashi T, Honda Y and Morimoto K**. Nucleocapsid formation and/or subsequent conformational change of rabies virus nucleoprotein (N) is a prerequisite step for acquiring the phosphatase-sensitive epitope of monoclonal antibody 5-2-26. **Virology** (**1999**)263:395-407.
204. **Kawashima K and Fujii T**. The lymphocytic cholinergic system and its contribution to the regulation of immune activity. **Life sciences** (**2003**)74:675-696.
205. **Kelly RM and Strick PL**. Rabies as a transneuronal tracer of circuits in the central nervous system. **Journal of neuroscience methods** (**2000**)103:63-71.
206. **Kelly RM and Strick PL**. Cerebellar loops with motor cortex and prefrontal cortex of a nonhuman primate. **The Journal of neuroscience : the official journal of the Society for Neuroscience** (**2003**)23:8432-8444.
207. **Kiba T**. The role of the autonomic nervous system in liver regeneration and apoptosis--recent developments. **Digestion** (**2002**)66:79-88.
208. **Koenig E and Giuditta A**. Protein-synthezising machinery in the axon compartment. **Neuroscience** (**1999**)89:5-15.
209. **Kohno T, Mori S and Mito M**. Cells of origin innervating the liver and their axonal projections with synaptic terminals into the liver parenchyma in rats. **[Hokkaido igaku zasshi] The Hokkaido journal of medical science** (**1987**)62:933-946.
210. **Komarova AV, Real E, Borman AM, Brocard M, England P, Tordo N, Hershey JWB, Kean KM and Jacob Y**. Rabies virus matrix protein interplay with eIF3, new insights into rabies virus pathogenesis. **Nucl. Acids Res.** (**2007**)35:1522-1532.
211. **Kopp UC, Olson LA and DiBona GF**. Renorenal reflex responses to mechano- and chemoreceptor stimulation in the dog and rat. **The American journal of physiology** (**1984**)246:F67-77.
212. **Kouznetzoff A, Buckle M and Tordo N**. Identification of a region of the rabies virus N protein involved in direct binding to the viral RNA. **The Journal of general virology** (**1998**)79:1005-1013.
213. **Krebs JW, Noll H, Rupprecht CE and Childs JE**. Rabies surveillance in the United States during 2001. **Journal of the American Veterinary Medical Association** (**2002**)221:1690-1701.
214. **Kristensson K, Dastur D, Manghani D, Tsiang H and Bentivoglio M**. Rabies: interactions between neurons and viruses. A review of the history of Negri inclusion bodies. **Neuropathology and applied neurobiology** (**1996**)22:179-187.
215. **Kumar P, Wu H, McBride JL, Jung K-E, Kim MH, Davidson BL, Lee SK, Shankar P and Manjunath N**. Transvascular delivery of small interfering RNA to the central nervous system. **Nature** (**2007**)448:39-43.
216. **Kurilla MG, Cabradilla CD, Holloway BP and Keene JD**. Nucleotide sequence and host La protein interactions of rabies virus leader RNA. **Journal of virology** (**1984**)50:773-778.
217. **Kuzmin IV, Hughes G, Botvinkin AD, Orciari LA and Rupprecht CE**. Phylogenetic relationships of Irkut and West caucasian bat viruses within the lyssavirus genus and suggested quantititavie criteria based on the N gene sequence for lyssavirus genotype definitions. **Virus research** (**2005**)111:28-43.
218. **Kuzmin IV, Orciari LA, Arai YT, Smith JS, Hanlon CA, Kameoka Y and Rupprecht CE**. Bat lyssaviruses (Aravan and Khujand) from Central Asia: phylogenetic relationships according to N, P and G gene sequences. **Virus research** (**2003**)97:65-79.
219. **Lafon M, Bourhy H and Sureau P**. Immunity against the European bat rabies (Duvenhage) virus induced by

rabies vaccines: an experimental study in mice. **Vaccine** (**1988**)6:362-368.

220. **Lafon M, Herzog M and Sureau P**. Human rabies vaccines induce neutralising antibodies against the European bat rabies virus. **Lancet** (**1986**)2:515.
221. **Langevin C, Jaaro H, Bressanelli S, Fainzilber M and Tuffereau C**. Rabies virus glycoprotein (RVG) is a trimeric ligand for the N-terminal cysteine-rich domain of the mammalian p75 neurotrophin receptor. **The Journal of biological chemistry** (**2002**)277:37655-37662.
222. **Lee LG, Connell CR and Bloch W**. Allelic discrimination by nick-translation PCR with fluorgenic probes. **Nucleic acids research** (**1993**)21:3761-3766.
223. **Leger J, Croll RP and Smith FM**. Regional distribution and extrinsic innervation of intrinsic cardiac neurons in the guinea pig. **The Journal of comparative neurology** (**1999**)407:303-317.
224. **Lentz TL**. Rabies virus binding to an acetylcholine receptor alpha-subunit peptide. **Journal of molecular recognition : JMR** (**1990**)3:82-88.
225. **Lentz TL, Benson R, Klimowicz D, Wilson P and Hawrot E**. Binding of rabies virus to purified Torpedo acetylcholine receptor. **Brain research** (**1986**)387:211-219.
226. **Lentz TL, Burrage T, Smith AL, Crick J and Tignor GH**. Is the acetylcholine receptor a rabies virus receptor? **Science** (**1982**)215:182-184.
227. **Lentz TL, Wilson P, Hawrot E and Speicher D**. Amino acid sequence similarity between rabies virus glycoprotein and snake venom curaremimetic neurotoxins. **Science** (**1984**)226:847-848.
228. **Levine B and Griffin DE**. Persistence of viral RNA in mouse brains after recovery from acute alphavirus encephalitis. **Journal of virology** (**1992**)66:6429-6435.
229. **Levine B, Hardwick J, Trapp B, Crawford T, Bollinger R and Griffin DE**. Antibody-mediated clearance of alphavirus infection from neurons. **Science** (**1991**)254:856-860.
230. **Lewis P, Fu Y and Lentz TL**. Rabies virus entry into encosomes in IMR-32 human neuroblastoma cells. **Experimental neurology** (**1998**)153:65-73.
231. **Lewis P, Fu Y and Lentz TL**. Rabies virus entry at the neuromuscular junction in nerve-muscle cocultures. **Muscle & nerve** (**2000**)23:720-730.
232. **Lewis P and Lentz TL**. Rabies virus entry into cultured rat hippocampal neurons. **Journal of neurocytology** (**1998**)27:559-573.
233. **Li J, McGettigan JP, Faber M, Schnell MJ and Dietzschold B**. Infection of monocytes or immature dendritic cells (DCs) with an attenuated rabies virus results in DC maturation and a strong activation of the NFkappaB signaling pathway. **Vaccine** (**2008**)26:419-426.
234. **Li X-Q, Sarmento L and Fu ZF**. Degeneration of Neuronal Processes after Infection with Pathogenic, but not Attenuated, Rabies Viruses. **Journal of virology** (**2005**)79:10063-10068.
235. **Li Y, Luo L, Schubert M, Wagner RR and Kang CY**. Viral liposomes released from insect cells infected with recombinant baculovirus expressing the matrix protein of vesicular stomatitis virus. **Journal of virology** (**1993**)67:4415-4420.
236. **Li Z, Feng Z and Ye H**. Rabies viral antigen in human tongues and salivary glands. **The Journal of tropical medicine and hygiene** (**1995**)98:330-332.
237. **Lima K, Megid J, Silva A and Cortez A**. The heminested RT-PCR for the study of rabies virus pathogenesis. **Journal of virological methods** (**2005**)124:79-85.
238. **Lin AC and Holt CE**. Local translation and directional steering in axons. **The EMBO journal** (**2007**)Jul 26 Epub ahead of print.
239. **Liu L and Barajas L**. Nitric oxide synthase immunoreactive neurons in the rat kidney. **Neuroscience Letters** (**1993**)161:145-148.
240. **Liu L, Liu GL and Barajas L**. Colocalization of NADPH-diaphorase and dopamine beta-hydroxylase in the neuronal somata of the rat kidney. **Neuroscience Letters** (**1995**)202:69-72.
241. **Liu L, Liu GL and Barajas L**. Distribution of nitric oxide synthase-containing ganglionic neuronal somata and postganglionic fibers in the rat kidney. **The Journal of comparative neurology** (**1996**)369:16-30.
242. **Livak K, Flood S, Marmaro J, Giusti W and Deetz K**. Oligonucleotides with fluorescent dyes at opposite ends provide a quenched probe system useful for detecting PCR product and nucleic acid hybridization. **PCR methods and applications** (**1995**)4:357-362.
243. **Lodmell DL, Dimcheff DE and Ewalt LC**. Viral RNA in the bloodstream suggest viremia occurs in clinically ill rabies-infected mice. **Virus research** (**2006**)116:114-118.

244. **Lodmell DL and Ewalt LC**. Pathogenesis of street rabies virus infections in resistant and susceptible strains of mice. **Journal of virology** (**1985**)55:788-795.
245. **Lumio J, Hillbom M, Roine R, Ketonen L, Haltia M, Valle M, Neuvonen E and Lähdevirta J**. Human rabies of bat origin in Europe. **Lancet** (**1986**)1:378.
246. **Lycke E and Tsiang H**. Rabies virus infection of cultured rat sensory neurons. **Journal of virology** (**1987**)61:2733-2741.
247. **Lyles DS and McKenzie MO**. Reversible and irreversible steps in assembly and disassembly of vesicular stomatitis virus: equilibria and kinetics of dissociation of nucleocapsid-M protein complexes assembled in vivo. **Biochemistry** (**1998**)37:439-450.
248. **Lyles DS, McKenzie MO and Parce JW**. Subunit interactions of vesicular stomatitis virus envelope glycoprotein stabilized by binding to viral matrix protein. **Journal of virology** (**1992**)66:349-358.
249. **Lyles DS, Puddington L and McCreedy BJ, Jr**. Vesicular stomatitis virus M protein in the nuclei of infected cells. **Journal of virology** (**1988**)62:4387-4392.
250. **Madhusudana S, Nagaraj D, Uday M, Ratnavalli E and Kumar M**. Partial recovery from rabies in a six-year-old girl. **International journal of infectious diseases : IJID : official publication of the International Society for Infectious Diseases** (**2002**)6:85-86.
251. **Magni F and Carobi C**. The afferent and preganglionic parasympathetic innervation of the rat liver, demonstrated by the retrograde transport of horseradish peroxidase. **Journal of the autonomic nervous system** (**1983**)8:237-260.
252. **Martin R, Vaida B, Bleher R, Crispino M and Giuditta A**. Protein synthesizing units in presynaptic and postsynaptic domains of squid neurons. **Journal of cell science** (**1998**)111:3157-3166.
253. **Massa PT, Ozato K and McFarlin DE**. Cell type-specific regulation of major histocompatibility complex (MHC) class I gene expression in astrocytes, oligodendrocytes, and neurons. **Glia** (**1993**)8:201-207.
254. **Masters PS and Banerjee AK**. Complex formation with vesicular stomatitis virus phosphoprotein NS prevents binding of nucleocapsid protein N to nonspecific RNA. **Journal of virology** (**1988**)62:2658-2664.
255. **Masters PS and Banerjee AK**. Resolution of multiple complexes of phosphoprotein NS with nucleocapsid protein N of vesicular stomatitis virus. **Journal of virology** (**1988**)62:2651-2657.
256. **Mavrakis M, Mehouas S, Real E, Iseni F, Blondel D, Tordo N and Ruigrok RW**. Rabies virus chaperone: Identification of the phosphoprotein peptide that keeps nucleoprotein soluble and free from non-specific RNA. **Virology** (**2006**)349:422-429.
257. **Mawe GM, Talmage EK, Lee KP and Parsons RL**. Expression of choline acetyltransferase immunoreactivity in guinea pig cardiac ganglia. **Cell and tissue research** (**1996**)285:281-286.
258. **McColl K, Gould AR, Selleck P, Hooper P, Westbury H and Smith JS**. Polymerase chain reaction and other laboratory techniques in the diagnosis of long incubation rabies in Australia. **Australian veterinary journal** (**1993**)70:84-89.
259. **McCreedy BJ, Jr and Lyles DS**. Distribution of M protein and nucleocapsid protein of vesicular stomatitis virus in infected cell plasma membranes. **Virus research** (**1989**)14:189-205.
260. **McKenna OC and Angelakos ET**. Acetylcholinesterase-containing nerve fibers in the canine kidney. **Circulation research** (**1968**)23:645-651.
261. **Mebatsion T**. Extensive attenuation of rabies virus by simultaneously modifying the dynein light chain binding site in the P protein and replacing Arg333 in the G protein. **Journal of virology** (**2001**)75:11496-11502.
262. **Mebatsion T, König M and Conzelmann K-K**. Budding of rabies virus particles in the absence of the spike glycoprotein. **Cell** (**1996**)84:941-951.
263. **Mebatsion T, Weiland F and Conzelmann K-K**. Matrix protein of rabies virus is responsible for the assembly and budding of bullet-shaped particles and interacts with the transmembrane spike glycoprotein G. **Journal of virology** (**1999**)73:242-250.
264. **Meinl E, Krumbholz M and Hohlfeld R**. B lineage cells in the inflammatory central nervous system environment: Migration, maintenance, local antibody production, and therapeutic modulation. **Annals of neurology** (**2006**)59:880-892.
265. **Meltzer M and Rupprecht CE**. A review of the economics of the prevention and control of rabies. Part 1: Global impact and rabies in humans. **PharmacoEconomics** (**1998**)14:365-383.

266. **Mifune K, Ohuchi M and Mannen K**. Hemolysis and cell fusion by rhabdoviruses. **FEBS letters** (**1982**)137:293-297.
267. **Miller CS**. Pleiotropic mechanisms of virus survival and persistence. **Oral surgery, oral medicine, oral pathology, oral radiology, and endodontology** (**2005**)100:S27-S36.
268. **Misak A**. Rabies after solid organ transplantation. **CMAJ : Canadian Medical Association journal = journal de l'Association medicale canadienne** (**2004**)171:327.
269. **Mitchell GAG**. The renal nerves. **British journal of urology** (**1950**)22:269-280.
270. **Mitrabhakdi E, Shuangshoti S, Wannakrairot P, Lewis RA, Susuki K, Laothamatas J and Hemachudha T**. Difference in neuropathogenic mechanisms in human furious and paralytic rabies. **Journal of the neurological sciences** (**2005**)238:3-10.
271. **Moravec M and Moravec J**. Adrenergic neurons and short proprioceptive feedback loops involved in the integration of cardiac function in the rat. **Cell and tissue research** (**1989**)258:381-385.
272. **Moravec M, Moravec J and Forsgren S**. Catecholaminergic and peptidergic nerve components of intramural ganglia in the rat heart. An immunohistochemical study. **Cell and tissue research** (**1990**)262:315-327.
273. **Morimoto K, Foley HD, McGettigan JP, Schnell MJ and Dietzschold B**. Reinvestigation of the role of the rabies virus glycoprotein in viral pathogenesis using a reverse genetics approach. **Journal of neurovirology** (**2000**)6:373-381.
274. **Morimoto K, Hooper DC, Spitsin S, Koprowski H and Dietzschold B**. Pathogenicity of different rabies virus variants inversely correlates with apoptosis and rabies virus glycoprotein expression in infected primary neuron cultures. **Journal of virology** (**1999**)73:510-518.
275. **Morimoto K, Patel M, Corisedo S, Hooper DC, Fu ZF, Rupprecht CE, Koprowski H and Dietzschold B**. Characterization of a unique variant of bat rabies virus responsible for newly emerging human cases in North America. **Proceedings of the National Academy of Sciences of the United States of America** (**1996**)93:5653-5658.
276. **Morris T, Robertson B and Gallagher M**. Rapid reverse transcription-PCR detection of hepatitis C virus RNA in serum by using the TaqMan fluorogenic detection system. **Journal of clinical microbiology** (**1996**)34:2933-2936.
277. **Moss NG**. Renal function and renal afferent and efferent nerve activity. **The American journal of physiology** (**1982**)243:F425-433.
278. **Müller T, Cox J, Peter W, Schäfer R, Johnson N, McElhinney LM, Geue J, Tjornehoj K and Fooks AR**. Spill-over of European bat lyssavirus type 1 into a stone marten (Martes foina) in Germany. **Journal of veterinary medicine. B, Infectious diseases and veterinary public health** (**2004**)51:49-54.
279. **Murphy F and Bauer S**. Early street rabies virus infection in striated muscle and later progression to the central nervous system. **Intervirology** (**1974**)3:256-268.
280. **Nagaraj T, Vasanth JP, Desai A, Kamat A, Madhusudana S and Ravi V**. Ante mortem diagnosis of human rabies using saliva samples: Comparison of real time and convetional RT-PCR techniques. **Journal of Clinical Virology** (**2006**).
281. **Nathwani D, McIntyre PG, White K, Shearer A, Reynolds N, Walker D, Orange G and Fooks AR**. Fatal human rabies caused by European bat lyssavirus type 2a infection in Scotland. **Clinical infectious diseases : an official publication of the Infectious Diseases Society of America** (**2003**)37:598-601.
282. **Nelson DA and Berry RG**. Fatal rabies associated with extensive demyelination. **Archives of neurology** (**1993**)50:317-323.
283. **Neumann H, Cavalié A, Jenne DE and Wekerle H**. Induction of MHC class I genes in neurons. **Science (New York, NY)** (**1995**)269:549-552.
284. **Newcomb WW and Brown JC**. Role of the vesicular stomatitis virus matrix protein in maintaining the viral nucleocapsid in the condensed form found in native virions. **Journal of virology** (**1981**)39:295-299.
285. **Ni Y, Iwatani Y, Morimoto K and Kawai A**. Studies on unusual cytoplasmic structures which contain rabies virus envelope proteins. **The Journal of general virology** (**1996**)77 (Pt 9): 2137-2147.
286. **Noah DL, Drenzek CS, Smith JS, Krebs JW, Orciari LA, Shaddock J, Sanderlin D, Whitfield S, Fekadu M, Olson JG, Rupprecht CE and Childs JE**. Epidemiology of human rabies in the United States, 1980 to 1996. **Annals of internal medicine** (**1998**)128:922-930.

287. **Norgren R and Smith GP**. Central distribution of subdiaphragmatic vagal branches in the rat. **The Journal of comparative neurology** (**1988**)273:207-223.
288. **Norvell JE and Anderson JM**. Assessment of possible parasympathetic innervation of the kidney. **Journal of the autonomic nervous system** (**1983**)8:291-294.
289. **Ono K, Dubois-Dalcq ME, Schubert M and Lazzarini RA**. A mutated membrane protein of vesicular stomatitis virus has an abnormal distribution within the infected cell and causes defective budding. **Journal of virology** (**1987**)61:1332-1341.
290. **Orciari LA, Niezgoda M, Hanlon CA, Shaddock JH, Sanderlin DW, Yager PA and Rupprecht CE**. Rapid clearance of SAG-2 rabies virus from dogs after oral vaccination. **Vaccine** (**2001**)19:4511-4518.
291. **Pape WJ, Fitzsimmons TD and Hoffman RE**. Risk for rabies transmission from encounters with bats, Colorado, 1977-1996. **Emerging infectious diseases** (**1999**)5:433-437.
292. **Park C-H, Kondo M, Inoue S, Noguchi A, Oyamada T, Yoshikawa H and Yamada A**. The histopathogenesis of paralytic rabies in six-week-old C57BL/6J mice following inoculation of the CVS-11 strain into the right triceps surae muscle. **The Journal of veterinary medical science / the Japanese Society of Veterinary Science** (**2006**)68:589-595.
293. **Pattnaik AK, Hwang LN, Li T, Englund N, Mathur M, Das T and Banerjee AK**. Phosphorylation within the amino-terminal acidic domain I of the phosphoprotein of vesicular stomatitis virus is required for transcription but not for replication. **Journal of virology** (**1997**)71:8167-8175.
294. **Patton JT, Davis NL and Wertz GW**. N protein alone satisfies the requirement for protein synthesis during RNA replication of vesicular stomatitis virus. **Journal of virology** (**1984**)49:303-309.
295. **Pauza DH, Pauziene N, Pakeltyte G and Stropus R**. Comparative quantitative study of the intrinsic cardiac ganglia and neurons in the rat, guinea pig, dog and human as revealed by histochemical staining for acetylcholinesterase. **Annals of anatomy = Anatomischer Anzeiger : official organ of the Anatomische Gesellschaft** (**2002**)184:125-136.
296. **Paxinos G and Franklin KB**. The mouse brain in stereotaxic coordinates, 2nd ed. Academic Press, San Diego, California (**2001**).
297. **Perry LL and Lodmell DL**. Role of CD4+ and CD8+ T Cells in Murine Resistance to Street Rabies Virus. **Journal of virology** (**1991**)65:3429-3434.
298. **Phares TW, Kean RB, Mikheeva T and Hooper DC**. Regional Differences in Blood-Brain Barrier Permeability Changes and Inflammation in the Apathogenic Clearance of Virus from the Central Nervous System. **Journal of immunology (Baltimore, Md. : 1950)** (**2006**)176:7666-7675.
299. **Picard-Meyer E, Bruyère V, Barrat J, Tissot E, Barrat M and Cliquet F**. Development of a hemi-nested RT-PCR method for the specific determination of European Bat Lyssavirus 1: Comparison with other rabies diagnostic methods. **Vaccine** (**2004**)22:1921-1929.
300. **Piper M and Holt CE**. RNA translation in axons. **Annual review of cell and developmental biology** (**2004**)20:505-523.
301. **Porras C, Barboza J, Fuenzalida E, Adaros H, Oviedo A and Furst J**. Recovery from rabies in man. **Annals of internal medicine** (**1976**)85:44-48.
302. **Prabhakar BS, Fischman HR and Nathanson N**. Recovery from Experimental Rabies by Adoptive Transfer of Immune Cells. **The Journal of general virology** (**1981**)56:25-31.
303. **Prabhakar BS and Nathanson N**. Acute rabies death mediated by antibody. **Nature** (**1981**)290:590-591.
304. **Preuss MA**. [Verbreitung und Replikation verschiedener Rabies-Virusstämme in der Peripherie und der Effekt von rekombinantem TNF auf die Pathogenität von Rabies-Virus im murinen Trigeminalganglion]. Philipps-Universität Marburg, Marburg (**2005**).
305. **Pringle CR**. The order *Mononegavirales*. **Archives of virology** (**1991**)117:137-140.
306. **Prosniak M, Hooper DC, Dietzschold B and Koprowski H**. Effect of rabies virus infection on gene expression in mouse brain. **Proceedings of the National Academy of Sciences of the United States of America** (**2001**)98:2758-2763.
307. **Pulmanausahakul R, Li J, Schnell MJ and Dietzschold B**. The glycoprotein and matrix protein of rabies virus affect pathogenicity by regulating viral replication and facilitating cell-to-cell spread. **Journal of virology** (**2008**)82:2330-2338.
308. **Rasalingam P, Rossiter JP and Jackson AC**. Recombinant rabies virus vaccine strain SAD-L16 inoculated intracerebrally in young mice produces a severe encephalitis with extensive

neuronal apoptosis. **The Canadian Journal of Veterinary Research** (**2005**)69:100-105.

309. **Raux H, Flamand A and Blondel D**. Interaction of the rabies virus P protein with the LC8 dynein light chain. **Journal of virology** (**2000**)74:10212-10216.
310. **Ray NB, Ewalt IC and Lodmell DL**. Rabies virus replication in primary murine bone marrow macrophages and in human and murine macrophage-like cell lines: implications for viral persistence. **Journal of virology** (**1995**)69:764-772.
311. **Ray NB, Power C, Lynch W, Ewalt LC and Lodmell DL**. Rabies viruses infect primary cultures of murine, feline, and human microglia and astrocytes. **Archives of virology** (**1997**)142:1011-1019.
312. **Reagan KJ and Wunner WH**. Rabies virus interaction with various cell lines is independent of the acetylcholine receptor. **Archives of virology** (**1985**)84:277-282.
313. **Recordati G, Genovesi S, Cerati D and di Cintio R**. Reno-renal and reno-adrenal reflexes in the rat. **Clinical science (London, England : 1979)** (**1980**)59 Suppl 6:323s-325s.
314. **Recordati GM, Moss NG and Waselkov L**. Renal chemoreceptors in the rat. **Circulation research** (**1978**)43:534-543.
315. **Reddy D, Schnitzlein W and Reichmann M**. Use of defective interfering particle RNA probes in the determination of the order of in vitro transcription of vesicular stomatitis virus genes. **Journal of virology** (**1977**)21:432-434.
316. **Reilly FD, McCuskey PA and McCuskey RS**. Intrahepatic distribution of nerves in the rat. **The Anatomical record** (**1978**)191:55-67.
317. **Richardson JB**. Recent progress in pulmonary innervation. **The American review of respiratory disease** (**1983**)128:S65-68.
318. **Robison CS and Whitt MA**. The membrane-proximal stem region of vesicular stomatitis virus G protein confers efficient virus assembly. **Journal of virology** (**2000**)74:2239-2246.
319. **Roche S and Gaudin Y**. Evidence that rabies virus forms different kinds of fusion machines with different pH tresholds for fusion. **Journal of virology** (**2004**)78:8746-8752.
320. **Rodríguez EM, Herrera H, Peruzzo B, Rodríguez S, Hein S and Oksche A**. Light- and electron-microscopic immunocytochemistry and lectin histochemistry of the subcommissural organ: evidence for processing of the secretory material. **Cell and tissue research** (**1986**)243:545-559.
321. **Rønn L, Hartz B and Bock E**. The neural cell adhesion molecule (NCAM) in development and plasticity of the nervous system. **Experimental gerontology** (**1998**)33:853-864.
322. **Rupprecht CE, Hanlon CA and Hemachudha T**. Rabies re-examined. **Lancet Infect Dis** (**2002**)2:327-343.
323. **Sacramento D, Bourhy H and Tordo N**. PCR technique as an alternative method for diagnosis and molecular epidemiology of rabies virus. **Molecular and cellular probes** (**1991**)5:229-240.
324. **Sakaguchi T**. Alterations in gastric acid secretion following hepatic portal injections of D-glucose and its anomers. **Journal of the autonomic nervous system** (**1982**)5:337-344.
325. **Samaratunga H, Searle JW and Hudson N**. Non-rabies lyssavirus human encephalitis from fruit bats: Australian bat lyssavirus (pteropid lyssavirus) infection. **Neuropathology and applied neurobiology** (**1998**)24:331-335.
326. **Sato M, Maeda N, Yoshida H, Urade M and Saito S**. Plaque formation of herpes virus hominis type 2 and rubella virus in variants isolated from the colonies of BHK21/WI-2 cells formed in soft agar. **Archives of virology** (**1977**)53:269-273.
327. **Schindler R**. Studies on the pathogenesis of rabies. **Bulletin of the World Health Organization** (**1961**)25:119-126.
328. **Schneider L, Dietzschold B, Dierks R, Matthaeus W, Enzmann P and Strohmaier K**. Rabies group-specific ribonucleoprotein antigen and a test system for grouping and typing of rhabdoviruses. **Journal of virology** (**1973**)11:748-755.
329. **Schnell MJ, Buonocore L, Boritz E, Gosh HP, Chernish R and Rose JK**. Requirement for a non-specific glycoprotein cytoplasmic domain sequence to drive efficient budding of vesicular stomatitis virus. **The EMBO journal** (**1998**)17:1289-1296.
330. **Schnell MJ, Mebatsion T and Conzelmann K-K**. Infectious rabies viruses from cloned cDNA. **The EMBO journal** (**1994**)13:4195-4203.
331. **Schnell MJ, Tan GS and Dietzschold B**. The application of reverse genetics technology in the study of rabies virus (RV) pathogenesis and for the development of novel RV vaccines. **Journal of neurovirology** (**2005**)11:76-81.

332. **Selimov M, Tatarov A, Botvinkin AD, Klueva E, Kulikova L and Khismatullina N**. Rabies-related Yuli virus; identification with a panel of monoclonal antibodies. **Acta virologica** (**1989**)33:542-546.
333. **Serra-Cobo J, Amengual B, Abellán C and Bourhy H**. European bat lyssavirus infection in Spanish bat populations. **Emerging infectious diseases** (**2002**)8:413-420.
334. **Shankar V, Dietzschold B and Koprowski H**. Direct entry of rabies virus into the central nervous system without prior local replication. **Journal of virology** (**1991**)65:2736-2738.
335. **Sheikh KA, Ramos-Alvarez M, Jackson AC, Li CY, Asbury AK and Griffin JW**. Overlap of pathology in paralytic rabies and axonal Guillain-Barre syndrome. **Annals of neurology** (**2005**)57:768-772.
336. **Sikes RK, Cleary WF, Koprowski H, Wiktor TJ and Kaplan MM**. Effective protection of monkeys against death from street virus by post-exposure administration of tissue-culture rabies vaccine. **Bulletin of the World Health Organization** (**1971**)45:1-11.
337. **Simon OR and Schramm LP**. The spinal course and medullary termination of myelinated renal afferents in the rat. **Brain research** (**1984**)290:239-247.
338. **Singh S, Johnson PI, Javed A, Gray TS, Lonchyna VA and Wurster RD**. Monoamine- and histamine-synthesizing enzymes and neurotransmitters within neurons of adult human cardiac ganglia. **Circulation** (**1999**)99:411-419.
339. **Smart NL and Charlton KM**. The distribution of Challenge virus standard rabies virus versus skunk street rabies virus in the brains of experimentally infected rabid skunks. **Acta neuropathologica** (**1992**)84:501-508.
340. **Smith JS**. Mouse model for abortive rabies infection of the central nervous system. **Infection and Immunity** (**1981**)31:297-308.
341. **Smith JS**. Monoclonal antibody studies of rabies in insectivorous bats of the United States. **Reviews of infectious diseases** (**1988**)10:S637-643.
342. **Smith JS**. New aspects of rabies with emphasis on epidemiology, diagnosis, and prevention of the disease in the United States. **Clinical microbiology reviews** (**1996**)9:166-176.
343. **Smith JS, Fishbein DB, Rupprecht CE and Clark K**. Unexplained rabies in three immigrants in the United States. A virologic investigation. **The New England journal of medicine** (**1991**)324:205-211.
344. **Smith JS, McCelland C, Reid F and Baer G**. Dual role of the immune response in street rabies virus infection of mice. **Infection and Immunity** (**1982**)35:213-221.
345. **Sokol F and Clark HF**. Phosphoproteins, structural components of rhabdoviruses. **Virology** (**1973**)52:246-263.
346. **Sokol F, Schlumberger HD, Wiktor TJ, Koprowski H and Hummeler K**. Biochemical and biophysical studies on the nucleocapsid and on the RNA of rabies virus. **Virology** (**1969**)38:651-665.
347. **Srinivasan A, Burton EC, Kuehnert MJ, Rupprecht CE, Sutker WL, Ksiazek TG, Paddock CD, Guarner J, Schih W-J, Goldsmith C, Hanlon CA, Zoretic J, Fischbach B, Niezgoda M, El-Feky WH, Orciari LA, Sanchez EQ, Likos A, Klintmalm GB, Cardo D, LeDuc J, Chamberland ME, Jernigan DB and Zaki SR**. Transmission of rabies virus from an organ donor to four transplant recipients. **The New England journal of medicine** (**2005**)352:1103-1111.
348. **Steele PA, Gibbins IL, Morris JL and Mayer B**. Multiple populations of neuropeptide-containing intrinsic neurons in the guinea-pig heart. **Neuroscience** (**1994**)62:241-250.
349. **Sugamata M, Miyazawa M, Mori S, Spangrude GJ, Ewalt LC and Lodmell DL**. Paralysis of Street Rabies Virus-Infected Mice Is Dependent on T Lymphocytes. **Journal of virology** (**1992**)66:1252-1260.
350. **Superti F, Derer M and Tsiang H**. Mechanism of rabies virus entry into CER cells. **The Journal of general virology** (**1984**)65:781-789.
351. **Superti F, Seganti L, Tsiang H and Orsi N**. Role of phospholipids in rhabdovirus attachment to CER cells. **Archives of virology** (**1984**)81:321-328.
352. **Tan GS, Preuss MA, Williams JC and Schnell MJ**. The dynein light chain 8 binding motif of rabies virus phosphoprotein promotes efficient viral transcription. **Proceedings of the National Academy of Sciences of the United States of America** (**2007**)104:7229-7234.
353. **Tang Y, Rampin O, Giuliano F and Ugolini G**. Spinal and brain circuits to motoneurons of the bulbospongiosus muscle: retrograde transneuronal tracing with rabies virus. **The Journal of comparative neurology** (**1999**)414:167-192.
354. **Thoulouze M-I, Lafage M, Montano-Hirose JA and Lafon M**. Rabies virus

infects mouse and human lymphocytes and induces apoptosis. **Journal of virology** (**1997**)71:7372-7380.

355. **Thoulouze M-I, Lafage M, Schachner M, Hartmann U, Cremer H and Lafon M**. The neural cell adhesion molecule is a receptor for rabies virus. **Journal of virology** (**1998**)72:7181-7190.
356. **Thoulouze M-I, Lafage M, Yuste VJ, Kroemer G, Susin SA, Israel N and Lafon M**. Apoptosis Inversely Correlates with Rabies Virus Neurotropism. **Ann N Y Acad Sci** (**2003**)1010:598-603.
357. **Tirawatnpong S, Hemachudha T, Manutsathit S, Shuangshoti S, Phanthumchinda K and Phanuphak P**. Regional distribution of rabies viral antigen in central nervous system of human encephalitic and paralytic rabies. **Journal of the neurological sciences** (**1989**)92:91-99.
358. **Tomomatsu T, Ino T and Matsumoto E**. Experimental studies on neurogenic mechanism of renal circulation. **Japanese circulation journal** (**1962**)26:585-595.
359. **Tordo N, Poch O, Ermine A, Keith G and Rougeon F**. Walking along the rabies genome: is the large G-L intergenic region a remnant gene? **Proceedings of the National Academy of Sciences of the United States of America** (**1986**)83:3914-3918.
360. **Tsiang H**. Neuronal function impairment in rabies-infected rat brain. **The Journal of general virology** (**1982**)61:277-281.
361. **Tsiang H**. Rabies virus infection of myotubes and neurons as elements of the neuromuscular junction. **Reviews of infectious diseases** (**1988**)10:S733-738.
362. **Tsiang H, Atanasiu P, Chermann J and Jasmin C**. Inhibition of rabies virus in vitro by the ammonium-5-tungsto-2-antimoniate. **The Journal of general virology** (**1978**)40:665-668.
363. **Tsiang H, de La Porte S, Ambroise D, Derer M and Koenig J**. Infection of cultured rat myotubes and neurons from the spinal cord by rabies virus. **Journal of neuropathology and experimental neurology** (**1986**)45:28-42.
364. **Tsiang H, Derer M and Taxi J**. An in vivo and in vitro study of rabies virus infection of the rat superior cervical ganglia. **Archives of virology** (**1983**)76:231-243.
365. **Tsiang H, Koulakoff A, Bizzini B and Berwald-Netter Y**. Neurotropism of rabies virus. An *in vitro* study. **Journal of neuropathology and experimental neurology** (**1983**)42:439-452.
366. **Tsiang H, Lycke E, Ceccaldi P-E, Ermine A and Hirardot X**. The anterograde transport of rabies virus in rat sensory dorsal root ganglia neurons. **The Journal of general virology** (**1989**)70:2075-2085.
367. **Tuffereau C, Bénéjean J, Blondel D, Kieffer B and Flamand A**. Low-affinity nerve-growth factor receptor (P75NTR) can serve as a receptor for rabies virus. **The EMBO journal** (**1998**)17:7250-7259.
368. **Tuffereau C, Benejean J, Roque Alfonso A-M, Flamand A and Fishman MC**. Neuronal cell surface molecules mediate specific binding to rabies virus glycoprotein expressed by a recombinant baculovirus on the surfaces of lepidopteran cells. **Journal of virology** (**1998**)72:1085-1091.
369. **Turnley AM, Starr R and Bartlett PF**. Failure of sensory neurons to express class I MHC is due to differential SOCS1 expression. **Journal of Neuroimmunology** (**2002**)123:35-40.
370. **Twiss JL and van Minnen J**. New insights into neuronal regeneration: the role of axonal protein synthesis in pathfinding and axonal extension. **Journal of neurotrauma** (**2006**)23:295-308.
371. **Tyor W, Wesselingh S, Levine B and Griffin DE**. Long term intraparenchymal Ig secretion after acute viral encephalitis in mice. **Journal of immunology (Baltimore, Md. : 1950)** (**1992**)149:4016-4020.
372. **Ugolini G**. Specificity of rabies virus as a transneuronal tracer of motor networks: transfer from hypoglossal motoneurons to connected second-order and higher order central nervous system cell groups. **The Journal of comparative neurology** (**1995**)356:457-480.
373. **Uyama N, Geerts A and Reynaert H**. Neural connections between the hypothalamus and the liver. **The anatomical record Part A, Discoveries in molecular, cellular, and evolutionary biology** (**2004**)280:808-820.
374. **van der Poel WH, Lina PH and Kramps JA**. Public health awareness of emergin zoonotic viruses of bats: a European perspective. **Vector borne and zoonotic diseases (Larchmont, N.Y.)** (**2006**)6:315-324.
375. **van Minnen J**. Axonal localization of neuropeptide-encoding mRNA in identified neurons of the snail Lymnaea stagnalis. **Cell and tissue research** (**1994**)276:155-161.
376. **Villarreal LP, Breindl M and Holland JJ**. Determination of molar ratios of vesicular stomatitis virus induced RNA species in BHK21 cells. **Biochemistry** (**1976**)15:1663-1667.

377. **Vos A, Müller T, Neubert L, Zurbriggen A, Botteron C, Pohle D, Schoon H, Haas L and Jackson AC**. Rabies in red foxes (Vulpes vulpes) experimentally infected with European bat lyssavirus type 1. **Journal of veterinary medicine. B, Infectious diseases and veterinary public health** (**2004**)51:327-332.
378. **Watson HD, Tignor GH and Smith AL**. Entry of rabies virus into the peripheral nerves of mice. **The Journal of general virology** (**1981**)56:371-382.
379. **Weiland F, Cox JH, Meyer S, Dahme E and Reddehase MJ**. Rabies Virus Neuritic Paralysis: Immunopathogenesis of Nonfatal Paralytic Rabies. **Journal of virology** (**1992**)66:5096-5099.
380. **Weitsen HA and Norvell JE**. Cholinergic innervation of the autotransplanted canine kidney. **Circulation research** (**1969**)25:535-541.
381. **Wellenberg G, Audry L, Rønsholt L, van der Poel WH, Bruschke C and Bourhy H**. Presence of European bat lyssavirus RNAs in apparently healthy Rousettus aegyptiacus bats. **Archives of virology** (**2002**)147:349-361.
382. **Wessler I, Kirkpatrick C and Racké K**. The cholinergic 'pitfall': acetylcholine, a universal cell molecule in biological systems, including humans. **Clinical and experimental pharmacology & physiology** (**1999**)26:198-205.
383. **Whitt MA, Buonocore L, Prehaud C and Rose JK**. Membrane fusion activity, oligomerization, and assembly of the rabies virus glycoprotein. **Virology** (**1991**)185:681-688.
384. **Wickersham IR, Finke S, Conzelmann K-K and Callaway EM**. Retrograde neuronal tracing with a deletion-mutant rabies virus. **Nature Methods** (**2007**)4:47-49.
385. **Wiktor TJ, Doherty PC and Koprowski H**. Suppression of cell-mediated immunity by street rabies virus. **The Journal of experimental medicine** (**1977**)145:1617-1622.
386. **Wiktor TJ, Fernandes M and Koprowski H**. Cultivation of rabies virus in human diploid cell strain WI38. **Journal of immunology (Baltimore, Md. : 1950)** (**1964**)93:353-366.
387. **Wiktor TJ, Macfarlan R, Foggin C and Koprowski H**. Antigenic analysis of rabies and Mokola virus from Zimbabwe using monoclonal antibodies. **Developments in biological standardization** (**1984**)57:199-211.
388. **Williams JC, Roulhac PL, Roy AG, Vallee RB, Fitzgerald MC and Hendrickson WA**. Structural and thermodynamic characterization of a cytoplasmic dynein light chain-intermediate chain complex. **Proceedings of the National Academy of Sciences of the United States of America** (**2007**)104:10028-10033.
389. **Willis DE, Li KW, Zheng J-Q, Chang JH, Smit A, Kelly T, Merianda TT, Sylvester J, van Minnen J and Twiss JL**. Differential transport and local translation of cytoskeletal, injury-response, and neurodegeneration protein mRNAs in axons. **The Journal of neuroscience : the official journal of the Society for Neuroscience** (**2005**)25:778-791.
390. **Willis DE and Twiss JL**. The evolving roles of axonally sythesized proteins in regeneration. **Current Opinion in Neurobiology** (**2006**)16:111-118.
391. **Willoughby RE, Jr, Tieves KS, Hoffman GM, Ghanayem NS, Amlie-Lefond CM, Schwabe MJ, Chusid MJ and Rupprecht CE**. Survival after treatment of rabies with induction of coma. **The New England journal of medicine** (**2005**)352:2508-2514.
392. **Wilson T and Lenard J**. Interaction of wild-type and mutant M protein of vesicular stomatitis virus with nucleocapsids in vitro. **Biochemistry** (**1981**)20:1349-1354.
393. **Winkler W, Baker EJ and Hopkins C**. An outbreak of non-bite transmitted rabies in a laboratory animal colony. **American journal of epidemiology** (**1972**)95:267-277.
394. **Winkler W, Fashinell T, Leffingwell L, Howard P and Conomy P**. Airborne rabies transmission in a laboratory worker. **JAMA : the journal of the American Medical Association** (**1973**)226:1219-1221.
395. **Winkler W, Shaddock J and Bowman C**. Rabies virus in salivary glands of raccoons (Procyon lotor). **Journal of wildlife diseases** (**1985**)21:297-298.
396. **Wu X, Gong X, Foley HD, Schnell MJ and Fu ZF**. Both viral transcription and replication are reduced when the rabies virus nucleoprotein is not phosphorylated. **Journal of virology** (**2002**)76:4153-4161.
397. **Wunner WH, Reagan KJ and Koprowski H**. Characterization of saturable binding sites for rabies virus. **Journal of virology** (**1984**)50:691-697.
398. **Xi X, Randall WC and Wurster RD**. Morphology of intracellularly labeled canine intracardiac ganglion cells. **The Journal of comparative neurology** (**1991**)314:396-402.
399. **Yang J, Hooper DC, Wunner WH, Koprowski H, Dietzschold B and Fu ZF**. The specificity of rabies virus RNA

encapsidation by nucleoprotein. **Virology** (**1998**)242:107-117.

400. **Yang J, Koprowski H, Dietzschold B and Fu ZF**. Phosphorylation of rabies virus nucleoprotein regulates viral RNA transcription and replication by modulating leader RNA encapsidation. **Journal of virology** (**1999**)73:1661-1664.
401. **Ye Z, Sun W, Suryanarayana K, Justice PA, Robinson D and Wagner RR**. Membrane-binding domains and cytopathogenesis of the matrix protein of vesicular stomatitis virus. **Journal of virology** (**1994**)68:7386-7396.
402. **Yi CX, van der Vliet J, Dai J, Yin G, Ru L and Buijs RM**. Ventromedial arcuate nucleus communicates peripheral metabolic information to the suprachiasmatic nucleus. **Endocrinology** (**2006**)147:283-294.
403. **Yin HH, Davis MI, Ronesi JA and Lovinger DM**. The role of protein synthesis in striatal long-term depression. **The Journal of neuroscience : the official journal of the Society for Neuroscience** (**2006**)26:11811-11820.
404. **Zheng J-Q, Kelly TK, Chang B, Ryazantsev S, Rajasekaran AK, Martin KC and Twiss JL**. A functional role for intra-axonal protein synthesis during axonal regeneration from adult sensory neurons. **The Journal of neuroscience : the official journal of the Society for Neuroscience** (**2001**)21:9291-9303.

10. Appendix

10.1. Curriculum Vitae: Mirjam Preuß (July 2, 2008)

Address

Alte Kasseler Straße 20
35039 Marburg
Germany

Personal history

name:	Preuß, Mirjam Anna Rita
birth date:	July 4, 1981
place of birth:	Wertheim, Germany
nationality:	German
maritial status:	married

School education

1987 – 1991	Elementary School Sendelbach in Lohr am Main, Germany
1991 – 2000	Franz-Ludwig v. Erthal – Gymnasium in Lohr am Main, Germany
2000	Abitur (university entrance qualification)

University education

2000 – 2005	studies in human biology (theoretical medicine) at the Philipps University Marburg, Germany
Major:	neurobiology
Minor:	immunology

Diploma thesis:
Spread and replication of various rabies virus strains in the periphery and the effect of recombinant TNF on the pathogenicity of rabies virus in the murine trigeminal ganglion
(Department of Molecular Neuroscience: Prof. Dr. E Weihe, PD Dr. M Bette)

2005*:*	diploma of human biology

Scientific occupations

Current position since 04.2007
Scientific assistant in the Department of Molecular Neuroscience (Prof. Dr. E Weihe), Institute of Anatomy and Cell Biology, Philipps-University Marburg, Germany

06.2005 – 03.2007
Research technician in the Department of Microbiology (MJ Schnell, PhD, B Dietzschold, DVM), Thomas Jefferson University, Philadelphia, PA, USA
(in context of the doctoral thesis)

Teaching experience

at the Philipps University Marburg, Germany:
- Anatomical dissection course for human biology students
- Neurobiology workshop for human biology students
- Anatomical lecture for biomedical science students
- Histology course for medical students
- Neuroanatomy course for medical students
- Basic laboratory training for human biology students

Co-authorships

Weihe E, Bette M, **Preuss MAR**, Faber M, Schäfer MKH, Rehnelt J, Schnell MJ, Dietzschold B:
Role of virus-induced neuropeptides in the brain in the pathogenesis of rabies.
In: Towards the Elimination of Rabies in Eurasia.
Karger, Eds: Dodet B, Fooks AR, Müller T, Tordo N. **Dev Biologicals 2008**; 73-81.

Faber M, Faber M-L, Li J, **Preuss MAR**, Schnell MJ, Dietzschold B:
Dominance of a Nonpathogenic Glycoprotein Gene over a Pathogenic Glycoprotein Gene in Rabies Virus.
Journal of Virology 2007; 81(13):7041-7047.

Tan GS, **Preuss MAR**, Williams JC, Schnell MJ:
The dynein light chain 8 binding motif of rabies virus phosphoprotein promotes efficient viral transcription.
Proceedings of the National Academy of Sciences U S A 2007; 104(17):7229-7234.

Smith JA, Nunnari G, **Preuss M**, Pomerantz RJ and Daniel R:
Pentoxifylline Suppresses Transduction by HIV-1-Based Vectors.
Intervirology 2007; 50(5):377-386.

Faber M, Bette M, **Preuss MAR**, Pulmanausahakul R, Rehnelt J, Schnell MJ, Dietzschold B, Weihe E:
Overexpression of Tumor Necrosis Factor Alpha by a Recombinant Rabies Virus Attenuates Replication in Neurons and Prevents Lethal Infection in Mice.
Journal of Virology 2005; 79(24):15405-15416.

Published abstracts & Contributions to Conferences

Preuss MAR, Bette M, Krieger T, Faber M, Schäfer MK-H, Schnell MJ, Dietzschold B, Weihe E:
Immunosubversion by Rabies virus through upregulation of the immunosuppressive neuropeptide CGRP in the central nervous system
European Journal of Cell Biology 2008; 87(Suppl. 58):32.

Preuss M, Dietzschold B, Faber M-L, Tan G, Weihe E, Schnell MJ:
Rabies virus replication outside the CNS - implications for transmission of new emerging RV strains
Third European Congress of Virology, September 1-5, **2007**; Nürnberg, Germany.

10.2. List of Academic Teachers

My academic teachers in Marburg were the professors:

Aumüller, Berndt, Besedovsky, Bremmer, Czubayko, Daut, del Rey, Eilers, Elsässer, Feuser, Garten, Gromes, Gudermann, Hasilik, Heeg, Heimbrodt, Jungclas, Kirchner, Koolman, Kunz, Lang, Lill, Löffler, Lohoff, Moll, Müller, Petz, Renkawitz-Pohl, Renz, Röhm, Röper, Schäfer, Seitz, Seitz, Steiniger, Suske, Voigt, Weihe

10.3. Acknowledgments

I would like to express my gratitude to the following persons for their very appreciated help and support without which this thesis would have never been written:

My supervisors and advisors:
Matthias J Schnell, Bernhard Dietzschold, Eberhard Weihe
Michael Bette
Martin K-H Schäfer, Reiner Westermann
For excellent mentoring, valuable incitation and discussion as well as inspiring and critical comments for the conception of my study.

My present and former coworkers and colleagues from Philadelphia:
Gene S Tan, Rojjanaporn Pulmanausahakul, Martin Koser, Amy Papaneri, James McGettigan Marie-Luise Faber, Mary-Ellen Smith, Christoph Wirblich, Jianwei Li, Milosz Faber
and
The present and former technical personnel from E. Weihe's lab:
Romy Weber, Petra Lattermann, Michael Schneider, Heidemarie Schneider
For very good collaboration, the pleasant atmosphere in the labs, valuable comments and excellent technical support.

My family:
Alfred and Petra Preuss, Marliese and Karl-Heinz Schumm, Nabil Bertoune